

PARTICLE FREEZE-OUT IN SELF-CONSISTENT RELATIVISTIC HYDRODYNAMICS

Kyrill A. Bugaev¹ and Mark I. Gorenstein²

Institut für Theoretische Physik, Goethe Universität Frankfurt, Germany
and
Bogolyubov Institute for Theoretical Physics, Kiev, Ukraine

¹e-mail: bugaev@th.physik.uni-frankfurt.de

²e-mail: goren@th.physik.uni-frankfurt.de

Abstract

The particle emission in relativistic hydrodynamic model is formulated assuming a sharp 3-dimensional space-time freeze-out hypersurface. The boundary conditions correspond to the energy-momentum and charge conservation between fluid and the gas of free particles. The emission and possible feedback of particles are included into the self-consistent hydrodynamic scheme. For the time-like parts of the freeze-out hypersurface the obtained results are different from the well known Cooper-Frye formula and lead to the shock-like freeze-out. A simple-wave hydrodynamic solution is considered in detail to illustrate some aspects of new freeze-out procedure.

Key words: freeze-out, particle spectra, conservation laws, freeze-out shock
PACS numbers: 24.10.Nz, 25.75.-q

1. Introduction

During last three years an essential progress has been achieved in the understanding of the freeze-out problem in relativistic hydrodynamics. A generalization of the well known Cooper–Frye (CF) formula [1] to the case of the time-like freeze-out hypersurfaces (hereafter **FHS**) was suggested in Ref. [2]. This formula does not contain negative particle number contributions on time-like **FHS** appeared in the CF procedure from those particles which cannot leave the hydrodynamical system during its expansion. The new distribution function has the cut-off factor, and we'll call it the cut-off distribution function (CO). Once the CO distribution function is defined, the energy-momentum tensor of the gas of free particles is known. In contrast to the CF formula the expressions derived in Ref. [2] show the explicit dependence on the parameters of the time-like **FHS**.

The freeze-out procedure of Ref. [2] has been further developed in a series of publications [3, 4, 5, 6, 7]. However, many important questions have not yet been studied. The aim of the present paper is to clarify the connection between new freeze-out procedure of Ref. [2] and the fluid hydrodynamics. We show that the system evolution is consistently split into the differential equations for the fluid motion and particle emission from **FHS**: smooth CF freeze-out on its space-like parts and the shock-like freeze-out with CO formula on time-like ones. The conservation laws and consistency of the full system of equations are shown.

High energy nucleus-nucleus collisions presumably give us the possibility to study strongly interacting matter in the framework of relativistic hydrodynamics (see [8, 9, 10] and references therein). It is evident that the hydrodynamic description of the fluid created in A+A collisions could be meaningful in the finite space-time region only. The relativistic hydrodynamics has to be combined self-consistently with the free stream of final particles towards the detectors at the latest stage of A+A reaction.

In Section 2 several transparent examples are presented to show the difference between the results obtained with the traditional CF formula and those with CO distribution. The form of the distribution function of the gas of free particles is discussed accounting for both the emission and (possible) feedback of the particles from the various time-like **FHS**.

In Section 3 we study all possible boundary conditions between the perfect fluid and the gas of free particles. The fluid equations of motion are derived there. The global energy-momentum and charge conservation holds for the whole system consisting of the fluid and the gas of free particles.

The equations for the time-like parts of the **FHS** are studied in Section 4. The general scheme of their solution together with the hydrodynamical equations for the fluid is discussed and applied to hydrodynamical motions in 1+1 dimensions. Thermodynamical and mechanical stability of the *freeze-out shock* is discussed there. The freeze-out problem of the simple wave for the massless gas of free particles is solved analytically. Momentum spectra for the freeze-out of the simple wave are found and compared with those obtained from the Cooper-Frye formula.

In Appendix A we present the systematic analysis of the angular and momentum integrations for the gas of free particles. Appendix B gives the complete comparison of the Eckart and the Landau-Lifshitz definitions of the hydrodynamic velocities for the massless gas of free particles. The spatial anisotropy of the energy-momentum tensor in the Landau-Lifshitz frame is found.

A short resume of the above results and conclusions are given in Section 5.

2. Particle Spectra on the Time-like Hypersurfaces

Originally the idea of freeze-out was postulated by Landau [11]. It states, that if the mean free path of the particles of the rarefied gas becomes comparable with the size of the whole system, one can assume that the collisions between particles cease to exist on some hypersurface and the particles freely move to the detector. Here we shall not consider the justification of this assumption, but we shall show that it leads to rather strong restrictions on the possible freeze-out procedure. The first, crucial step for showing this is to obtain the correct formula for the particle spectra emitted from both space-like and time-like freeze-out hypersurfaces.

2.1. Short Derivation of the Cut-off Formula

The correct formula for the particle spectra emitted from an arbitrary hypersurface was obtained in [2] by the method developed earlier [12]. However, we would like to rederive it here in a less rigorous, but more transparent way. In what follows we shall use the Landau-Lifshitz convention for the metric tensor and 4-intervals. Thus $ds^2 > 0$ ($ds^2 < 0$) is a time-like (space-like) interval. In contrast to Ref. [4] we shall specify the hypersurfaces by their intervals.

First, let us consider a small element dS_\perp of the boundary between gas and vacuum and let us count the number of particles dN that will cross this element during the time dt , assuming that the mentioned boundary is at rest (this assumption is very essential because it is valid only for the time-like hypersurfaces). Let $\phi(\mathbf{x}, t, \mathbf{p})$ be a distribution function which describes the probability to find a particle with 3-momentum \mathbf{p} and energy $p_0 = \sqrt{m^2 + \mathbf{p}^2}$ at the space-time coordinate (\mathbf{x}, t) . Let \mathbf{n} denote a unit 3-vector of the external normal to the surface element dS_\perp . Then the desired number of particles is given by the expression

$$dN = \phi(\mathbf{x}, t, \mathbf{p}) d^3p \mathbf{v} \cdot \mathbf{n} dt dS_\perp \Theta(\mathbf{v} \cdot \mathbf{n}) . \quad (2.1)$$

The presence of the Θ -function in the above formula is evident: it ensures that only particles with positive projection of the velocity on the external normal can cross the surface (cosine of the angle between the vectors \mathbf{v} and \mathbf{n} must be positive). Particles with negative projection of the velocity on the normal never cross the surface and should not be taken into account.

Next we take into account the shift of the surface $d\mathbf{x}$ with the time as follows:

$$dN = \phi(\mathbf{x}, t, \mathbf{p}) d^3p [\mathbf{v}dt - d\mathbf{x}] \cdot \mathbf{n} dS_\perp \Theta([\mathbf{v}dt - d\mathbf{x}] \cdot \mathbf{n}) . \quad (2.2)$$

The second term in the last equation describes the change of the flux through the element dS_\perp due to the displacement $d\mathbf{x}$ of the surface element in time dt (it is still not the most general choice of the **FHS**). Then it can be written in the fully covariant form,

$$p_0 \frac{dN^{cut-off}}{d^3p} = \phi(\mathbf{x}, t, \mathbf{p}) p_\nu d\sigma^\nu \Theta(p_\rho d\sigma^\rho) , \quad (2.3)$$

where $d\sigma^\mu$ is the external normal 4-vector to the freeze-out hypersurface. This relation differs from the Cooper–Frye one by the presence of the Θ -function which plays an important role for the time-like **FHS**, as we saw it during the derivation. On the other hand it completely agrees with the *CF* formula [1] for the space-like **FHS**. In the latter case the Θ -function is equal to unity because of the inequality $p_\nu d\sigma^\nu > 0$. Thus, Eq. (2.3) is the *CF* formula [1], but without negative particle numbers that appear for the time-like **FHS**!

2.2. Consideration of the Sun-like Object

As a simple application of the derived formula let us consider the Sun-like object¹ (hereafter “the Sun,” for simplicity), i.e., spherical object with the constant radius R_\odot , $\frac{dR_\odot}{dt} = 0$, with the phase space distribution function of photons $f_\gamma(\frac{p_0}{T})$, which is isotropic in the momentum space and is spherically symmetric in the coordinate one. Here p_0 is the photon energy and $T = T(|\mathbf{R}|)$ is the Sun temperature on its radius $|\mathbf{R}|$.

Then one can easily find the total number of the emitted photons by the *CF* formula. With the help of the following expression for the normal 4-vector $d\sigma_\mu$

$$d\sigma_\mu = \left(0, \frac{\mathbf{R}}{|\mathbf{R}|}\right) dS_\perp dt ,$$

one can trivially perform the integration over momenta in spherical coordinates. Indeed, the number of emitted photons per unit time and per unit area is given by the *CF* formula

$$\frac{dN_\gamma^{CF}}{dtdS_\perp} = \int d^3\mathbf{p} f_\gamma\left(\frac{p_0}{T}\right) \frac{\mathbf{p} \cdot \mathbf{R}}{p_0|\mathbf{R}|} = 2\pi \int dp_0 p_0^2 f_\gamma\left(\frac{p_0}{T}\right) \int_0^\pi d\theta_p \sin(\theta_p) \cos(\theta_p) , \quad (2.4)$$

where we decouple the angular and energy integrations because of the spherical symmetry, choose the angle θ_p between Z -axis and the vector of 3-momentum as one of the spherical angles, and perform a trivial integration over the other spherical angle.

Then one sees that the integration over all possible values of the angle θ_p gives zero:

$$\frac{dN_\gamma^{CF}}{dtdS_\perp} \sim \int_{-1}^{+1} dx x = 0 . \quad (2.5)$$

The calculation of the emitted energy can be done similarly, and again one gets zero for the energy emitted by the Sun. In other words, according to the Cooper-Frye formula all stars are invisible!

In contrast to this, our formula (or Eq. (2.3)) gives the correct answer because in this case the angular integral contains the Θ -function which ensures that only outgoing photons are taken into account:

$$\frac{dN_\gamma^{cut-off}}{dtdS_\perp} \sim \int_0^\pi d\theta_p \sin(\theta_p) \cos(\theta_p) \Theta(\cos(\theta_p)) \sim \int_{-1}^{+1} dx x \Theta(x) \neq 0 . \quad (2.6)$$

¹This nice example was first suggested to one of us, K.A.B., by D.H. Rischke

This is one of the best examples showing an inapplicability of the *CF* -formula for time-like hypersurfaces.

2.3. Other Formulae for the Invariant Spectrum

In this subsection we would like to comment our generalization of the *CF* result for the case of time-like hypersurfaces. An attempt to modify the *CF* formula for time-like FHS was made by Sinyukov in Ref. [13]. This formulation was recently used in Ref. [14].

In the derivation presented in Ref. [13], the decay of a small element of the gas of free particles was considered inside the box with the real wall. This is a suitable treatment for the space-like **FHS** [12]. It appears to be, however, not applicable for the time-like one. The treatment of the box wall in Ref. [12] was just an auxiliary trick in order to simplify the derivation. It means an introduction of the identical element of the gas behind the wall (see Figs. 1–3). Reflection of the particle trajectories from the wall means nothing but only an extension of their trajectories behind the wall and emission of those particles with corresponding momenta from the symmetric element behind the wall. Counting all particles which cross the time-like **FHS** as it was done in work [2], one can easily see where the reflection from the wall gives a wrong contribution.

Let us briefly show this. Suppose that in the rest frame of the small element Δx the phase space distribution function $\phi(\mathbf{x}, t, \mathbf{p})$ is given. Following Ref. [2], we call this frame the rest frame of the gas before the decay, or, in short, the reference frame of the gas (hereafter **RFG**). It is convenient to perform the whole consideration in a two-dimensional case for the sake of simplicity.

The first contribution corresponds to those particles with negative momenta that leave the element Δx without a reflection from the wall *BD* in the meaning of the paper [13] (see Fig.1)

$$\frac{dN_1}{d^2p_\perp dS_\perp} = \phi(\mathbf{x}, t, \mathbf{p}) \Delta x dp^x \Theta(-p^x) . \quad (2.7)$$

where p_\perp is the transverse momentum of the particle.

Then, let us count the number of particles with negative momenta that are reflected from the wall *BD*. This is equivalent to the consideration of the particles from the element $BC = \Delta x$ (see Fig. 2.). For example, the real trajectory of the particle emitted in the point *A* is *AG*, but its reflection from the wall *BD* is *EF*. This corresponds to the particle emitted in the point *C* with the passage *CF*. One can easily find out that this procedure gives the correct result for the low values of momenta, namely $-\frac{AB}{BD} = -\frac{\Delta x}{\Delta t} \leq \frac{p^x}{p^0}$, otherwise it is wrong.

The correct contribution is given by the particles with negative momenta from the element $BH = -\frac{p^x}{p^0} \Delta t$ (Fig. 3.)

$$\frac{dN_2}{d^2p_\perp dS_\perp} = -\phi(\mathbf{x}, t, \mathbf{p}) \frac{p^x}{p^0} \Delta t dp^x \Theta(-p^x) . \quad (2.8)$$

Since the size of the element $BH = -\frac{p^x}{p^0} \Delta t$ depends upon the momentum p^x , then for the high negative momenta $-1 \leq \frac{p^x}{p^0} < -\frac{AB}{BD} = -\frac{\Delta x}{\Delta t}$ the contribution from the element

$CH = -\frac{p^x}{p^0}\Delta t - \Delta x$ (Fig. 3.) cannot be obtained by the reflection procedure used in Ref. [13]. In fact, there is no ‘wall’ in the considered physical problem.

We also have to mention that the energy-momentum tensor derived with the distribution function of Ref. [13] is not symmetric, and hence there are difficulties with the conservation of the angular momentum. This fact makes it impossible to diagonalize the energy-momentum tensor and, therefore, creates a problem in defining the hydrodynamical velocity according to the Landau-Lifshitz prescription.

It is also evident that for the space-like **FHS** such a reflection procedure gives the correct result because the inequality $-1 \leq \frac{p^x}{p^0} < -\frac{AB}{BD} = -\frac{\Delta x}{\Delta t}$ is not fulfilled anymore.

The last contribution comes from the particles with positive momenta p^x from the element $\Delta x - \frac{p}{p_0}\Delta t$. We should stress, however, that those particles will cross the freeze-out hypersurface BD if and only if their velocity $\frac{p^x}{p^0}$ is smaller than the derivative $\frac{\Delta x}{\Delta t}$ of the **FHS** in the $t - x$ plane. Thus, the third term reads as follows (see Fig.4):

$$\frac{dN_3}{d^2p_\perp dS_\perp} = \phi(\mathbf{x}, t, \mathbf{p}) \left[\Delta x - \frac{p^x}{p^0}\Delta t \right] dp^x \Theta(p^x) \Theta\left(\frac{\Delta x}{\Delta t} - \frac{p^x}{p^0}\right). \quad (2.9)$$

In a previous paper [2] it was shown that Eqs. (2.7) – (2.9) can be reduced after some algebra to Eq. (2.3) which we derived at the beginning of this section.

Another example for the momentum distribution function can be found in Ref. [15] and it reads as

$$p_0 \frac{dN}{d^3p} = \phi(\mathbf{x}, t, \mathbf{p}) p_\mu u^\mu u_\nu d\sigma^\nu, \quad (2.10)$$

where u^ν is the 4-vector of the hydrodynamical velocity. It is clear that this formula gives a correct result in the absence of the hydrodynamical motion only.

Thus, we completed the correct generalization of the CF -formula for the case of arbitrary **FHS**.

2.4. Interpretation of the Cut-off formula

Here we would like to give an additional interpretation of the CO -formula for the invariant spectrum. The presence of the Θ -function in the momentum distribution, which cuts off the unphysical contributions of negative particle number, is also important in the coordinate space. This is schematically shown for the 2-dimensional case (when the hypersurfaces become just curves) in Figs. 5 and 6 for convex and concave hypersurfaces, respectively.

Situation with the convex freeze-out hypersurface (see Fig. 5) is evident since no particles can reenter the fluid. Then, for the fixed velocity $v^x = \frac{p^x}{p^0}$ of the particles measured by a detector, the cut-off function gives the integration limits in coordinate space which are obtained from the condition $p^\mu d\sigma_\mu = 0$, or

$$v_\sigma \equiv \frac{dx^*(t)}{dt} = \frac{p^x}{p^0}, \quad (2.11)$$

where the freeze-out hypersurface is given by the equation $x = x^*(t)$. The above equation gives the tangent points of the particle velocity to the freeze-out hypersurface in the t - x plane.

For the concave **FHS** (see Fig. 6.) the freeze-out picture is more complicated because there might be a feedback of the particles emitted earlier. In this case the presence of such a cut-off term $\Theta(p^\mu d\sigma_\mu)$ cannot, of course, exclude reentering particles from the consideration. They are necessary for the balance of the energy and momentum and have (in principle) to be taken into account. In what follows we shall always mean that only particles which were emitted before can reenter the fluid at the concave parts of hypersurface and that, on the other hand, particles of the gas with rescattered momenta are not allowed.

Having this in mind, we can write the distribution function of the gas and each of its moments on the **FHS** denoted by coordinates \mathbf{x}^* for time t as a sum of two terms

$$\phi_g(\mathbf{x}^*, t, \mathbf{p}) = \left(\phi_{g.emit}(\mathbf{x}^*, t, \mathbf{p}) \Theta(p^\mu d\sigma_\mu) + \phi_{g.fback}(\mathbf{x}^*, t, \mathbf{p}) \Theta(-p^\mu d\sigma_\mu) \right), \quad (2.12)$$

$$N_{c.g}^\mu(\mathbf{x}^*, t) = \int \frac{d^3\mathbf{p}}{p_0} p^\mu \left(\phi_{c.g.emit}(\mathbf{x}^*, t, \mathbf{p}) \Theta(p^\mu d\sigma_\mu) + \phi_{c.g.fback}(\mathbf{x}^*, t, \mathbf{p}) \Theta(-p^\mu d\sigma_\mu) \right), \quad (2.13)$$

$$T_g^{\mu\nu}(\mathbf{x}^*, t) = \int \frac{d^3\mathbf{p}}{p_0} p^\mu p^\nu \left(\phi_{g.emit}(\mathbf{x}^*, t, \mathbf{p}) \Theta(p^\mu d\sigma_\mu) + \phi_{g.fback}(\mathbf{x}^*, t, \mathbf{p}) \Theta(-p^\mu d\sigma_\mu) \right), \quad (2.14)$$

where the first terms in the right-hand side correspond to the emitted particles, but the second ones describe the feedback of the previously emitted particles into the fluid, the vector $d\sigma^\mu$ being an external normal to the **FHS** with respect to fluid. We shall also assume that the feedback part vanishes if **FHS** is convex. The notations are as follows: $N_{c.g}^\mu$ is the 4-vector of the current associated with the chemical potential μ_c and $T_g^{\mu\nu}$ is energy-momentum tensor of the gas. Throughout this paper we have also adopted that the distribution functions with the additional subscript "c" denote the difference of the particles and antiparticles contributions, whereas the other ones stand for their sum.

The above expressions show a main difference between the gas of free particles and the usual fluid. One might think of the fluid distribution function cast in the way similar to Eq. (2.12) for some hypersurface with a normal vector $d\sigma_\mu$. Formally it is true, but the meaning is very different. In the element inside of the fluid the particles with positive (negative) product $p^\mu d\sigma_\mu$ are leaving (entering) this element for (from) neighboring element of the fluid. But in the gas of free particles there is no neighboring element on one of the sides, and only the reentering particles are coming from the earlier emitted gas elements which may be quite remote.

Such a situation should always happen at the time-like boundary of the fluid with the vacuum because the traditional hydrodynamics is not applicable at the sharp boundary. Hence, at the boundary one has to introduce the "transition matter" that differs from the fluid. The main difference between the usual fluid and the "transition matter" is due to the cut-off distribution function (2.12) at the boundary with the vacuum. Then one should not allow the fluid to have the boundary with vacuum, but should allow the "transition matter" to exist between fluid and vacuum on the time-like parts of the boundary. Thus we call the emitted particles or the "transition matter" as the gas of free particles in order to distinguish it from and to stress its principal difference with the fluid on the time-like **FHS**.

Eqs. (2.12) – (2.14) are the "compromise" between the hydrodynamics and kinetics, based on the approximation of a sharp boundary. In sections 4.2 and 4.3 we shall consider some justification of this approximation. Hereafter we shall also approximate the distribution functions of the emitted particles $\phi_{g.emit}$ by the equilibrium ones. The latter is consistent with the hydrodynamical approach, which implies also the thermodynamical equilibrium. Then the adopted assumptions do not seem to be very restrictive because in reality the transition region for the time-like **FHS** has to exist, where, we suppose, there is a fast transformation from the fluid into the gas, and due to sufficiently high rate of collisions inside the transition region the distribution function of the gas of free particles may be close to the equilibrium one.

The correct formula for one-particle spectra should be applied to the calculation of the HBT-correlations from the shock-like freeze-out boundary. First it was done by Sinyukov [13] with his one-particle spectrum, and recently the comparison of the Cooper-Frye and Sinyukov's formula was made by Heiselberg [14] under very simple assumptions about **FHS**. The same calculation with the correct formula should give new estimations for the observables.

The calculation of the feedback contribution in a closed form is a very interesting task, but it is, however, beyond the scope of the present work. We would like only to mention some important results with respect to the emission part. In the previous work [2] we gave the general expression for the energy-momentum tensor in the **RFG** and wrote explicitly its components for the massless non-interacting gas for the left hemisphere as an example. In the subsequent work [4] on the similar subject the expressions for the case of massive non-interacting Boltzmann gas were presented. Unfortunately, all their formulae are valid for the left hemisphere only, and are lacking certain terms in the expressions for energy-momentum tensor and the 4-vector of particle number. These results were corrected in part in Ref. [5], but in terms of the newly adopted definition for $\mathcal{K}_n(a, b)$ functions. Therefore, we would like to give in this work a brief technical summary on how to calculate such integrals for the time-like **FHS** which is presented in Appendix A.

3. Conservation Laws on the Surface between Fluid and Gas

In the previous section we discussed the derivation of the correct formula for the momentum spectra on the time-like **FHS**. From the example of the Sun-like object we saw that the Cooper-Frye formula gives wrong results when it is applied for the time-like **FHS**. This property is known for a long time, but the *CF* formula was used so often in the past because it is consistent with the conservation laws of usual relativistic hydrodynamics. However, we think it is so because of the mutual cancelation of two mistakes: first, the fact of the decay of the small element of the fluid on the time-like **FHS** has to affect its further evolution (a recoil problem, hereafter) and, therefore, has to be taken into account into the equations of motion of the fluid, which is ignored in the traditional approach, and, second, for those **FHS** the *CF* formula of the particle spectra gives incorrect result, but in such a way that both mistakes "compensate" each other and hence both are consistent with each other!

We feel, nevertheless, that it is worth to discuss this problem in more details before the formulation of the right approach.

3.1. Energy-Momentum Conservation in the Traditional Hydrodynamics and the *CF* formula

We would like to consider a simple model of freeze-out assuming that the system consists of the fluid and the gas of free particles. The transition region between them is not considered in this paper. Then fluid evolution is described by the energy-momentum and charge conservation equations, or equations of motion in a differential form

$$\partial_\mu T_f^{\mu\nu}(\mathbf{x}, t) = 0, \quad (3.1)$$

$$\partial_\mu N_{c.f}^\mu(\mathbf{x}, t) = 0, \quad (3.2)$$

with the evident notations for the energy-momentum tensor $T_f^{\mu\nu}$ and the charge 4-current $N_{c.f}^\nu$ of the perfect fluid, which are given by the standard formulae

$$T_f^{\mu\nu}(\mathbf{x}, t) = (\varepsilon_f + p_f) u_f^\mu u_f^\nu - p_f g^{\mu\nu}, \quad (3.3)$$

$$N_{c.f}^\nu(\mathbf{x}, t) = n_{c.f} u_f^\nu, \quad (3.4)$$

where p_f , ε_f and $n_{c.f}$ are the pressure, energy and charge density of the fluid, respectively, and the 4-vector of the hydrodynamic velocity is denoted as $u_f^\mu = \frac{1}{\sqrt{1-\mathbf{v}^2}}(1, \mathbf{v})$.

System of these equations has to be completed by the *Additional Conditions* such as

- **i)** the initial conditions given on the initial hypersurface $\Sigma_{in}(\mathbf{x}, t)$;
- **ii)** the equation of state (*EoS*) of the fluid;
- **iii)** the freeze-out criterion, which defines the equation of the **FHS** denoted as $\Sigma_{fr}(\mathbf{x}, t)$.

We shall assume that the freeze-out criterion follows from some requirement beyond the hydrodynamics (for the discussion see, for instance, Refs. [17, 18] and references therein) and we shall use just the simplest choice as an example² to be specific

$$T_g(\mathbf{x}, t) = T^* = Const \Rightarrow \{x^*\} \Leftrightarrow x^{1*} = x^1(x^2, x^3, t), \quad (3.5)$$

i.e., that decay of the gas of free particles happens at the given freeze-out temperature T^* , and the solution of the left Eq. (3.5) exists. In principle the relevant freeze-out criterion should follow from the problem under consideration. For our purpose, however, it is sufficient to assume its existence for the gas of free particles and hence it will define the form of the **FHS**.

We shall denote the latter as x^* in the general case, or as x^{1*} with the corresponding arguments, when it is necessary to distinguish the 4- and 2-dimensions.

For the sake of simplicity we shall also assume that the **FHS** is x_a^* , $a \in \{l, r\}$, and it consists of two single-valued parts which are denoted as "left" and "right" ones (in Fig. 5, for example, the initial hypersurface Σ_{in} is AB , and two parts of the **FHS** one, Σ_{fr} , are AEF and BGF , respectively).

² In the previous paper [2] we also considered such criterion as an example only. It is evident that for any other choice of the freeze-out criterion, the derived equations can be obtained in the similar way.

Let us prove the following *Statement 1*: Conservation laws in the integral form on the **FHS** follow from the differential ones (3.1) – (3.2) and *Additional Conditions* if the Cooper-Frye formula for the spectrum of the emitted particles is used.

First we recall the definition of the 4-momentum from the kinetic theory [16] in terms of the momentum distribution function

$$P^\nu \equiv \int d^3\mathbf{p} \, p^\nu \frac{d^3N}{dp^3} \quad (3.6)$$

Identifying the gas of free particles with the fluid on the **FHS**, one can substitute the Cooper-Frye formula into the previous equation and thus can obtain the four-momentum of the gas of free particles in terms of the fluid energy-momentum tensor

$$P_{g.fr}^\nu = \int \frac{d^3\mathbf{p}}{p^0} p^\nu \int_{\Sigma_{fr}} d\sigma_\mu p^\mu \phi_f \left(\frac{p_\rho u_f^\rho}{T^*} \right) = \int_{\Sigma_{fr}} d\sigma_\mu T_f^{\mu\nu}(x^*, t), \quad (3.7)$$

where we interchanged the order of the integrations and substituted then the expression for the ideal fluid energy-momentum tensor in terms of its distribution function ϕ_f .

Next we integrate the fluid equations of motion (3.1) over the 4-volume of the fluid V_f surrounded by the closed hypersurface $\Sigma_f = \Sigma_{in} \oplus \Sigma_{fr}$ with the help of the Gauss theorem

$$\int_{V_f} d^4x \, \partial_\mu T_f^{\mu\nu}(\mathbf{x}, t) = \oint_{\Sigma_f} d\sigma_\mu T_f^{\mu\nu}(\mathbf{x}, t) = 0, \quad (3.8)$$

transforming it into the integral over the closed hypersurface Σ_f . The last step of the proof is to rewrite the above integral over closed hypersurface as a sum of two over the initial and the final hypersurfaces Σ_{in} and Σ_{fr} , respectively

$$P_{f.in}^\nu \equiv - \int_{\Sigma_{in}} d\sigma_\mu T_f^{\mu\nu}(\mathbf{x}, t) = \int_{\Sigma_{fr}} d\sigma_\mu T_f^{\mu\nu}(x^*, t) = P_{g.fr}^\nu, \quad (3.9)$$

where we have changed the sign in the first equality because $d\sigma_\mu$ is the vector of the external normal with respect to the fluid. The above equation is just the energy-momentum conservation of the fluid in the integral form.

For the conserved current (3.4) the proof is similar.

We have to stress that in such a consideration there is no difference between the fluid and the gas of free particles. Usually this fact is understood implicitly. In the previous section it was shown that the gas of free particles has the cut-off distribution function and, hence, differs from the fluid. Thus, the identification of the fluid and gas for the time-like parts of the **FHS** leads to the incorrect freeze-out which, nevertheless, is formally consistent with the energy-momentum conservation in the traditional hydrodynamics. Due to the same reason, there is no recoil of the particle emission from the time-like parts of the **FHS** onto the fluid evolution. This is seen from the fact that the equation for the **FHS** (see the freeze-out criterion after the identification $T_f = T^*$) does not depend on the expansion of the fluid and therefore it can be formulated independently from the equations of motion, which should not be the case for the time-like hypersurfaces. Moreover, we know that only a part of the particles from the fluid can be emitted from the time-like hypersurfaces and be

detected then, and the rest of particles should reenter the fluid. Both of these facts have to be taken into account.

On the other hand, *Statement 1* suggests also that the traditional hydrodynamics is not consistent with the cut-off formula for the particles emitted from the time-like hypersurface. Thus, we are left with the only possibility to use the modified hydrodynamics together with the correct formula for particle spectra.

3.2. Hydrodynamics with Specific Boundary Conditions and the Cut-off formula

Following previous work [2], we write the energy-momentum tensor of the whole system consisting of the sum of the fluid and the gas of free particles terms given by Eqs. (3.3) and (2.14), respectively. In order to clarify the presentation, we use a very simple example of the **FHS** with left and right boundaries only as it was introduced in the previous subsection (see also Fig. 5 for the 2-dimensional case). Then total energy-momentum tensor and charge current read as

$$T_{tot}^{\mu\nu} = T_f^{\mu\nu} \Theta [x_r^{1*} - x^1] \Theta [x^1 - x_l^{1*}] + T_g^{\mu\nu} \left\{ \Theta [x^1 - x_r^{1*}] + \Theta [x_l^{1*} - x^1] \right\}, \quad (3.10)$$

$$N_{tot}^\mu = N_{c.f}^\mu \Theta [x_r^{1*} - x^1] \Theta [x^1 - x_l^{1*}] + N_{c.g}^\mu \left\{ \Theta [x^1 - x_r^{1*}] + \Theta [x_l^{1*} - x^1] \right\}, \quad (3.11)$$

where the unimportant arguments are dropped for simplicity.

The meaning of this expression is obvious – it states that the whole system consists of the fluid which is "surrounded"³ by the gas of free particles and on the boundary between them, x^{1*} , there is exchange of energy and momentum. When the hydrodynamical evolution is over, there is only a gas of free particles. A similar consideration can be trivially done for the conserved currents, but we do not repeat it just to reduce the complications for the reader. In what follows it is assumed that the derivatives of the fluid and gas hydrodynamical quantities are continuous and finite everywhere in the corresponding domain including the **FHS**.

The equations of motion of the whole system are the energy-momentum and charge conservation laws in the differential form:

$$\partial_\mu T_{tot}^{\mu\nu} = 0, \quad (3.12)$$

$$\partial_\mu N_{tot}^\mu = 0. \quad (3.13)$$

Let us study *the boundary conditions* first.

Integrating equations (3.12) over the 4-volume around the vicinity of the **FHS**, namely $x^1 \in [x^{1*} - \delta^2; x^{1*} + \delta^2]$ and the corresponding finite limits for the other coordinates (see parts *BDE* and *BCE*, respectively, on Fig. 7), and applying the Gauss theorem as it was done in previous subsection, one obtains the energy-momentum conservation on the part $\tilde{\Sigma}_{fr}$ of the **FHS**

³ For the time-like parts of the **FHS** it is true, because there is a spatial separation between fluid and gas. But for the space-like ones they are separated in time.

$$\int_{\tilde{\Sigma}_{fr}-\delta^2} d\sigma_\mu T_{tot}^{\mu\nu} = \int_{\tilde{\Sigma}_{fr}+\delta^2} d\sigma_\mu T_{tot}^{\mu\nu} , \quad (3.14)$$

where in both sides of the equality $d\sigma_\mu$ is the external normal with respect to the fluid.

Then in the limit $\delta \rightarrow 0$ for the energy-momentum tensor defined by the Eqs. (3.10), one easily gets the conservation laws for both the energy-momentum and the charge on the **FHS** as follows

$$d\sigma_\mu T_f^{\mu\nu} \Big|_{x^{1*}} = d\sigma_\mu T_g^{\mu\nu} \Big|_{x^{1*}} , \quad (3.15)$$

$$d\sigma_\mu N_{c.f}^\mu \Big|_{x^{1*}} = d\sigma_\mu N_{c.g}^\mu \Big|_{x^{1*}} , \quad (3.16)$$

or, writing it explicitly,

$$d\sigma_\mu \int \frac{d^3\mathbf{p}}{p^0} p^\mu p^\nu \phi_f \left(\frac{p_\rho u_f^\rho}{T} \right) \Big|_{x^{1*}} = \quad (3.17)$$

$$d\sigma_\mu \int \frac{d^3\mathbf{p}}{p_0} p^\mu p^\nu \left(\phi_{g.emit}(\mathbf{p}) \Theta(p^\mu d\sigma_\mu) + \phi_{g.fback}(\mathbf{p}) \Theta(-p^\mu d\sigma_\mu) \right) \Big|_{x^{1*}} ,$$

$$d\sigma_\mu \int \frac{d^3\mathbf{p}}{p^0} p^\mu \phi_{c.f} \left(\frac{p_\rho u_f^\rho}{T} \right) \Big|_{x^{1*}} = \quad (3.18)$$

$$d\sigma_\mu \int \frac{d^3\mathbf{p}}{p_0} p^\mu \left(\phi_{c.g.emit}(\mathbf{p}) \Theta(p^\mu d\sigma_\mu) + \phi_{c.g.fback}(\mathbf{p}) \Theta(-p^\mu d\sigma_\mu) \right) \Big|_{x^{1*}} ,$$

where we have dropped the space-time dependence in the distribution functions above for the sake of convenience.

From the expressions (3.17) and (3.18) it is clear that there are two distinct cases, namely **(i)** when the distribution function of the gas of free particles coincides with that one of the fluid (or the *EoS* is the same for both) and **(ii)** when they are entirely different. In the latter case there is no criterion which equation of state is preferable. This should be defined by the physics of the considered task. We believe that the full solution of the problem can be given within the kinetic approach only. However, since we adopted the hydrodynamical approach which implies also the thermodynamical equilibrium, in what follows it is assumed that at least the emission part is described by the equilibrium distribution function.

Statement 2: If the fluid and the gas have same *EoS*, then on the space-like parts of the **FHS** their distribution functions are identical, on the convex parts of the time-like **FHS** there exists a *freeze-out shock* transition, and on the concave ones there is a *parametric freeze-out shock* transition (see below).

Let us demonstrate this. Indeed, a simple analysis shows that for the case **(i)** there are the following possibilities:

(i.a) if $\Theta(p^\mu d\sigma_\mu) = 1$ for $\forall \mathbf{p}$, i.e., on the *space-like* parts of the **FHS** or on the light cone, there is no feedback and then there is only a trivial solution given by the *CF*-formula $\phi_f \left(\frac{p_\rho u_f^\rho}{T} \right) \Big|_{x^{1*}} = \phi_{g.emit}(\mathbf{p}) \Big|_{x^{1*}}$ with the fluid temperature being equal to the freeze-out one. Note that the discontinuity through such a hypersurface (or the time-like shocks, as the authors of Ref. [19] call it) is impossible in this case as it was shown in Gorenstein's work [20].

(i.b) for the *convex time-like* parts of the **FHS** the feedback term vanishes as we discussed before (see also Fig. 5) and hence there is a *freeze-out shock* between the fluid and the gas of free particles (actually, the same fluid, but with the freeze-out temperature and *CO* distribution function; for details see later). It is reasonable to call it this way because the pressure and the energy density of the gas of free particles are not the usual ones, but have extra dependence on the parameters of the **FHS**. The hydrodynamic parameters of the fluid should be found from the conservation laws on the discontinuity

$$d\sigma_\mu \int \frac{d^3\mathbf{p}}{p_0} p^\mu p^\nu \phi_f \left(\frac{p_\rho u_f^\rho}{T} \right) \Big|_{x^{1*}} = d\sigma_\mu \int \frac{d^3\mathbf{p}}{p_0} p^\mu p^\nu \phi_f \left(\frac{p_\rho u'^\rho}{T^*} \right) \Theta(p^\mu d\sigma_\mu) \Big|_{x^{1*}}, \quad (3.19)$$

$$d\sigma_\mu \int \frac{d^3\mathbf{p}}{p_0} p^\mu \phi_{c.f} \left(\frac{p_\rho u_f^\rho}{T} \right) \Big|_{x^{1*}} = d\sigma_\mu \int \frac{d^3\mathbf{p}}{p_0} p^\mu \phi_{c.f} \left(\frac{p_\rho u'^\rho}{T^*} \right) \Theta(p^\mu d\sigma_\mu) \Big|_{x^{1*}}. \quad (3.20)$$

(i.c) for the *concave time-like* parts of the **FHS** the feedback term does not vanish (see also Fig. 6) and hence it is a new type of shock between the fluid and the gas of free particles which can be called a *parametric freeze-out shock* with the contribution of the feedback particles being a parameter in the general meaning. In this case the equations on the discontinuity, i.e. Eqs. (3.17) and the similar one for the conserved charge, should be studied. However, it requires the knowledge of the expressions for the feedback particles emitted from arbitrary hypersurface which is outside the scope of this paper. In addition, the assumption of the instant thermalization of the feedback particles has to be investigated, but this is far beyond the hydrodynamical approach.

Statement 3: If the fluid and the gas have entirely different *EoS*, then on the space-like parts of the **FHS** time-like shocks [19] can exist, on the convex parts of the time-like **FHS** there is a *freeze-out shock* transition, and on the concave ones there is a *parametric freeze-out shock*.

The proof is similar to the previous consideration. If the fluid and the gas *EoS* are different, [case (ii)], one has the following options:

(ii.a) if $\Theta(p^\mu d\sigma_\mu) = 1$ for $\forall \mathbf{p}$, i.e., on the *space-like* parts of the **FHS** or on the light cone, again the feedback contribution is zero, but there is no trivial solution in contrast to the case (i.a). And the time-like shocks [19] are possible as it was discussed in Ref. [20]. They are defined by the following conservation laws

$$d\sigma_\mu \int \frac{d^3\mathbf{p}}{p_0} p^\mu p^\nu \phi_f \left(\frac{p_\rho u_f^\rho}{T} \right) \Big|_{x^{1*}} = d\sigma_\mu \int \frac{d^3\mathbf{p}}{p_0} p^\mu p^\nu \phi_{g.emit} \left(\frac{p_\rho u'^\rho}{T^*} \right) \Big|_{x^{1*}}, \quad (3.21)$$

$$d\sigma_\mu \int \frac{d^3\mathbf{p}}{p_0} p^\mu \phi_{c.f} \left(\frac{p_\rho u_f^\rho}{T} \right) \Big|_{x^{1*}} = d\sigma_\mu \int \frac{d^3\mathbf{p}}{p_0} p^\mu \phi_{c.g.emit} \left(\frac{p_\rho u'^\rho}{T^*} \right) \Big|_{x^{1*}}, \quad (3.22)$$

where the equilibrium distribution functions for the gas of free particles $\phi_{g.emit} \left(\frac{p_\rho u'^\rho}{T^*} \right)$ and $\phi_{c.g.emit} \left(\frac{p_\rho u'^\rho}{T^*} \right)$ are used.

More recent results on this subject can be found in Refs. [21, 22]. However, this kind of solutions can probably exist only under very special conditions, namely for the supercooled quark-gluon plasma. It is difficult to imagine the reason for the fluid near the freeze-out state (when all interactions between particles are very weak) to convert suddenly without any cause into the gas of free particles with entirely different *EoS*.

(ii.b) for the *convex time-like* parts of the **FHS** the feedback term again vanishes and therefore there is a shock transition between the fluid and the gas of free particles, but now fluid and gas being completely different states! Outside the fluid, the gas should be described by the *CO* distribution function. The hydrodynamic parameters of the fluid then are defined by the conservation laws on the discontinuity

$$d\sigma_\mu \int \frac{d^3\mathbf{p}}{p_0} p^\mu p^\nu \phi_f \left(\frac{p_\rho u_f^\rho}{T} \right) \Big|_{x^{1*}} = d\sigma_\mu \int \frac{d^3\mathbf{p}}{p_0} p^\mu p^\nu \phi_{g.emit} \left(\frac{p_\rho u'^\rho}{T^*} \right) \Theta(p^\mu d\sigma_\mu) \Big|_{x^{1*}}, \quad (3.23)$$

$$d\sigma_\mu \int \frac{d^3\mathbf{p}}{p_0} p^\mu \phi_{c.f} \left(\frac{p_\rho u_f^\rho}{T} \right) \Big|_{x^{1*}} = d\sigma_\mu \int \frac{d^3\mathbf{p}}{p_0} p^\mu \phi_{c.g.emit} \left(\frac{p_\rho u'^\rho}{T^*} \right) \Theta(p^\mu d\sigma_\mu) \Big|_{x^{1*}}. \quad (3.24)$$

(ii.c) for the *concave time-like* parts of the **FHS** the feedback term does not vanish and therefore the *parametric freeze-out shock* introduced above should exist. This kind of the shock solution should satisfy the conservation laws in the most general form of Eqs. (3.17) and (3.18). However, the detailed consideration of that solution would lead us too far off the main topic of this work.

Thus, we have given the full analysis of all possible boundary conditions. The conservation laws equations discussed above have to be solved together with the equations of motion for the fluid in order to find out the **FHS**. Next subsection is devoted to the derivation of the equations of motion of the fluid alone and their consistency with the boundary conditions.

Note that the conservation laws on the boundary between the fluid and the gas of free particles discussed in [4] (see Eqs. (6), (7) therein) were just postulated and are not related to any hydrodynamical evolution of the fluid at all. Moreover, those equations, in the integral form as presented in Ref. [4], cannot be used to solve them together with the hydrodynamical equations of the fluid. In this sense those equations are *ad hoc* ones, and thus of a rather restricted use.

To summarize, we have presented above the full and complete analysis of the possible boundary conditions, following the original idea of the paper [2]. The derived formalism allows us not only to find out the new class of the shock transitions, i.e. the *parametric freeze-out shock*, but also to formulate the hydrodynamical approach in the way consistent with the emission of the particles from an arbitrary **FHS**.

3.3. Consistency Theorem

Let us study the consistence of the equations of motion for the whole system with the boundary conditions derived in the previous subsection. For our present purpose the explicit form of the energy-momentum tensor and the conserved 4-current for the gas of free particles is not important, but we should remember that those quantities have to satisfy the conservation laws in the differential form, i.e.,

$$\partial_\mu T_g^{\mu\nu} = 0, \quad (3.25)$$

$$\partial_\mu N_{c.g}^\mu = 0 \quad (3.26)$$

in the domain where the gas of free particles exists.

Exploiting this fact, we can rewrite the original conservation laws (3.12) and (3.13) as equations of motion of the fluid alone

$$\partial_\mu \left\{ \Theta \left[x_r^{1*} - x^1 \right] \Theta \left[x^1 - x_l^{1*} \right] T_f^{\mu\nu} \right\} = - \sum_{a \in l, r} \delta \left(x_a^{1*} - x^1 \right) n_\mu(f_a) \times \quad (3.27)$$

$$\int \frac{d^3 \mathbf{p}}{p_0} p^\mu p^\nu \left(\phi_{g.emit}(\mathbf{p}) \Theta(p^\mu n_\mu(f_a)) + \phi_{g.fback}(\mathbf{p}) \Theta(-p^\mu n_\mu(f_a)) \right) \Big|_{x_a^{1*}},$$

$$\partial_\mu \left\{ \Theta \left[x_r^{1*} - x^1 \right] \Theta \left[x^1 - x_l^{1*} \right] N_{c.f}^\mu \right\} = - \sum_{a \in l, r} \delta \left(x_a^{1*} - x^1 \right) n_\mu(f_a) \times \quad (3.28)$$

$$\int \frac{d^3 \mathbf{p}}{p_0} p^\mu \left(\phi_{c.g.emit}(\mathbf{p}) \Theta(p^\mu n_\mu(f_a)) + \phi_{c.g.fback}(\mathbf{p}) \Theta(-p^\mu n_\mu(f_a)) \right) \Big|_{x_a^{1*}},$$

with $n_\mu(f_a)$ being the external normal 4-vector with respect to the fluid and being defined as follows

$$n_\mu(f_a) = \left(-\partial_0 x_a^{1*}; 1; -\partial_2 x_a^{1*}; -\partial_3 x_a^{1*} \right) \begin{cases} -1, & a = l, \\ +1, & a = r, \end{cases} \quad (3.29)$$

i.e., having the positive projection on the X-axis for the right hemisphere and the negative projection for the left one (see also Appendix A and Fig. 8.).

Equations (3.27) and (3.28) look like the hydrodynamical equations of motion with the source terms, the first of them describes *the loss* of the energy-momentum flux through the **FHS** due to emission of the "frozen" particles and the second one is responsible for *the gain* by the reentering particles at the concave parts of the time-like **FHS**. It is evident because the Θ -function in the first term takes into account only positive values of the product $p^\mu n_\mu(f_a) > 0$, while the second one is nonvanishing only for its negative values, i.e., $p^\mu n_\mu(f_a) < 0$.

However, it is easy to show that there are no source terms in fact because they disappear due to the boundary conditions studied in the previous subsection! Indeed, taking derivatives of the remaining Θ -functions in the left hand side of Eqs. (3.27) and (3.28), one obtains source-like terms with the fluid energy-momentum tensor and with the conserved 4-current, respectively,

$$\Theta \left[x_r^{1*} - x^1 \right] \Theta \left[x^1 - x_l^{1*} \right] \partial_\mu T_f^{\mu\nu} - \sum_{a \in l, r} \delta \left(x_a^{1*} - x^1 \right) n_\mu(f_a) T_f^{\mu\nu} \Big|_{x_a^{1*}} = - \sum_{a \in l, r} \delta \left(x_a^{1*} - x^1 \right) \times$$

$$n_\mu(f_a) \int \frac{d^3 \mathbf{p}}{p_0} p^\mu p^\nu \left(\phi_{g.emit}(\mathbf{p}) \Theta(p^\mu n_\mu(f_a)) + \phi_{g.fback}(\mathbf{p}) \Theta(-p^\mu n_\mu(f_a)) \right) \Big|_{x_a^{1*}}, \quad (3.30)$$

$$\Theta \left[x_r^{1*} - x^1 \right] \Theta \left[x^1 - x_l^{1*} \right] \partial_\mu N_{c.f}^\mu - \sum_{a \in l, r} \delta \left(x_a^{1*} - x^1 \right) n_\mu(f_a) N_{c.f}^\mu \Big|_{x_a^{1*}} = - \sum_{a \in l, r} \delta \left(x_a^{1*} - x^1 \right) \times$$

$$n_\mu(f_a) \int \frac{d^3 \mathbf{p}}{p_0} p^\mu \left(\phi_{c.g.emit}(\mathbf{p}) \Theta(p^\mu n_\mu(f_a)) + \phi_{c.g.fback}(\mathbf{p}) \Theta(-p^\mu n_\mu(f_a)) \right) \Big|_{x_a^{1*}}, \quad (3.31)$$

which automatically cancel the corresponding contributions from the gas of free particles due to the general boundary conditions (or conservation laws) on the **FHS** given by Eqs. (3.17) and (3.18). Then the equations of motion of the fluid acquire the familiar form

$$\Theta \left[x_r^{1*} - x^1 \right] \Theta \left[x^1 - x_l^{1*} \right] \partial_\mu T_f^{\mu\nu} = 0, \quad (3.32)$$

$$\Theta \left[x_r^{1*} - x^1 \right] \Theta \left[x^1 - x_l^{1*} \right] \partial_\mu N_{c.f}^\mu = 0. \quad (3.33)$$

These equations complete the proof of the following *Theorem 1*: If the gas of free particles with the emission part defined by cut-off distribution and with known feedback part is described by the equations of motion (3.25) and (3.26), then the equations of motion (3.12) and (3.13) of the whole system consisting of the perfect fluid and the gas of free particles split up into the system of the fluid equations of motion (3.32) and (3.33), and of the boundary conditions in the general form of Eqs. (3.17) and (3.18) on the **FHS**.

It is necessary to stress that Eqs. (3.32) and (3.33) have only one, but a crucial point of difference with the equations of motion of traditional hydrodynamics, although they look very similar. Evidently, a solution of the traditional hydrodynamic equations under the given *Additional Conditions* is also a solution of Eqs. (3.32) and (3.33). Moreover, the solution of the latter has to be understood this way. However, the Θ -functions in front of the Eqs. (3.32) and (3.33) ensure that the fluid exists inside of the **FHS** (i.e., in the fluid domain) defined by the freeze-out criterion for the gas. Thus, the effect of the particle emission is implicitly taken into account into the equations of motion of the fluid alone, and is expressed explicitly in the boundary conditions between the fluid and the gas.

Theorem 1 leads also to the fact that inclusion of the source terms which are proportional to the δ -function on the **FHS** into the equations of motion of the fluid will always require their vanishing, unless the derivatives of the fluid energy-momentum tensor or the gas one contain similar singularities. This is a very important consequence of the *Theorem 1* which is easy to understand recalling the fact that singularities like δ -function and its derivatives (if they appear) are of different order and should be considered independently. Therefore, if these singularities enter the same equality, then singularities of the same order will generate independent equations.

Now we are in a position to consider the consistency problem of the energy-momentum and the current conservation of the fluid given by Eqs. (3.12) and (3.13) with the emission of the "frozen" particles of the gas described by the *CO*-distribution function like it was shown for the usual hydrodynamics and the *CF*-formula.

Theorem 2: Energy, momentum and charge of the initial fluid together with the corresponding contribution of the reentering particles from the concave parts of the **FHS** are equal to the corresponding quantities of the emitted from this hypersurface free particles with the cut-off momentum distribution function, i.e., those quantities are conserved.

Proof. First we apply the results of the *Statement 1* to the derived equations (3.32) and (3.33) of the fluid evolution. Evidently one can use it. Then we obtain an integral form of the energy-momentum conservation, for instance, for the fluid alone, which is identical to Eqs. (3.9)

$$P_{f.in}^\nu \equiv - \int_{\Sigma_{in}} d\sigma_\mu T_f^{\mu\nu}(\mathbf{x}, t) = \int_{\Sigma_{fr}} d\sigma_\mu T_f^{\mu\nu}(x^*, t).$$

Due to the boundary conditions (3.17) on the **FHS** which are just conservation laws on the boundary between fluid and gas, one obtains the following equality

$$\begin{aligned} & - \int_{\Sigma_{in}} d\sigma_\mu T_f^{\mu\nu}(\mathbf{x}, t) - \int_{\Sigma_{fr}} d\sigma_\mu \int \frac{d^3\mathbf{p}}{p_0} p^\mu p^\nu \phi_{g.fback}(\mathbf{p}) \Theta(-p^\mu d\sigma_\mu) \Big|_{x^{1*}} = \\ & \int_{\Sigma_{fr}} d\sigma_\mu \int \frac{d^3\mathbf{p}}{p_0} p^\mu p^\nu \phi_{g.emit}(\mathbf{p}) \Theta(p^\mu d\sigma_\mu) \Big|_{x^{1*}}, \end{aligned} \quad (3.34)$$

which actually states the energy-momentum conservation in the integral form and also shows that the sum of the energy-momentum of the fluid and the particles reentering the fluid during its evolution are exactly transformed into the energy-momentum of the emitted particles with the correct distribution function!

A proof for the conserved current can be obtained in a similar way.

4. Equations of the Freeze-out Hypersurface

These equations for the time-like parts of the **FHS** follow from the boundary conditions (3.17) and (3.18). They have to be solved together with the solution of the usual hydrodynamical equations of the fluid and allow us to find the **FHS** as a solution of the system of the coupled partial differential equations. It is worth to make a close investigation of these equations due to necessity of further applications in both academic and numeric aspects.

As a good example of applying the derived scheme, we consider an important problem of relativistic hydrodynamics – the freeze-out of the simple wave.

4.1. Freeze-out Calculus: General scheme

General expressions for the corresponding shock solution on the boundary can be obtained from Eqs. (3.17) and (3.18) by the substitution of the formula (3.29) for the normal vector in terms of the derivatives of the **FHS**. In what follows we shall neglect the contribution of the feedback particles in order to simplify consideration. Then we shall not distinguish the *freeze-out* and the *parametric freeze-out shocks*.

Let us obtain now the full system of all necessary equations. First, we shall suppose that the **FHS** exist and then we derive its equations. For this it is convenient to evaluate the boundary conditions in the rest frame of the fluid (hereafter **RFF**) before the freeze-out shock, where the energy-momentum tensor of the fluid is diagonal. We choose the local coordinate system with one of the axes, let it be the X -axis, being parallel to the normal 3-vector. The latter then is reduced to

$$n_\mu(f_a) = \left(-\partial_0 x_a^{1*}; 1; 0; 0 \right) \begin{cases} -1, & a = l, \\ +1, & a = r. \end{cases} \quad (4.1)$$

Next, we mention that the velocity of the gas of free particles cannot have nonzero projection on any tangential direction to the normal 3-vector in this frame. It can be shown directly by manipulation with formulae, but it is evident from the simple reason that an oblique shock (see corresponding chapter in Ref. [23]) should have continuous tangent velocities on the both sides of shock. Then it follows for the **RFF** that the gas velocity can be parallel or antiparallel to the normal 3-vector only.

This statement is valid for the **RFG** as well, and the expression for the normal 4-vector in this frame is evidently similar to the Eq. (4.1). In order to distinguish them, hereafter we shall write the corresponding subscript.

Boundary conditions (3.17) and (3.18) have a simplest representation in the **RFG** since the moments of the *CO* distribution function do not look too much complicated in this frame:

$$T_f^{X0}(v_{f\mathbf{G}}) - T_f^{00}(v_{f\mathbf{G}})v_{s\mathbf{G}} = T_g^{X0}(v_{s\mathbf{G}}) - T_g^{00}(v_{s\mathbf{G}})v_{s\mathbf{G}} , \quad (4.2)$$

$$T_f^{XX}(v_{f\mathbf{G}}) - T_f^{X0}(v_{f\mathbf{G}})v_{s\mathbf{G}} = T_g^{XX}(v_{s\mathbf{G}}) - T_g^{X0}(v_{s\mathbf{G}})v_{s\mathbf{G}} , \quad (4.3)$$

$$N_{c.f}^X(v_{f\mathbf{G}}) - N_{c.f}^0(v_{f\mathbf{G}})v_{s\mathbf{G}} = N_{c.g}^X(v_{s\mathbf{G}}) - N_{c.g}^0(v_{s\mathbf{G}})v_{s\mathbf{G}} , \quad (4.4)$$

where the energy-momentum tensor and 4-current of the fluid have standard form of Eqs. (3.3) and (3.4), respectively, with the 3-velocity $v_{f\mathbf{G}}$. In the above formula the velocity $v_{s\mathbf{G}} = \partial_0 x^{1*}$ is the time derivative of the freeze-out hypersurface in the **RFG**, or velocity of the shock in this frame. Note, however, that in contrast to the usual shocks the above equations look like the conservation laws in the arbitrary Lorentz frame (not the rest frame of the gas!) where the nondiagonal components of the energy-momentum tensor are nonzero.

Introducing the following notations for the "effective" energy density, pressure and charge density of the gas of free particles

$$\tilde{\varepsilon}_g(v_{s\mathbf{G}}) = T_g^{00}(v_{s\mathbf{G}}) - T_g^{X0}(v_{s\mathbf{G}})v_{s\mathbf{G}}^{-1} , \quad (4.5)$$

$$\tilde{p}_g(v_{s\mathbf{G}}) = T_g^{XX}(v_{s\mathbf{G}}) - T_g^{X0}(v_{s\mathbf{G}})v_{s\mathbf{G}} , \quad (4.6)$$

$$\tilde{n}_{c.g}(v_{s\mathbf{G}}) = N_{c.g}^0(v_{s\mathbf{G}}) - N_{c.g}^X(v_{s\mathbf{G}})v_{s\mathbf{G}}^{-1} , \quad (4.7)$$

one can transform the right-hand side of Eqs. (4.2) – (4.4) to the familiar expressions of the relativistic shocks [23] written in the rest frame of the matter behind the discontinuity. In contrast to the usual shock, however, Eqs. (4.2) – (4.4) do not form the closed system together with the *EoS*, but they are dynamical equations for the trajectory of freeze-out. Then velocities of fluid and shock in the **RFG** can be expressed by the standard relations

$$v_{f\mathbf{G}}^2 = \frac{(\varepsilon_f - \tilde{\varepsilon}_g(v_{s\mathbf{G}}))(p_f - \tilde{p}_g(v_{s\mathbf{G}}))}{(\varepsilon_f + \tilde{p}_g(v_{s\mathbf{G}}))(p_f + \tilde{\varepsilon}_g(v_{s\mathbf{G}}))} , \quad (4.8)$$

$$v_{s\mathbf{G}}^2 = \frac{(p_f - \tilde{p}_g(v_{s\mathbf{G}}))(\varepsilon_f + \tilde{p}_g(v_{s\mathbf{G}}))}{(\varepsilon_f - \tilde{\varepsilon}_g(v_{s\mathbf{G}}))(p_f + \tilde{\varepsilon}_g(v_{s\mathbf{G}}))} . \quad (4.9)$$

Now it is clearly seen that last relation is a transcendental equation for the $v_{s\mathbf{G}}$ – velocity of the **FHS** in the **RFG**. It cannot be solved analytically for an arbitrary *EoS*. In addition we have to transform it to the fluid rest frame in order to complete it with the solution of the hydrodynamical equations for the fluid

$$v_{s\mathbf{F}} = \frac{v_{s\mathbf{G}} - v_{f\mathbf{G}}}{1 - v_{s\mathbf{G}} v_{f\mathbf{G}}} . \quad (4.10)$$

Fortunately, there exist a simple expression for the square of this velocity, namely

$$v_{s\mathbf{F}}^2 = \frac{(p_f - \tilde{p}_g(v_{s\mathbf{G}}))(p_f + \tilde{\varepsilon}_g(v_{s\mathbf{G}}))}{(\varepsilon_f - \tilde{\varepsilon}_g(v_{s\mathbf{G}}))(\varepsilon_f + \tilde{p}_g(v_{s\mathbf{G}}))} , \quad (4.11)$$

which can be easily understood if one recalls that in the theory of relativistic shocks the above relation has a meaning of the shock velocity in the rest frame of the initial fluid.

Equation for the charge density becomes

$$n_{c.f}^2 = \tilde{n}_{c.g}^2(v_{s\mathbf{G}}) \frac{(p_f + \varepsilon_f)}{(p_f + \tilde{\varepsilon}_g(v_{s\mathbf{G}}))} \cdot \frac{(\tilde{p}_g(v_{s\mathbf{G}}) + \varepsilon_f)}{(\tilde{p}_g(v_{s\mathbf{G}}) + \tilde{\varepsilon}_g(v_{s\mathbf{G}}))}. \quad (4.12)$$

Evidently, it can be cast in the form of usual Taub adiabat [24]. Together with equations for the shock velocity in **RFG** and **RFF**, Eqs. (4.9) and (4.11) respectively, it forms a complete system of boundary conditions.

Let us discuss the boundary conditions and how to solve these equations together with the hydrodynamic equations for the fluid. In what follows we shall assume that the solution of hydrodynamical equations (3.32) and (3.33) for the fluid is known in the center of mass frame (hereafter **C.M.**) for the whole available space-time volume, and hydrodynamical quantities, for instance, T_f, μ_f and $u_{f\mathbf{C.M.}}^\nu = (1; \mathbf{v}_{f\mathbf{C.M.}}) / \sqrt{1 - \mathbf{v}_{f\mathbf{C.M.}}^2}$, are given in each space-time point $X_{f\mathbf{C.M.}}^\nu$ with $\nu \in \{0; 1; 2; 3\}$. Having this solution, one can map it into the **RFF** by the Lorentz transformation

$$X_{\mathbf{F}}^i = \frac{1}{\sqrt{1 - \mathbf{v}_{f\mathbf{C.M.}}^2}} \left(X_{\mathbf{C.M.}}^i - X_{\mathbf{C.M.}}^0 v_{f\mathbf{C.M.}}^i \right), \quad (4.13)$$

$$X_{\mathbf{F}}^0 = \frac{1}{\sqrt{1 - \mathbf{v}_{f\mathbf{C.M.}}^2}} \left(X_{\mathbf{C.M.}}^0 - X_{\mathbf{C.M.}}^i v_{f\mathbf{C.M.}}^i \right), \quad (4.14)$$

with $i \in \{1; 2; 3\}$. Then all hydrodynamical quantities are defined in the **RFF**.

After this transformation into the **RFF**, the obtained coordinate system does not necessarily coincide with the original system that was used for the derivation of the shock-like expressions (4.9), (4.11) and (4.12) on the boundary between fluid and gas. Suppose that in the **RFF** the 3-vector of the shock velocity $v_{s\mathbf{F}}$ is described by the standard set of spherical coordinates with the angles ϕ and θ . Exploiting this fact, one can derive differential equation for the **FHS** in **RFF** as follows.

First, it is necessary to project the shock velocity $\vec{v}_{s\mathbf{F}}$ on the coordinate axes of the **RFF**. The shock velocity was assumed to be parallel to the X' -axis of the original coordinate system. Using the spherical coordinates of the **RFF** obtained from the **C.M.** frame, one can find the projections of the shock velocity $\vec{v}_{s\mathbf{F}}$ on the coordinate axes as follows

$$\left. \frac{\partial X^1}{\partial X^0} \right|_{s\mathbf{F}} = \{\vec{v}_{s\mathbf{F}}\}^1 = v_{s\mathbf{F}} \sin \theta \cos \phi, \quad (4.15)$$

$$\left. \frac{\partial X^2}{\partial X^0} \right|_{s\mathbf{F}} = \{\vec{v}_{s\mathbf{F}}\}^2 = v_{s\mathbf{F}} \sin \theta \sin \phi, \quad (4.16)$$

$$\left. \frac{\partial X^3}{\partial X^0} \right|_{s\mathbf{F}} = \{\vec{v}_{s\mathbf{F}}\}^3 = v_{s\mathbf{F}} \cos \theta, \quad (4.17)$$

where superscripts denote respective coordinates. The system obtained above can be used in numerical studies of the **FHS** for the unknown function $X^{*0}(X^1; X^2; X^3)$.

Next, we reexpress it for the unknown functions $X^{*1}(X^2; X^3; X^0)$ as the derivatives of the implicit function:

$$\left. \frac{\partial X^{*1}}{\partial X^0} \right|_{s\mathbf{F}} = v_{s\mathbf{F}} \sin \theta \cos \phi, \quad (4.18)$$

$$\left. \frac{\partial X^{*1}}{\partial X^2} \right|_{s\mathbf{F}} = -\frac{1}{\tan \phi} , \quad (4.19)$$

$$\left. \frac{\partial X^{*1}}{\partial X^3} \right|_{s\mathbf{F}} = -\tan \theta \cos \phi , \quad (4.20)$$

This is a desired system of equations for $X^{*1}(X^2; X^3; X^0)$ which can be employed in numerical investigations.

Finally, one can exclude the spherical angles by the simple manipulations and find the following equation instead of the system above

$$\left. \frac{\partial X^{*1}}{\partial X^0} \right|_{s\mathbf{F}}^2 \left[1 + \left. \frac{\partial X^{*1}}{\partial X^3} \right|_{s\mathbf{F}}^2 \left(1 + \left. \frac{\partial X^{*1}}{\partial X^2} \right|_{s\mathbf{F}}^{-2} \right) \right] = v_{s\mathbf{F}}^2 \left. \frac{\partial X^{*1}}{\partial X^3} \right|_{s\mathbf{F}}^2 , \quad (4.21)$$

which has to be solved along with equations (4.9) , (4.11) and (4.12) obtained from the boundary conditions, and with the solution of the hydrodynamic equations for the fluid which is mapped into the **RFF**.

Let us now show how to do this. For that we rewrite all necessary equations in a more convenient form using both EqS

$$F_{nf}(T_f, \mu_f, \mu_g, v_{s\mathbf{G}}) \equiv \frac{n_{c,f}^2}{\tilde{n}_{c,g}^2(v_{s\mathbf{G}})} - \frac{(p_f + \varepsilon_f)}{(p_f + \tilde{\varepsilon}_g(v_{s\mathbf{G}}))} \cdot \frac{(\tilde{p}_g(v_{s\mathbf{G}}) + \varepsilon_f)}{(\tilde{p}_g(v_{s\mathbf{G}}) + \tilde{\varepsilon}_g(v_{s\mathbf{G}}))} = 0 , \quad (4.22)$$

$$F_{v_{s\mathbf{F}}}(T_f, \mu_f, \mu_g, v_{s\mathbf{G}}, v_{s\mathbf{F}}) \equiv v_{s\mathbf{F}}^2 - \frac{(p_f - \tilde{p}_g(v_{s\mathbf{G}}))(p_f + \tilde{\varepsilon}_g(v_{s\mathbf{G}}))}{(\varepsilon_f - \tilde{\varepsilon}_g(v_{s\mathbf{G}}))(\varepsilon_f + \tilde{p}_g(v_{s\mathbf{G}}))} = 0 , \quad (4.23)$$

$$F_{v_{s\mathbf{G}}}(T_f, \mu_f, \mu_g, v_{s\mathbf{G}}) \equiv v_{s\mathbf{G}}^2 - \frac{(p_f - \tilde{p}_g(v_{s\mathbf{G}}))(\varepsilon_f + \tilde{p}_g(v_{s\mathbf{G}}))}{(\varepsilon_f - \tilde{\varepsilon}_g(v_{s\mathbf{G}}))(p_f + \tilde{\varepsilon}_g(v_{s\mathbf{G}}))} = 0 , \quad (4.24)$$

where the most important arguments are shown.

The above derivation can be formulated as the following *Theorem 3*: If solutions of the transcendental Eqs. (4.22) – (4.24) exist, then **FHS** on the time-like boundary between fluid and gas is described by the differential equation (4.21) .

To prove it let us, first, resolve the transcendental equation (4.24) for the mapped solution of the hydrodynamic equations into **RFF**. Suppose it exists and is denoted as

$$v_{s\mathbf{G}} = v_{s\mathbf{G}}(T_f(X^{*1}), \mu_f(X^{*1}), \mu_g) . \quad (4.25)$$

Substituting it into equation of the charge conservation (4.22) , one finds the relation between the chemical potentials of gas and fluid, and fluid temperature. Assume it can be expressed as follows

$$\mu_g = \mu_g(T_f(X^{*1}), \mu_f(X^{*1})) . \quad (4.26)$$

Having substitute this solution into Eq. (4.25) and then both equations into expression (4.23) , one defines the shock velocity $v_{s\mathbf{F}}(T_f(X^{*1}), \mu_f(X^{*1}))$ in terms of the hydrodynamical solution mapped into the **RFF**. The last result completes the differential equation (4.21) for the time-like parts of the **FHS** in the **RFF**. The space-like ones should be obtained in accordance with the traditional Cooper-Frye prescription. On the light cones both parts should match and this is a requirement to choose the correct root of the transcendental equations for the time-like **FHS**.

In the case of zero charge the above consideration simplifies because both chemical potentials and equation of the charge conservation should be left out.

Thus, the principal way how to find the time-like **FHS** is described. Let us now consider the freeze-out problem in $1 + 1$ dimensions.

4.2. Freeze-out in $1 + 1$ Dimensional Hydrodynamics

A. Construction of the Solution

According to the *Theorems 1* and *3* we have to conjugate the *freeze-out shock* with the hydrodynamical solution for the fluid. In $1+1$ dimensions the original system of equations (4.21) – (4.24) for the **FHS** is greatly simplified. Setting formally $dX^{*2}, dX^{*3} \rightarrow 0$ in Eq. (4.21), one finds then in the **RFF**

$$\left. \frac{dX^*}{dX^0} \right|_{s\mathbf{F}} = v_{s\mathbf{F}}(T_f(X^*)), \quad (4.27)$$

or, rewriting it in the **C.M.** frame, one gets

$$\left. \frac{dX^*}{dX^0} \right|_{s\mathbf{C.M.}} = \frac{v_{f\mathbf{C.M.}} + v_{s\mathbf{F}}}{1 + v_{f\mathbf{C.M.}} v_{s\mathbf{F}}} \quad (4.28)$$

by the relativistic addition of the fluid velocity in **C.M.**.

Dividing Eq. (4.24) by Eq. (4.23), one obtains the following important expression after getting rid of the squares

$$v_{s\mathbf{G}}^\pm = \pm v_{s\mathbf{F}} \frac{\varepsilon_f + \tilde{p}_g(v_{s\mathbf{G}})}{p_f + \tilde{\varepsilon}_g(v_{s\mathbf{G}})}. \quad (4.29)$$

Substituting next Eq. (4.29) into Eq. (4.24), one obtains the second equation for velocities

$$v_{s\mathbf{F}} v_{s\mathbf{G}}^\pm = \pm \frac{p_f - \tilde{p}_g(v_{s\mathbf{G}})}{\varepsilon_f - \tilde{\varepsilon}_g(v_{s\mathbf{G}})}, \quad (4.30)$$

where we denote possible sign values by the corresponding superscript.

For the sake of simplicity we shall consider the fluid and gas without charge. Then Eq. (4.22) becomes an identity. In what follows we shall impose that the *EoS* of the fluid is

$p_f = c_s^2 \sigma_f T_f^{\frac{1+c_s^2}{c_s^2}} = c_s^2 \varepsilon_f$, and gas of free particles has the *EoS* of the ideal gas of massless particles $p_g = \frac{\sigma_g}{3} T_g^4 = \varepsilon_g/3$.

Such an example is meaningful because intuitively it is clear that once the interaction is not important for the gas and its particles are nearly free, then the most natural choice for its *EoS* is the ideal gas one. In order to simplify presentation we consider the massless gas. However, this simple choice shows us conceptually most important physical features of the freeze-out model.

The same might be valid for the fluid as well, but we would like to study a more general case of the fluid *EoS*. Then, the case when both *EoS* are the same is included by the proper choice of the speed of sound $c_s = \sqrt{\frac{dp}{d\varepsilon}}$ of the fluid.

Using the results of Appendix B, it is easy to obtain the effective energy density and pressure of the gas of free particles

$$\tilde{\varepsilon}_g = -\varepsilon_g(T^*) \frac{(1 - v_{s\mathbf{G}})^2}{4v_{s\mathbf{G}}} , \quad (4.31)$$

$$\tilde{p}_g = \varepsilon_g(T^*) \frac{(1 - v_{s\mathbf{G}})^2 (2 + v_{s\mathbf{G}})}{12} , \quad (4.32)$$

where we employ the results for the right hemisphere. In the further study we shall consider only single boundary between the fluid and the gas of free particles, assuming that fluid occupied the left hemisphere at the beginning and the gas to be appeared in the right hemisphere (in the meaning of the Appendix A).

It is a remarkable fact that the effective pressure \tilde{p}_g for the massless case is exactly the same as the pressure in the perpendicular direction to the 3-normal vector (c.f. Eq. (B.4)).

In this section we shall adopt the freeze-out criterion as it was introduced in Eq. (3.5). We only mention here that one can introduce, for instance, the freeze-out criterion by the energy density in the Landau-Lifshitz frame (see Appendix B) or by the effective energy density from the equation above. The latter might simplify a consideration essentially.

Introducing the new variable

$$R \equiv \frac{\sigma_f(T_f)^{\frac{1+c_s^2}{c_s^2}}}{\sigma_g(T^*)^4} > 0 , \quad (4.33)$$

one can rewrite Eqs. (4.29) and (4.30) with the help of the relations (4.31) and (4.32) as follows

$$\frac{v_{s\mathbf{G}}^\pm}{v_{s\mathbf{F}}} = \pm \frac{R + \frac{(1-v_{s\mathbf{G}}^\pm)^2(2+v_{s\mathbf{G}}^\pm)}{12}}{R c_s^2 - \frac{(1-v_{s\mathbf{G}}^\pm)^2}{4v_{s\mathbf{G}}^\pm}} , \quad (4.34)$$

$$v_{s\mathbf{F}} v_{s\mathbf{G}}^\pm = \pm \frac{R c_s^2 - \frac{(1-v_{s\mathbf{G}}^\pm)^2(2+v_{s\mathbf{G}}^\pm)}{12}}{R + \frac{(1-v_{s\mathbf{G}}^\pm)^2}{4v_{s\mathbf{G}}^\pm}} , \quad (4.35)$$

and, excluding the variable R , one finds from Eqs. (4.34) and (4.35)

$$\frac{\frac{c_s^2}{v_{s\mathbf{F}}} \mp v_{s\mathbf{G}}^\pm}{1 \mp \frac{c_s^2}{v_{s\mathbf{F}}} v_{s\mathbf{G}}^\pm} = - \frac{v_{s\mathbf{F}} \pm \frac{(2+v_{s\mathbf{G}}^\pm)}{3}}{1 \pm v_{s\mathbf{F}} \frac{(2+v_{s\mathbf{G}}^\pm)}{3}} . \quad (4.36)$$

Using the hyperbolic tangent function one can easily find solutions of Eq. (4.36). Since its solution $v_{s\mathbf{G}}^\pm = 1$ is unphysical, we are left only with the following ones

$$v_{s\mathbf{G}}^\pm = \mp 2v_{s\mathbf{F}} \frac{1 + c_s^2}{v_{s\mathbf{F}}^2 + c_s^2} - 3 . \quad (4.37)$$

For the left hemisphere one has to change only the overall sign in the left-hand side of the above equation.

Then we shall analyze the solution $v_{s\mathbf{G}}^+$ only, because other case can be obtained by the substitution $v_{s\mathbf{F}} \rightarrow -v_{s\mathbf{F}}$. From the inequality $|v_{s\mathbf{G}}^+| < 1$ the available range of the velocity $v_{s\mathbf{F}}$ follows

$$-1 < v_{s\mathbf{F}} < -c_s^2. \quad (4.38)$$

The maximal value of $v_{s\mathbf{G}}^+$ corresponds to $v_{s\mathbf{F}} = -c_s$ (see also Fig. 9).

Inequalities (4.38) show the limiting values of the shock velocity in the **RFF** which are derived by the conservation laws and relativistic causality condition. However, the entropy growth condition will give the narrower interval for the allowed values of the velocity $v_{s\mathbf{F}}$ (see below).

After some algebra one obtains an expression for the unknown quantity R by substituting Eq. (4.38) into Eq. (4.34) or (4.35)

$$R^+ = \frac{(2c_s^2 + 2v_{s\mathbf{F}}^2 + v_{s\mathbf{F}}(1 + c_s^2))^2 (v_{s\mathbf{F}} - 1)}{3 (v_{s\mathbf{F}} + c_s^2) (v_{s\mathbf{F}}^2 + c_s^2)^2}. \quad (4.39)$$

Finally, the result for the unknown fluid temperature on the boundary with the gas reads as

$$T_f = \left[\frac{\sigma_g (T^*)^4 (2c_s^2 + 2v_{s\mathbf{F}}^2 + v_{s\mathbf{F}}(1 + c_s^2))^2 (v_{s\mathbf{F}} - 1)}{3 \sigma_f (v_{s\mathbf{F}} + c_s^2) (v_{s\mathbf{F}}^2 + c_s^2)^2} \right]^{\frac{c_s^2}{1+c_s^2}}. \quad (4.40)$$

The formal solution of the freeze-out problem in 1+1 dimensions follows from the last equation: solving it for $v_{s\mathbf{F}}(T_f(X^*))$ and integrating Eq. (4.28) with the known hydrodynamical solution for the fluid, one finds the desired answer.

From Eq. (4.40) it is seen that freeze-out criteria $T_g = T^*$ and $T_f = T^*$ are not equivalent in general. The only exception is when the **FHS** is a straight line in (X^0, X) plane. This occurs in the freeze-out process of the simple wave (see subsection 4.2.C). The criterion $T_f = T^*$ looks technically simpler because the time derivative of the **FHS** $v_{s\mathbf{F}}(T_f(X^*))$ is defined by the hydrodynamical solution for the fluid. Then one has to find the gas temperature. However, it might be that under the "bad choice" of the freeze-out criterion, the gas temperature becomes too low (in the limit $v_{s\mathbf{F}}(T_f(X^*)) \rightarrow -c_s^2$ it follows $T_g \rightarrow 0$) for the applicability of both thermodynamics and hydrodynamics.

Using the above results, one finds the relative velocity of the fluid in the **RFG** from Eq. (4.8)

$$(v_{f\mathbf{G}}^+)^2 = \frac{(v_{s\mathbf{F}}^2 + 2v_{s\mathbf{F}} + 3c_s^2)^2}{(3v_{s\mathbf{F}}^2 + 2v_{s\mathbf{F}}c_s^2 + c_s^2)^2}, \quad (4.41)$$

where the superscript "+" corresponds to the solution $v_{s\mathbf{G}}^+$. Causality condition (4.38) plays the very same role for the relative velocity of the fluid.

Dependence of the fluid temperature and the relative velocity of the fluid in the **RFG** on $v_{s\mathbf{F}}$ for $c_s^2 = \frac{1}{3}$ is presented in Figs. 10 and 11, respectively. From the Fig. 10 it is seen that fluid temperature is always larger than that the gas one. This fact is born in a more general statement, namely the energy density of the fluid $\varepsilon_f(T_f)$ always exceeds the gas one $\varepsilon_g(T^*)$ one for $c_s^2 \geq \frac{1}{3}$. To show its validity we mention only that inequalities $R^+(v_{s\mathbf{F}} = -1) = \frac{2}{3(1-c_s^2)} \geq 1$ and $\frac{d \ln R^+}{d v_{s\mathbf{F}}} \geq 0$ hold for $v_{s\mathbf{F}} \leq 0$ and $c_s^2 \geq \frac{1}{3}$.

B. Entropy Production in the Freeze out Shock

Next we would like to study the problem of the thermodynamical stability, or in other words the entropy production in the freeze-out shock. This question is of a special interest for us because it proves that the freeze-out shock is a new kind of the discontinuity in which entropy increases in the rarefaction transition for thermodynamically normal media [25].

The fluid entropy flux through the **FHS** in an arbitrary Lorentz frame is given by

$$s_f^\mu = s_f u_f^\mu, \quad (4.42)$$

$$\mathcal{S}_f = \int_{\Sigma_{fr}} d\sigma_\mu s_f^\mu. \quad (4.43)$$

With the help of the previous section the entropy flux in **RFG** can be written in the general form

$$s_f^\mu n_\mu = s_f \left(\frac{(p_f - \tilde{p}_g(v_{s\mathbf{G}})) (\tilde{\varepsilon}_g(v_{s\mathbf{G}}) + \tilde{p}_g(v_{s\mathbf{G}}))}{(\varepsilon_f - \tilde{\varepsilon}_g(v_{s\mathbf{G}})) (p_f + \varepsilon_f)} \right)^{\frac{1}{2}}, \quad (4.44)$$

where the normal vector n_μ acquires the form $n_\mu = (-v_{s\mathbf{G}}; 1)$ in $1 + 1$ dimensions.

The corresponding expression for the gas of free particles has to be found from the cut-off distribution function. In the **RFG** it is evident that the entropy of outgoing particles is accounted by the change of the momentum integration volume $d^3p \rightarrow \Theta(p_\rho d\sigma^\rho) d^3p$ in the standard expressions for both classical and quantum statistics. For the Boltzmann distribution function ϕ [16], for example, it yields

$$s_g^\mu = \int \frac{d^3\mathbf{p}}{p^0} p^\mu \phi [1 - \ln \phi] \Theta(p_\rho d\sigma^\rho), \quad (4.45)$$

$$\mathcal{S}_g = \int_{\Sigma_{fr}} d\sigma_\mu s_g^\mu. \quad (4.46)$$

The results of Appendix B (see Eq. (B.2)) then lead to the following expressions of the entropy flux of the massless gas

$$s_g^\nu(v_{s\mathbf{G}}, T) = s_g(T^*) \left(\frac{1 - v_{s\mathbf{G}}}{2}; \frac{1 - v_{s\mathbf{G}}^2}{4} \right), \quad (4.47)$$

$$\mathcal{S}_g = \int_{\Sigma_{fr}} dX^0 n_\mu s_g^\mu, \quad (4.48)$$

where $s_g(T^*)$ is the entropy density of the gas at the freeze-out temperature.

One can find then the ratio of the entropy flux on the both sides of the freeze-out shock

$$P_s = \left(\frac{s_g^\mu n_\mu}{s_f^\mu n_\mu} \right)^4, \quad (4.49)$$

which becomes

$$P_s^+ \Big|_{c_s^2=\frac{1}{3}} = \frac{\sigma_g (3 v_{s\mathbf{F}}^2 + 1)^2 (3 v_{s\mathbf{F}} + 1)}{16 \sigma_f v_{s\mathbf{F}}^4 (v_{s\mathbf{F}} - 1)} \quad (4.50)$$

for the solution $v_{s\mathbf{F}}^+$ with $c_s^2 = \frac{1}{3}$.

Fig. 12 shows the limiting values of $v_{s\mathbf{F}}$ obtained by the thermodynamical stability criterion

$$P_s^+ \Big|_{c_s^2=\frac{1}{3}} \geq 1 \Rightarrow -1 < v_{s\mathbf{F}} \leq -0.479 \text{ for } \sigma_g = \sigma_f. \quad (4.51)$$

The maximal value of the entropy production in the freeze-out shock for the same *EoS* of the fluid is

$$\max \left(P_s^+ \Big|_{c_s^2=\frac{1}{3}} \right)^{\frac{1}{4}} \approx 1.01088 \left(\frac{\sigma_g}{\sigma_f} \right)^{\frac{1}{4}}, \quad (4.52)$$

i.e., is about one percent for the same number of the internal degrees of freedom of fluid and gas.

Another problem of stability is the mechanical stability (see, for example, Ref. [26] and references therein) of the *freeze-out shock*. It is of the crucial importance for the freeze-out process because it is related to the recoil problem of the freeze-out process on the fluid expansion. Usually one might argue that the freeze-out of the small fluid element would affect the hydrodynamical solution in the whole future cone of this element.

However, it is known that in the thermodynamically normal matter the perturbations of the small amplitudes propagate with the speed of sound and the rarefaction shocks propagate with the subsonic velocity in the local rest frame of the fluid. Thus, one has to conclude that a *freeze-out shock* with the shock velocity in the following range

$$-1 < v_{s\mathbf{F}}^+ \leq -c_s \quad (4.53)$$

is also mechanically stable with respect to the perturbations of the fluid state (c.f. Fig. 12). The compression shocks in the fluid we do not consider because on the freeze-out boundary there is the energy loss, i.e., it is a rarefaction. Thus, we have proved *Statement 4*: For the *EoS* under consideration the perturbations of the fluid state on the time-like **FHS** are slower than the supersonic *freeze-out shock* and, hence, do not affect the hydrodynamical evolution of the fluid inside the **FHS**.

Now we see that in contrast to the usual approach the recoil problem is resolved for the supersonic velocities of the *freeze-out shock* in the **RFF**. This is one of the main goals of the suggested freeze-out scheme. However, an investigation of the mechanical stability of the *freeze-out shock* in full requires a separate consideration.

It is now worthwhile to verify the validity of the adopted approximations by the comparison of the mean free path λ in the fluid and in the gas of free particles. Since λ contains a cross-section, we rather prefer to study the ratio of the particle density on both sides of the freeze-out shock. Such estimation gives the lower limit because of the inequality

$$R_\rho \Big|_{c_s^2=\frac{1}{3}} = \frac{\rho_f}{\rho_g} \leq \frac{\lambda_g}{\lambda_f}. \quad (4.54)$$

Substituting the densities found in the corresponding rest frames (for the gas of free particles we use the results obtained in the Eckart frame that are presented in Appendix B), one gets

$$R_\rho^+ \Big|_{c_s^2=\frac{1}{3}} = \left(\frac{\sigma_f (v_{s\mathbf{F}} - 1)^3 (3v_{s\mathbf{F}}^2 + 1)^2}{16 \sigma_g (3v_{s\mathbf{F}} + 1)^3 v_{s\mathbf{F}}^2} \right)^{\frac{1}{4}} \quad (4.55)$$

for $c_s^2 = \frac{1}{3}$. It is easy to prove that for the same EoS with the same number of degrees of freedom the particle density in the fluid is larger than in the gas of free particles, i.e., the following inequalities hold (see also Fig. 13)

$$\frac{\lambda_g}{\lambda_f} \geq R_\rho^+ \Big|_{c_s^2=\frac{1}{3}} \geq 1 . \quad (4.56)$$

It would be a problem of internal consistency otherwise, because in the latter case the fluid with the larger mean free path should freeze-out before the gas of free particles and the whole consideration would become questionable.

It is yet clear that a very large mean free path in the gas of free particles might lead to the reduction of the collision rate and, hence, the usage of the cut-off equilibrium distribution function would not be justified. However, such a region of the velocity $v_{s\mathbf{F}} \rightarrow -c_s^2$ is not allowed by the thermodynamical stability condition (c. f. Eq. (4.51)). Thus, it is shown that the considered freeze-out scheme in 1 + 1 dimensions does not have internal contradictions.

C. Freeze out of the Simple Wave

Let us consider the freeze-out of the semi-infinite homogeneous normal matter without charge, occupying the left hemisphere in 1+1 dimensions. Then the hydrodynamical solution for the fluid is known – it is a simple wave [23]. This simple isentropic flow describes the propagation of the perturbations with small amplitudes in the thermodynamically normal media [25]. The characteristics of the simple wave and, therefore, its isotherms are just straight lines in the space-time variables originating at the initial position of the boundary with the vacuum. It is important to remind also that characteristics are the time-like hypersurfaces and, therefore, are of our special interest. A short and clear description of the simple wave can be found in the Appendix A of Ref. [26].

Adopting the EoS of the previous two subsections we can apply its results straightforward to describe the freeze-out of the simple wave. Making consideration in the **RFF**, we conclude that the shock velocity in this frame, namely $v_{s\mathbf{F}}$, has to be equal to the velocity of the simple wave there, i.e., to the velocity of sound c_s . Since both waves move to the left-hand side in **RFF**, we write

$$v_{s\mathbf{F}} = -c_s . \quad (4.57)$$

Hence the freeze-out of the simple wave corresponds to one particular choice of the freeze-out shock and it is only necessary to substitute relation (4.57) in all formula of previous subsections.

Thus, substitution of Eq. (4.57) into Eq. (4.37) yields

$$v_{s\mathbf{G}}^\pm = \pm \frac{1 + c_s^2}{c_s} - 3 . \quad (4.58)$$

The latter equation leads to the restrictions on the fluid EoS . Indeed, requiring the validity of the inequality $|v_{s\mathbf{G}}^+| < 1$, one gets the lower limit of the velocity of sound in the fluid, i.e.,

$$c_s^- \equiv 2 - \sqrt{3} < c_s < 1 < c_s^+ \equiv 2 + \sqrt{3} . \quad (4.59)$$

The lower boundary of the velocity of sound corresponds to the extremely soft *EoS* with $c_s^- \approx 0.26795$ or with the power of the temperature in the expression for the pressure being $\frac{1+c_s^2}{c_s^2} \approx 15$.

The ratio of the energy densities becomes

$$R^+ \Big|_{S.W.} = \frac{(1 - 4c_s + c_s^2)^2 (1 + c_s)}{12 c_s^3 (1 - c_s)}, \quad (4.60)$$

and the temperature of the fluid in the simple wave reduces to the expression

$$T_f \Big|_{S.W.} = \left[\frac{\sigma_g (T^*)^4 (1 - 4c_s + c_s^2)^2 (1 + c_s)}{12 \sigma_f c_s^3 (1 - c_s)} \right]^{\frac{c_s^2}{1+c_s^2}}. \quad (4.61)$$

In order to illustrate the scale of quantities let us study the case $c_s = \frac{1}{\sqrt{3}} \approx 0.57735$. Then the shock velocity in the **RFG** is $v_{sG}^+ = \frac{4}{\sqrt{3}} - 3 \approx -0.6906$, and the ratio R^+ is $R^+ \Big|_{S.W.} = \frac{8}{3\sqrt{3}} \approx 1.5396$. The freeze-out temperature of the fluid in the simple wave is

$$T_f \Big|_{S.W.} = \left[\frac{8 \sigma_g}{3 \sigma_f \sqrt{3}} \right]^{\frac{1}{4}} T^* \approx 1.1139 \left[\frac{\sigma_g}{\sigma_f} \right]^{\frac{1}{4}} T^*. \quad (4.62)$$

If the fluid and the gas of free particles possess the same number of the degrees of freedom, then the fluid temperature exceeds the freeze-out one only by 11 percent. Thus, no dramatical difference for the temperatures should be expected when both *EoS* are same.

The entropy growth in the simple wave corresponds to the maximal possible value

$$\left(P_s^+ \right)^{\frac{1}{4}} \Big|_{S.W.} = \max \left(P_s^+ \Big|_{c_s^2=\frac{1}{3}} \right)^{\frac{1}{4}} \approx 1.01088 \left(\frac{\sigma_g}{\sigma_f} \right)^{\frac{1}{4}}. \quad (4.63)$$

The ratio of the mean free paths on the both sides of freeze-out shock satisfies the inequality

$$\frac{\lambda_g}{\lambda_f} \Big|_{S.W.} \geq R_\rho^+ \Big|_{S.W.} \approx 1.655 \left(\frac{\sigma_f}{\sigma_g} \right)^{\frac{1}{4}}. \quad (4.64)$$

Thus, the freeze-out scheme of the simple wave is thermodynamically stable and leads to the increase of the mean free path in the gas of free particles compared to the fluid.

An application of the freeze-out of the simple wave in the relativistic nuclear collisions should be, of course, done with a more realistic *EoS*. However, present consideration already shows that for the pion rich matter which expands with Landau initial conditions one should expect the reduction of the emission volume in comparison with the standard *CF* freeze-out picture. It is so because the same freeze-out temperature of the emitted particles in the picture with freeze-out shock and without it corresponds to the different energy densities of the fluid in the simple wave. In the freeze-out shock the fluid temperature is larger than the freeze-out one, whereas in the traditional approach they are equal. It follows now that for the same initial condition the fluid velocity before the freeze-out is smaller for the larger energy density, i.e., in the picture with the freeze-out shock.

Due to this fact one should expect some reduction of the emission volume for the same expansion time for the suggested freeze-out of the simple wave in comparison with the traditional Cooper-Frye estimations. This is a clear indication of the "influence effect" of the particle emission on the evolution of the fluid in the simple wave.

Let us now find the spectra of massless particles (bosons to be specific) emitted by the simple wave within the cut-off freeze-out scheme and compare it with corresponding result obtained by the traditional Cooper-Frye one. Adopting the standard cylindric geometry (X-axis is longitudinal) in momentum space, one gets the following expression for the invariant spectra in the **C.M.** (after the angular integration)

$$\frac{dN^{cut-off}}{p_t dp_t dy_{\mathbf{C.M.}} dS_{\perp} dt} = \frac{E_t \cosh(y_{\mathbf{C.M.}}) (\tanh(y_{\mathbf{C.M.}}) - v_{\sigma}) \Theta(\tanh(y_{\mathbf{C.M.}}) - v_{\sigma})}{(2\pi)^2 \left(e^{\frac{E_t \cosh(y_{\mathbf{C.M.}} - \eta_G) - \mu_c}{T^*}} - 1 \right)}, \quad (4.65)$$

where $E_t = \sqrt{p_t^2 + m^2}$ is the transverse energy of the particle, p_t is its transverse momentum, $y_{\mathbf{C.M.}}$ is the **C.M.** particle rapidity, η_G is the rapidity of the **RFG** in the **C.M.** frame, and v_{σ} is a velocity of the *freeze-out shock* in the **C.M.** frame. For simplicity we consider only one internal degree of freedom.

For the massless particles without charge ($\mu_c = 0$) it is convenient to introduce the dimensionless variable $\tilde{p}_t = \frac{p_t}{T^*}$. Then Eq. (4.65) becomes

$$T^{*-3} \frac{dN^{cut-off}}{\tilde{p}_t d\tilde{p}_t dy_{\mathbf{C.M.}} dS_{\perp} dt} = \frac{\tilde{p}_t \cosh(y_{\mathbf{C.M.}}) (\tanh(y_{\mathbf{C.M.}}) - v_{\sigma}) \Theta(\tanh(y_{\mathbf{C.M.}}) - v_{\sigma})}{(2\pi)^2 (e^{\tilde{p}_t \cosh(y_{\mathbf{C.M.}} - \eta_G)} - 1)}. \quad (4.66)$$

Let us assume that initial fluid has the temperature T_{in} . Then the velocity v_f and the temperature T_f of the fluid in the simple wave are related through the expression

$$v_f(T_f) = \tanh \left(c_s^{-1} \ln \left(\frac{T_{in}}{T_f} \right) \right). \quad (4.67)$$

The *freeze-out shock* velocity in the **C.M.** frame is given by the formula

$$v_{\sigma} = \frac{v_f(T_f) - c_s}{1 - c_s v_f(T_f)}, \quad (4.68)$$

where the fluid temperature is taken on the freeze-out boundary with the gas and it is defined by Eq. (4.40).

Substituting $v_{s\mathbf{F}} = -c_s$ into Eq. (4.41), one gets the **RFG** velocity in the **C.M.** frame

$$\tanh(\eta_G) = \frac{v_f(T_f) - v_{f\mathbf{G}}^+(-c_s)}{1 - v_{f\mathbf{G}}^+(-c_s) v_f(T_f)}. \quad (4.69)$$

Figs. 14 and 15 show these velocities for the fluid EqS $c_s^2 = \frac{1}{3}$ as a function of the initial temperature T_{in} . For such an EqS the freeze-out temperature of the fluid is given by Eq. (4.62). Assuming that fluid and gas have the same number of degrees of freedom, one

obtains

$$v_f \Big|_{c_s^2=\frac{1}{3}}^{cut-off} \approx \tanh \left(\sqrt{3} \ln \left(\frac{T_{in}}{1.1139T^*} \right) \right) , \quad (4.70)$$

$$v_{f\mathbf{G}}^+ \Big|_{c_s^2=\frac{1}{3}}^{cut-off} \approx -.18835 . \quad (4.71)$$

The traditional freeze-out scheme based on the Cooper-Frye formula has several important differences. First of all, spectrum does not contain the cut-off Θ -function

$$T^{*-3} \frac{dN^{CF}}{\tilde{p}_t d\tilde{p}_t dy_{\mathbf{C.M.}} dS_{\perp} dt} = \frac{\tilde{p}_t \cosh(y_{\mathbf{C.M.}}) (\tanh(y_{\mathbf{C.M.}}) - v_{\sigma})}{(2\pi)^2 (e^{\tilde{p}_t \cosh(y_{\mathbf{C.M.}} - \eta_G)} - 1)} . \quad (4.72)$$

Second, the freeze-out fluid temperature coincides with the gas one, i.e., $T_f = T^*$. Thus, the freeze-out in the traditional scheme happens at smaller energy density and at larger velocity of the fluid in comparison with the one explained above. And, third, there is no difference between the rest frame of fluid and the frame of its decay. Therefore, the fluid velocity and the relative velocity of the emitted particles read as

$$v_f \Big|_{c_s^2=\frac{1}{3}}^{CF} = \tanh \left(\sqrt{3} \ln \left(\frac{T_{in}}{T^*} \right) \right) , \quad (4.73)$$

$$v_{f\mathbf{G}}^+ \Big|_{c_s^2=\frac{1}{3}}^{CF} = 0 . \quad (4.74)$$

Now it is easy to see that for the same initial temperature of the fluid the hydrodynamic motion of the fluid in the CF freeze-out scheme is more developed (see Figs. 14 and 15), i.e.,

$$v_{\sigma} \Big|_{c_s^2=\frac{1}{3}}^{CF}(T_{in}) > v_{\sigma} \Big|_{c_s^2=\frac{1}{3}}^{cut-off}(T_{in}) , \quad (4.75)$$

whereas the $\mathbf{C.M.}$ rapidities are nearly equal

$$\eta_G \Big|_{c_s^2=\frac{1}{3}}^{CF}(T_{in}) \leq \eta_G \Big|_{c_s^2=\frac{1}{3}}^{cut-off}(T_{in}) . \quad (4.76)$$

First inequality above leads to the important consequences: for the CO freeze-out scheme (i) the energy emission per unit time from the \mathbf{FHS} is larger, and (ii) the $\mathbf{C.M.}$ rapidity interval with the positive values of the particle spectra is more broad. Inequality (4.76) has a negligible effect on the difference of the CO and the CF results. Therefore, one immediately gets the following inequality

$$\frac{dN^{cut-off}}{\tilde{p}_t d\tilde{p}_t dy_{\mathbf{C.M.}} dS_{\perp} dt} \geq \frac{dN^{Cooper-Frye}}{\tilde{p}_t d\tilde{p}_t dy_{\mathbf{C.M.}} dS_{\perp} dt} , \quad (4.77)$$

which, evidently, holds for the spectra integrated over rapidity or transversal momentum.

Due to these reasons the integrated spectra in both schemes are very different. Figs. 16 – 26 show some typical examples of the spectra integrated over the rapidity and the transverse momenta for both schemes. Evidently, the spectra integrated in the small rapidity window about $y_{\mathbf{C.M.}} \approx 0$ are extremely different - for the high initial temperatures the Cooper-Frye formula gives negative particle numbers everywhere. This feature is hidden

if integration is carried for positive values of the rapidity. Nevertheless, the quantitative difference remains. The spectra integrated over the transverse momenta have, basically, similar features. However, these simple examples of the spectra show that some previous results based on the Cooper-Frye formula may be considerably revised while the correct freeze-out scheme is used.

An application of Eq. (4.77) to describe the finite systems requires the knowledge of the hydrodynamic evolution of the system. Nevertheless, it is clear that for the cut-off freeze-out scheme the fluid volume is reduced on the magnitude of about $\left(S_{\perp}^{CF}(t_{em}) v_{\sigma}^{CF} - S_{\perp}^{CO}(t_{em}) v_{\sigma}^{CO} \right) t_{em}$ in comparison with the *CF* one ($S_{\perp}(t_{em})$ is the area of the freeze-out 3-surface at the emission time t_{em}). The maximal difference of the velocities is about $v_{\sigma}^{CF} - v_{\sigma}^{CO} \approx 0.18$ and it corresponds to the initial temperature $T_{in} \approx 1.5T^*$. Such a reduction of the emitting source size might be in a better agreement with the results of the HBT analysis of the relativistic nuclear collisions.

In the considered example we gave the solution of the simple wave freeze-out problem. Due to the fact that characteristics and isotherms of the fluid in the simple wave are just straight lines in any Lorentz frame, one can show that the ratio of the partial derivatives of the temperatures on both sides of the shock is the same, i.e., $\frac{\partial_x T_f}{\partial_t T_f} = \frac{\partial_x T^*}{\partial_t T^*}$ in any frame. This is the simplest example against the statement of Ref. [4] that such a condition is unphysical. As was shown in this section, it is unnecessarily strong for the derivation of the equation for the **FHS** as it was supposed in the paper [2], but it appears in particular applications like the freeze-out of the simple wave.

5. Conclusions

In this work the solution of the freeze-out problem in relativistic hydrodynamics is presented within a zero width **FHS** approximation. We analyze the difference between the *CF* procedure and its *CO* generalization for time-like **FHS**. It is shown that a reformulation of the traditional hydrodynamic scheme is necessary in order to include particle emission from the time-like parts of the **FHS**. The modified self-consistent hydrodynamics with the specific boundary conditions is formulated and different types of shock-like freeze-out are studied.

The correct boundary conditions enable us to derive the equations of motion of the fluid alone, which do not contain any source term. We have also proved the energy-momentum and charge conservation in the integral form for hydrodynamics with the specific boundary conditions if the *CO* distribution function is used.

We analyze the equations for the time-like parts of the **FHS** and show how to solve them together with the equations of motion of the fluid. A complete analysis of the freeze-out problem for the time-like parts of the **FHS** in 1+1 dimensions is presented. The entropy growth and mechanical stability conditions as well as the “recoil problem” for the shock-like freeze-out are studied. As an application of the general scheme, the freeze-out of the simple wave is considered, and analytical solution of this problem for the massless gas of free particles is given. The spectra of the emitted particles are calculated and compared to those obtained in the *CF* procedure.

Acknowledgments

We would like to thank D.H. Rischke and S. Bernard for the enlightening discussions. K.A.B. gratefully acknowledges the warm hospitality of the Nuclear Theory Group of the Institute for Theoretical Physics of the University of Hannover, where an essential part of this work was done. M.I.G. acknowledges the financial support of DFG, Germany. K.A.B. is grateful to the Alexander von Humboldt Foundation for the financial support. K.A.B. is also cordially thankful to D.H. Rischke for the moral support, without which this work could not be completed.

Appendix A

The moments of the cut-off distribution function in 4-dimensions can be easily calculated in the **RFG**. This is a convenient frame for such a calculation.

A.1. Spherical Coordinates in Momentum Space

Let us assume for simplicity that in 4-dimensions the fluid occupies the left semi-infinite volume (see Fig. 8, case a) and its **FHS** has the following external normal vector with respect to the fluid ⁴

$$d\sigma_\mu^R = (-v_\sigma; 1; 0; 0) dt dy dz, \quad (\text{A.1})$$

with $v_\sigma = \frac{\partial x^*(t)}{\partial t}$ having the same meaning as in Eq. (2.11). From its explicit form it is clear that the above vector is always pointing outside the fluid (or to the right hand side of Fig. 8.) which we indicated by the Roman superscript in capital.

Then one can calculate, for example, the energy-momentum tensor in the **RFG** using spherical coordinates in momentum space. Evidently one can explicitly perform angular integration if the distribution function depends on the energy and not momentum. This is true for any equilibrium distribution function of the gas of free particles in the **RFG** because it is the rest frame of the original, non-cut, distribution function. However, the presence of the cut-off Θ -function makes it more complicated in general, because integrations over the energy and spherical angles are not decoupled. The only exception is the case of massless particles when integrations over the energy and spherical angles are independent as we saw it during the discussion of the emission spectrum for the Sun like object. Nevertheless, one can try to find the closed form for such integrals.

Now if we choose the spherical angle θ_p between X-axis and the vector of 3-momentum \mathbf{p} , then the integration over this angle is reduced to simple quadratures as follows

$$I_F^R(v_\sigma, p) \equiv \int_0^\pi d\theta_p \sin(\theta_p) F(\cos(\theta_p)) \Theta\left(\frac{p}{E} \cos(\theta_p) - v_\sigma\right) = \int_{-1}^{+1} dx F(x) \Theta\left(\frac{p}{E} x - v_\sigma\right), \quad (\text{A.2})$$

where we use the evident notations $p = |\mathbf{p}|$, $E = \sqrt{p^2 + m^2}$.

The geometrical meaning of this result is clear from the case a) of Fig. 8. The $\Theta(p^\mu d\sigma_\mu^R)$ -function cuts off the projections of the 3-velocity on the X-axis direction from the lower limit.

Similarly, for the fluid occupying the right semi-infinite volume (see Fig. 8, case b)) with the external normal vector to the fluid

$$d\sigma_\mu^L = (v_\sigma; -1; 0; 0) dt dy dz \quad (\text{A.3})$$

one has to calculate similar integrals

⁴ Note that this is not a very restrictive choice of the normal vector because the general case can be reduced to the considered one by the proper rotation of the coordinate system in each space point.

$$I_F^L(v_\sigma, p) \equiv \int_0^\pi d\theta_p \sin(\theta_p) F(\cos(\theta_p)) \Theta\left(v_\sigma - \frac{p}{E} \cos(\theta_p)\right) = \int_{-1}^{+1} dx F(x) \Theta\left(v_\sigma - \frac{p}{E} x\right). \quad (\text{A.4})$$

These integrals are connected by simple relations, for example,

$$I_F^R(v_\sigma, p) \equiv I_F^L(+1, p) - I_F^L(v_\sigma, p), \quad (\text{A.5})$$

and therefore knowing one of them is enough to find out the other one, and, hence, we shall give it just for the left case and then write it for the right one without detailed calculation.

A.2. Angular Integration

In order to find the angular integrals let us first change the variables

$$I_F^L(v_\sigma, p) = \int_{-1}^{+1} dx F(x) \Theta\left(v_\sigma - \frac{p}{E} x\right) = \frac{E}{p} \int_{-\frac{p}{E}}^{+\frac{p}{E}} d\tau F\left(\frac{E}{p} \tau\right) \Theta(v_\sigma - \tau). \quad (\text{A.6})$$

Then it is evident that the integral does not vanish only in two cases, i.e., when $v_\sigma > \frac{p}{E}$ and $-\frac{p}{E} < v_\sigma \leq \frac{p}{E}$, which can be written in terms of Θ -functions as follows

$$I_F^L(v_\sigma, p) = \begin{cases} \frac{E}{p} \int_{-\frac{p}{E}}^{+\frac{p}{E}} d\tau F\left(\frac{E}{p} \tau\right), & v_\sigma > \frac{p}{E} \\ \frac{E}{p} \int_{-\frac{p}{E}}^{+v_\sigma} d\tau F\left(\frac{E}{p} \tau\right), & -\frac{p}{E} < v_\sigma \leq \frac{p}{E} \\ 0, & v_\sigma < -\frac{p}{E} \end{cases} \quad (\text{A.7})$$

$$= \Theta\left(v_\sigma - \frac{p}{E}\right) \Theta(v_\sigma) \int_{-1}^{+1} dx F(x) + \Theta\left(\frac{p}{E} - v_\sigma\right) \Theta\left(v_\sigma + \frac{p}{E}\right) \int_{-1}^{v_\sigma \frac{E}{p}} dx F(x).$$

Now the integral is decoupled into two parts, the first of them looking like a space-like contribution because of the integration limits, and the second one reminds the time-like one! One can call it this way since in the limit of space-like **FHS** ($v_\sigma > 1$) all values of the spherical angle θ_p contribute and, hence, only the first term survives.

However, the meaning of the first term above is deeper: if **FHS** moves inside the fluid with the velocity v_σ and one considers the values of the particle velocity with the modulus $\frac{p}{E} < |v_\sigma|$, then particles with any projection of the velocity $\frac{p}{E}$ are emitted from the fluid, and this fact is taken into account by the limits of integration from -1 to $+1$. For the space-like **FHS** it is always so and the space-like term in Eq. (A.7) does not vanish. The second term

in Eq. (A.7) , evidently, describes the contribution of the velocity projection on the X -axis which exceeds the velocity of the **FHS** .

The same is valid for the right hemisphere as one can see from the expression below that was obtained with the help of the identity (A.5)

$$I_F^R(v_\sigma, p) = \Theta\left(-v_\sigma - \frac{p}{E}\right) \Theta(-v_\sigma) \int_{-1}^{+1} dx F(x) + \Theta\left(\frac{p}{E} - v_\sigma\right) \Theta\left(v_\sigma + \frac{p}{E}\right) \int_{v_\sigma \frac{E}{p}}^{+1} dx F(x), \quad (\text{A.8})$$

where we used the fact that for positive $\frac{p}{E} > 0$ the following product of Θ -functions always vanishes: $\Theta\left(-v_\sigma - \frac{p}{E}\right) \Theta\left(v_\sigma - \frac{p}{E}\right) = 0$.

Note that similar results hold for the case of the cylindrical geometry, with some simple modifications.

A.3. Momentum Integration

Since our next step is an integration over the modulus of momentum or energy, it is necessary to rewrite the above results in terms of energy. After some algebra, one gets the following result for the angular integrals

$$I_F^L(v_\sigma, p) = \Theta(E_\sigma - E) \Theta(v_\sigma) \int_{-1}^{+1} d\tau F(\tau) + \Theta(E - E_\sigma) \int_{-1}^{\frac{E}{p} v_\sigma} d\tau F(\tau), \quad (\text{A.9})$$

$$I_F^R(v_\sigma, p) = \Theta(E_\sigma - E) \Theta(-v_\sigma) \int_{-1}^{+1} d\tau F(\tau) + \Theta(E - E_\sigma) \int_{\frac{E}{p} v_\sigma}^{+1} d\tau F(\tau),$$

with $E_\sigma \equiv \frac{m}{\sqrt{1-v_\sigma^2}}$ for $v_\sigma^2 < 1$ and $E_\sigma = \infty$ for $v_\sigma^2 \geq 1$. Note that $\Theta(\pm v_\sigma)$ in front of the space-like integral above is of a crucial importance when one uses integration over the energy on the time-like **FHS** . For the space-like **FHS** (i.e., $v_\sigma^2 \geq 1$) it is trivial because the other Θ -function ensures that the correct value of v_σ is taken into account.

In the derivation of Eqs. (A.9) one has to use the following two relations for Θ -functions

$$\begin{aligned} \Theta\left(\frac{p}{E} - v_\sigma\right) \Theta\left(v_\sigma + \frac{p}{E}\right) &= \Theta\left(\frac{p}{E} - v_\sigma\right) \Theta\left(v_\sigma + \frac{p}{E}\right) [\Theta(v_\sigma) + \Theta(-v_\sigma)] \\ &= \Theta\left(\frac{p}{E} - v_\sigma\right) \Theta(v_\sigma) + \Theta\left(v_\sigma + \frac{p}{E}\right) \Theta(-v_\sigma), \quad (\text{A.10}) \end{aligned}$$

and

$$\Theta\left(\frac{p}{E} - v_\sigma\right) \Theta(v_\sigma) = \Theta(E - E_\sigma) \Theta(v_\sigma), \quad (\text{A.11})$$

from which all other necessary relations can be trivially found.

Usually one has to integrate such expressions over momentum or energy, i.e., to calculate the integrals of the following type:

$$I_{GF}^A(v_\sigma) \equiv \int_0^\infty dp p^2 G(p, E) I_F^A(v_\sigma, p) = \int_m^\infty dE E p(E) G(p(E), E) I_F^A(v_\sigma, p(E)), \quad (\text{A.12})$$

with $A \in \{L, R\}$ and $p(E) \equiv \sqrt{E^2 - m^2}$. Using Eqs. (A.9), one obtains the relations for momentum integrals in a closed form,

$$I_{GF}^L(v_\sigma) = \Theta(v_\sigma) \int_m^{E_\sigma} dE E p(E) G(p(E), E) \int_{-1}^{+1} d\tau F(\tau) + \int_{E_\sigma}^\infty dE E p(E) G(p(E), E) \int_{-1}^{v_\sigma \frac{E}{p(E)}} d\tau F(\tau), \quad (\text{A.13})$$

$$I_{GF}^R(v_\sigma) = \Theta(-v_\sigma) \int_m^{E_\sigma} dE E p(E) G(p(E), E) \int_{-1}^{+1} d\tau F(\tau) + \int_{E_\sigma}^\infty dE E p(E) G(p(E), E) \int_{v_\sigma \frac{E}{p(E)}}^{+1} d\tau F(\tau). \quad (\text{A.14})$$

It is evident that a sum of Eqs. (A.13) and (A.14) gives just the usual result without the cut-off Θ -function

$$I_{GF}^L(v_\sigma) + I_{GF}^R(v_\sigma) = I_{GF}^L(+1) = I_{GF}^R(-1) = \int_m^\infty dE E p(E) G(p(E), E) \int_{-1}^{+1} d\tau F(\tau), \quad (\text{A.15})$$

when integrations over spherical angle and energy are not connected. Another example of such a simplification is the case of massless particles, when the space-like contributions vanish, as it immediately follows from Eqs. (A.13) and (A.14)

$$I_{GF}^L(v_\sigma) \Big|_{m=0} = \int_0^\infty dE E^2 G(E, E) \int_{-1}^{v_\sigma} d\tau F(\tau), \quad (\text{A.16})$$

$$I_{GF}^R(v_\sigma) \Big|_{m=0} = \int_0^\infty dE E^2 G(E, E) \int_{v_\sigma}^{+1} d\tau F(\tau). \quad (\text{A.17})$$

All these relations can be greatly simplified for even or odd functions $F(\cos(\Theta_p))$ of the cosine of the spherical angle Θ_p which is usually the case for most applications. After trivial manipulations, one can easily prove the validity of the following relations between the integrals over left and right hemispheres

$$I_{GF}^R(v_\sigma) = \begin{cases} I_{GF}^L(-v_\sigma), & \text{even } F(\tau), \\ -I_{GF}^L(-v_\sigma), & \text{odd } F(\tau), \end{cases} \quad (\text{A.18})$$

which is one of the most useful and powerful relation.

An important consequence of this statement is that the terms proportional to $\Theta(\pm v_\sigma)$ do not vanish for even functions $F(\tau)$, and those terms are not present in the final expressions for odd functions $F(\tau)$. This is clearly seen from Eqs. (A.13) and (A.14) .

Using the results above, it is easy to find out expressions for the moments of the distribution function of the gas of free particles

A.4. Moments of the Cut-off Distribution Function

As a good example to apply the results of the previous subsection, let us consider a relativistic massive Boltzmann gas with the distribution function

$$\phi_g(\mathbf{x}, t, \mathbf{p}) = C_g e^{-\frac{E(\mathbf{p}) - \mu_c(\mathbf{x}, t)}{T(\mathbf{x}, t)}}, \quad (\text{A.19})$$

with the constant $C_g = \frac{d_g}{(2\pi)^3}$, where d_g is the degeneracy number of the gas. Then the components of the particle flow number of the emission part are

$$\begin{aligned} N_{g,L}^0(v_\sigma, T, \mu_c) &= 2\pi C_g T^3 e^{\frac{\mu_c}{T}} \left\{ \Theta(v_\sigma) \left[2\mathcal{K}_2\left(\frac{m}{T}; \frac{m}{T}\right) - \mathcal{K}_2\left(\frac{m}{T}; \frac{E_\sigma}{T}\right) \right] \right. \\ &\quad \left. + \Theta(-v_\sigma) \mathcal{K}_2\left(\frac{m}{T}; \frac{E_\sigma}{T}\right) + v_\sigma \mathcal{K}_2\left(0; \frac{E_\sigma}{T}\right) \right\}, \end{aligned} \quad (\text{A.20})$$

$$N_{g,L}^X(v_\sigma, T, \mu_c) = \pi C_g T^3 e^{\frac{\mu_c}{T}} \left\{ (v_\sigma^2 - 1) \mathcal{K}_2\left(0; \frac{E_\sigma}{T}\right) + \frac{m^2}{T^2} e^{-\frac{E_\sigma}{T}} \right\}, \quad (\text{A.21})$$

$$N_{g,L}^Y(v_\sigma, T, \mu_c) = N_{g,L}^Z(v_\sigma, T, \mu_c) = 0 \quad (\text{A.22})$$

for the left hemisphere, and

$$\begin{aligned} N_{g,R}^0(v_\sigma, T, \mu_c) &= 2\pi C_g T^3 e^{\frac{\mu_c}{T}} \left\{ \Theta(-v_\sigma) \left[2\mathcal{K}_2\left(\frac{m}{T}; \frac{m}{T}\right) - \mathcal{K}_2\left(\frac{m}{T}; \frac{E_\sigma}{T}\right) \right] \right. \\ &\quad \left. + \Theta(v_\sigma) \mathcal{K}_2\left(\frac{m}{T}; \frac{E_\sigma}{T}\right) - v_\sigma \mathcal{K}_2\left(0; \frac{E_\sigma}{T}\right) \right\}, \end{aligned} \quad (\text{A.23})$$

$$N_{g,R}^X(v_\sigma, T, \mu_c) = -\pi C_g T^3 e^{\frac{\mu_c}{T}} \left\{ (v_\sigma^2 - 1) \mathcal{K}_2\left(0; \frac{E_\sigma}{T}\right) + \frac{m^2}{T^2} e^{-\frac{E_\sigma}{T}} \right\}, \quad (\text{A.24})$$

$$N_{g,R}^Y(v_\sigma, T, \mu_c) = N_{g,R}^Z(v_\sigma, T, \mu_c) = 0 \quad (\text{A.25})$$

for the right one. Here we used the following notation for the \mathcal{K}_2 -function

$$\mathcal{K}_n(a; b) \equiv \frac{2^{n-1}(n-1)!}{(2n-2)!} \int_b^\infty dx x (x^2 - a^2)^{n-\frac{3}{2}} e^{-x}, \quad (\text{A.26})$$

which differs from the notation of the paper [4] and the book [16] by the dimensionless factor a^n .

With the help of the following identity

$$\mathcal{K}_2\left(0; \frac{E_\sigma}{T}\right) \equiv \left(2 + 2\frac{E_\sigma}{T} + \frac{E_\sigma^2}{T^2}\right) e^{-\frac{E_\sigma}{T}} \quad (\text{A.27})$$

we complete our analysis of the particle flow number.

One can see that in the expression for $N_{g,L}^0(v_\sigma, T, \mu_c)$ of Ref. [4] the factors with $\Theta(v_\sigma)$ and $\Theta(-v_\sigma)$ are missing, as well as in their expressions for the diagonal components of the energy-momentum tensor of the gas of free particles.

The results for the right hemisphere we give for the first time.

We also would like to emphasize the fact that the spatial projections of the particle flow 4-vector on other than the X-axis vanish in the **RFG** due to convenient choice of the normal vector. Same property one sees when evaluating components of the energy-momentum tensor.

Expressions for the nonzero components of the energy-momentum tensor of the emitted particles then read as

$$\begin{aligned} T_{g,L}^{00}(v_\sigma, T, \mu_c) &= 2\pi C_g T^4 e^{\frac{\mu_c}{T}} \left\{ \Theta(v_\sigma) \left[6\mathcal{K}_2\left(\frac{m}{T}; \frac{m}{T}\right) - 6\mathcal{K}_2\left(\frac{m}{T}; \frac{E_\sigma}{T}\right) - 2|v_\sigma| \frac{E_\sigma^3}{T^3} e^{-\frac{E_\sigma}{T}} \right] \right. \\ &+ \Theta(v_\sigma) 2\frac{m^2}{T^2} \left[\mathcal{K}_1\left(\frac{m}{T}; \frac{m}{T}\right) - \mathcal{K}_1\left(\frac{m}{T}; \frac{E_\sigma}{T}\right) \right] + 3\mathcal{K}_2\left(\frac{m}{T}; \frac{E_\sigma}{T}\right) + |v_\sigma| \frac{E_\sigma^3}{T^3} e^{-\frac{E_\sigma}{T}} \\ &+ \left. \frac{m^2}{T^2} \mathcal{K}_1\left(\frac{m}{T}; \frac{E_\sigma}{T}\right) + v_\sigma \left[3\mathcal{K}_2\left(0; \frac{E_\sigma}{T}\right) + \frac{E_\sigma^3}{T^3} e^{-\frac{E_\sigma}{T}} \right] \right\}, \end{aligned} \quad (\text{A.28})$$

$$\begin{aligned} T_{g,L}^{0X}(v_\sigma, T, \mu_c) &= \pi C_g T^4 e^{\frac{\mu_c}{T}} \left\{ (v_\sigma^2 - 1) \left[3\mathcal{K}_2\left(0; \frac{E_\sigma}{T}\right) + \frac{E_\sigma^3}{T^3} e^{-\frac{E_\sigma}{T}} \right] \right. \\ &+ \left. \frac{m^2}{T^2} \left(\frac{E_\sigma}{T} + 1 \right) e^{-\frac{E_\sigma}{T}} \right\}, \end{aligned} \quad (\text{A.29})$$

$$T_{g,L}^{X0}(v_\sigma, T, \mu_c) = T_{g,L}^{0X}(v_\sigma, T, \mu_c), \quad (\text{A.30})$$

$$\begin{aligned} T_{g,L}^{XX}(v_\sigma, T, \mu_c) &= 2\pi C_g T^4 e^{\frac{\mu_c}{T}} \left\{ \Theta(v_\sigma) \left[2\mathcal{K}_2\left(\frac{m}{T}; \frac{m}{T}\right) - \mathcal{K}_2\left(\frac{m}{T}; \frac{E_\sigma}{T}\right) - \frac{|v_\sigma|^3}{3} \frac{E_\sigma^3}{T^3} e^{-\frac{E_\sigma}{T}} \right] \right. \\ &+ \Theta(-v_\sigma) \left[\mathcal{K}_2\left(\frac{m}{T}; \frac{E_\sigma}{T}\right) + \frac{|v_\sigma|^3}{3} \frac{E_\sigma^3}{T^3} e^{-\frac{E_\sigma}{T}} \right] \\ &+ \left. \frac{v_\sigma^3}{3} \left[3\mathcal{K}_2\left(0; \frac{E_\sigma}{T}\right) + \frac{E_\sigma^3}{T^3} e^{-\frac{E_\sigma}{T}} \right] \right\}, \end{aligned} \quad (\text{A.31})$$

$$\begin{aligned} T_{g,L}^{YY}(v_\sigma, T, \mu_c) &= \pi C_g T^4 e^{\frac{\mu_c}{T}} \left\{ \Theta(v_\sigma) 2 \left[2\mathcal{K}_2\left(\frac{m}{T}; \frac{m}{T}\right) - \mathcal{K}_2\left(\frac{m}{T}; \frac{E_\sigma}{T}\right) - \frac{|v_\sigma|^3}{3} \frac{E_\sigma^3}{T^3} e^{-\frac{E_\sigma}{T}} \right] \right. \\ &+ 2\Theta(-v_\sigma) \left[\mathcal{K}_2\left(\frac{m}{T}; \frac{E_\sigma}{T}\right) + \frac{|v_\sigma|^3}{3} \frac{E_\sigma^3}{T^3} e^{-\frac{E_\sigma}{T}} \right] - \frac{m^2}{T^2} v_\sigma \left(\frac{E_\sigma}{T} + 1 \right) e^{-\frac{E_\sigma}{T}} \\ &+ \left. \left(v_\sigma - \frac{v_\sigma^3}{3} \right) \left[3\mathcal{K}_2\left(0; \frac{E_\sigma}{T}\right) + \frac{E_\sigma^3}{T^3} e^{-\frac{E_\sigma}{T}} \right] \right\}, \end{aligned} \quad (\text{A.32})$$

$$T_{g,L}^{ZZ}(v_\sigma, T, \mu) = T_{g,L}^{YY}(v_\sigma, T, \mu) \quad (\text{A.33})$$

for the left hemisphere. In deriving equations above we used several useful identities

$$\int_b^\infty dx x^2 (x^2 - a^2)^{\frac{1}{2}} e^{-x} = b^2 (b^2 - a^2)^{\frac{1}{2}} e^{-b} + 3\mathcal{K}_2(a; b) + a^2 \mathcal{K}_1(a; b), \quad (\text{A.34})$$

$$\int_b^\infty dx (x^2 - a^2)^{\frac{3}{2}} e^{-x} = (b^2 - a^2)^{\frac{3}{2}} e^{-b} + 3\mathcal{K}_2(a; b); \quad (\text{A.35})$$

The identities similar to these ones were used in Ref. [4], but the first terms in the r.h.s which appear after integration by parts were missing. For the further evaluation of the radicals above it is also convenient to use the identity $\left(\frac{E_\sigma^2}{T^2} - \frac{m^2}{T^2}\right)^{\frac{1}{2}} = |v_\sigma| \frac{E_\sigma}{T}$.

The formulae for the right hemisphere can be obtained in the similar way by a straightforward integration or with the help of Eq. (A.18)

$$\begin{aligned} T_{g,R}^{00}(v_\sigma, T, \mu_c) &= 2\pi C_g T^4 e^{\frac{\mu_c}{T}} \left\{ \Theta(-v_\sigma) \left[6\mathcal{K}_2\left(\frac{m}{T}; \frac{m}{T}\right) - 6\mathcal{K}_2\left(\frac{m}{T}; \frac{E_\sigma}{T}\right) - 2|v_\sigma| \frac{E_\sigma^3}{T^3} e^{-\frac{E_\sigma}{T}} \right] \right. \\ &+ \Theta(-v_\sigma) 2 \frac{m^2}{T^2} \left[\mathcal{K}_1\left(\frac{m}{T}; \frac{m}{T}\right) - \mathcal{K}_1\left(\frac{m}{T}; \frac{E_\sigma}{T}\right) \right] + 3\mathcal{K}_2\left(\frac{m}{T}; \frac{E_\sigma}{T}\right) + |v_\sigma| \frac{E_\sigma^3}{T^3} e^{-\frac{E_\sigma}{T}} \\ &+ \left. \frac{m^2}{T^2} \mathcal{K}_1\left(\frac{m}{T}; \frac{E_\sigma}{T}\right) - v_\sigma \left[3\mathcal{K}_2\left(0; \frac{E_\sigma}{T}\right) + \frac{E_\sigma^3}{T^3} e^{-\frac{E_\sigma}{T}} \right] \right\}, \end{aligned} \quad (\text{A.36})$$

$$\begin{aligned} T_{g,R}^{0X}(v_\sigma, T, \mu_c) &= -\pi C_g T^4 e^{\frac{\mu_c}{T}} \left\{ (v_\sigma^2 - 1) \left[3\mathcal{K}_2\left(0; \frac{E_\sigma}{T}\right) + \frac{E_\sigma^3}{T^3} e^{-\frac{E_\sigma}{T}} \right] \right. \\ &+ \left. \frac{m^2}{T^2} \left(\frac{E_\sigma}{T} + 1 \right) e^{-\frac{E_\sigma}{T}} \right\}, \end{aligned} \quad (\text{A.37})$$

$$T_{g,R}^{X0}(v_\sigma, T, \mu_c) = T_{g,R}^{0X}(v_\sigma, T, \mu_c), \quad (\text{A.38})$$

$$\begin{aligned} T_{g,R}^{XX}(v_\sigma, T, \mu_c) &= 2\pi C_g T^4 e^{\frac{\mu_c}{T}} \left\{ \Theta(-v_\sigma) \left[2\mathcal{K}_2\left(\frac{m}{T}; \frac{m}{T}\right) - \mathcal{K}_2\left(\frac{m}{T}; \frac{E_\sigma}{T}\right) - \frac{|v_\sigma|^3}{3} \frac{E_\sigma^3}{T^3} e^{-\frac{E_\sigma}{T}} \right] \right. \\ &+ \Theta(v_\sigma) \left[\mathcal{K}_2\left(\frac{m}{T}; \frac{E_\sigma}{T}\right) + \frac{|v_\sigma|^3}{3} \frac{E_\sigma^3}{T^3} e^{-\frac{E_\sigma}{T}} \right] \\ &- \left. \frac{v_\sigma^3}{3} \left[3\mathcal{K}_2\left(0; \frac{E_\sigma}{T}\right) + \frac{E_\sigma^3}{T^3} e^{-\frac{E_\sigma}{T}} \right] \right\}, \end{aligned} \quad (\text{A.39})$$

$$\begin{aligned} T_{g,R}^{YY}(v_\sigma, T, \mu_c) &= \pi C_g T^4 e^{\frac{\mu_c}{T}} \left\{ \Theta(-v_\sigma) 2 \left[2\mathcal{K}_2\left(\frac{m}{T}; \frac{m}{T}\right) - \mathcal{K}_2\left(\frac{m}{T}; \frac{E_\sigma}{T}\right) - \frac{|v_\sigma|^3}{3} \frac{E_\sigma^3}{T^3} e^{-\frac{E_\sigma}{T}} \right] \right. \\ &+ 2\Theta(v_\sigma) \left[\mathcal{K}_2\left(\frac{m}{T}; \frac{E_\sigma}{T}\right) + \frac{|v_\sigma|^3}{3} \frac{E_\sigma^3}{T^3} e^{-\frac{E_\sigma}{T}} \right] + \frac{m^2}{T^2} v_\sigma \left(\frac{E_\sigma}{T} + 1 \right) e^{-\frac{E_\sigma}{T}} \\ &- \left. \left(v_\sigma - \frac{v_\sigma^3}{3} \right) \left[3\mathcal{K}_2\left(0; \frac{E_\sigma}{T}\right) + \frac{E_\sigma^3}{T^3} e^{-\frac{E_\sigma}{T}} \right] \right\}, \end{aligned} \quad (\text{A.40})$$

$$T_{g,R}^{ZZ}(v_\sigma, T, \mu_c) = T_{g,R}^{YY}(v_\sigma, T, \mu_c) \quad (\text{A.41})$$

These expressions can be used for the approximate description of nucleons and baryon resonances in the numerical studies, with the only exception for the very low temperatures

where the Fermi statistics is essential. They also show us that even in the simplest case of the time-like **FHS** the derived expressions are more involved than in case of space-like one. The limit of the massless gas follows straightforwardly from the equations above.

Appendix B

In case of massless particles the formulae of the previous subsection become simpler. Note that for high enough temperatures, namely $T \geq m_\pi$, m_π is a pion mass, these results can be also used as a good approximation for the pion gas.

B.1. Moments of the Cut-off Distribution Function for the Massless Gas

Employing Eqs. (A.16) – (A.18) one obtains the following results for the particle flow number for the left and right hemispheres in the **RFG**

$$N_{g,L}^\nu(v_\sigma, T, \mu_c) = n_g(T, \mu_c) \left(\frac{1+v_\sigma}{2}; \frac{v_\sigma^2-1}{4}; 0; 0 \right), \quad (\text{B.1})$$

$$N_{g,R}^\nu(v_\sigma, T, \mu_c) = n_g(T, \mu_c) \left(\frac{1-v_\sigma}{2}; \frac{1-v_\sigma^2}{4}; 0; 0 \right), \quad (\text{B.2})$$

where $n_g(T, \mu_c)$ is usual particle density of the gas without cut-off with the temperature T and chemical potential μ . Similarly, the emission part of the energy-momentum tensor of the particles moving antiparallel to the X-axis is given by the formula

$$T_{g,L}^{\mu\nu}(v_\sigma, T, \mu_c) = \varepsilon_g(T, \mu_c) \begin{pmatrix} \frac{1+v_\sigma}{2} & \frac{v_\sigma^2-1}{4} & 0 & 0 \\ \frac{v_\sigma^2-1}{4} & \frac{1+v_\sigma^3}{6} & 0 & 0 \\ 0 & 0 & \frac{(1+v_\sigma)^2(2-v_\sigma)}{12} & 0 \\ 0 & 0 & 0 & \frac{(1+v_\sigma)^2(2-v_\sigma)}{12} \end{pmatrix}, \quad (\text{B.3})$$

where $\varepsilon_g(T, \mu_c)$ is the usual energy density of the gas with the temperature T and chemical potential μ_c , obtained for non-cut distribution function. It is remarkable that the above results do not depend on whether the statistics is Boltzmann, Fermi-Dirac or Bose-Einstein one! The corresponding formula for the case a) of Fig. 8. (or for the particles moving parallel to the X-axis) can be obtained similarly or employing Eqs. (A.5) , (A.16) – (A.18)

$$T_{g,R}^{\mu\nu}(v_\sigma, T, \mu_c) = \varepsilon_g(T, \mu_c) \begin{pmatrix} \frac{1-v_\sigma}{2} & \frac{1-v_\sigma^2}{4} & 0 & 0 \\ \frac{1-v_\sigma^2}{4} & \frac{1-v_\sigma^3}{6} & 0 & 0 \\ 0 & 0 & \frac{(1-v_\sigma)^2(2+v_\sigma)}{12} & 0 \\ 0 & 0 & 0 & \frac{(1-v_\sigma)^2(2+v_\sigma)}{12} \end{pmatrix}. \quad (\text{B.4})$$

B.2. Eckart and Landau–Lifshitz Velocities for the Massless Gas

This question was briefly discussed in Ref. [5]. We would like to discuss it in more details for the gas of massless particles because on this simplest example one can analytically show that the value of the Eckart velocity always exceeds the Landau-Lifshitz one.

First we find out the value of the velocity in the Eckart meaning. Instead of calculating it directly from the definition which can be found in text-books (see, for example, Ref. [16]), we remind the reader that in the Eckart frame the particle flow number has only the time component nonvanishing. Then, making the proper Lorentz transformation, we immediately obtain the expression for the Eckart velocity in the considered case

$$N_{g,A}^{X'}(v_\sigma, T, \mu_c) = \gamma \left(N_{g,A}^X(v_\sigma, T, \mu_c) - v_{E,A} N_{g,A}^0(v_\sigma, T, \mu_c) \right) = 0 \quad (\text{B.5})$$

$$\Rightarrow v_{E,A} = \frac{N_{g,A}^X(v_\sigma, T, \mu_c)}{N_{g,A}^0(v_\sigma, T, \mu_c)} = \begin{cases} \frac{v_\sigma - 1}{2}, & A = L, \\ \frac{v_\sigma + 1}{2}, & A = R. \end{cases} \quad (\text{B.6})$$

Note that such a transformation and, therefore, the first part of Eq. (B.6) are valid for massive gas as long as the normal vector to the **FHS** is chosen in the same way.

In accordance with the Eckart definition, the proper particle number density reads then as

$$n_{E,A} = n_g(T, \mu_c) \begin{cases} \frac{1+v_\sigma}{4} \sqrt{(1+v_\sigma)(3-v_\sigma)}, & A = L, \\ \frac{1-v_\sigma}{4} \sqrt{(1-v_\sigma)(3+v_\sigma)}, & A = R, \end{cases} \quad (\text{B.7})$$

which is, evidently, reduced in comparison with the value of $n_g(T, \mu_c)$.

Now we can find the Landau-Lifshitz velocity by the similar Lorentz transformation for the non-diagonal component of the symmetric energy-momentum tensor (dropping their arguments for simplicity)

$$T_{g,A}^{0X'}(v_\sigma, T, \mu_c) = \gamma^2 \left((1 + v_{LL,A}^2) T_{g,A}^{0X} - v_{LL,A} T_{g,A}^{00} - v_{LL,A} T_{g,A}^{XX} \right) = 0 \quad (\text{B.8})$$

$$\Rightarrow v_{LL,A} = \frac{T_{g,A}^{00} + T_{g,A}^{XX} - \sqrt{(T_{g,A}^{00} + T_{g,A}^{XX} - 2T_{g,A}^{0X})(T_{g,A}^{00} + T_{g,A}^{XX} + 2T_{g,A}^{0X})}}{2T_{g,A}^{0X}}, \quad (\text{B.9})$$

where we have chosen the physical solution of the Landau-Lifshitz velocity by the condition $v_{LL,A} \rightarrow 0$ when $T_{g,A}^{0X} \rightarrow 0$.

Applying the general result of Eq. (B.9) to the massless particle gas, one obtains more involved expressions for the Landau-Lifshitz velocity

$$v_{LL,A} \Big|_{m=0} = \begin{cases} \frac{(1+v_\sigma)\sqrt{7-4v_\sigma+v_\sigma^2} - (4-v_\sigma+v_\sigma^2)}{3(1-v_\sigma)}, & A = L, \\ -\frac{(1-v_\sigma)\sqrt{7+4v_\sigma+v_\sigma^2} - (4+v_\sigma+v_\sigma^2)}{3(1+v_\sigma)}, & A = R. \end{cases} \quad (\text{B.10})$$

To compare it with the Eckart velocity, let us find the limit $v_\sigma \rightarrow +1$ ($v_\sigma \rightarrow -1$) for the left (right) hemisphere. Then it is convenient to rewrite the previous expression in terms of the difference Δ

$$v_{LL,A} = \frac{(2 - \Delta) \sqrt{4 + 2\Delta + \Delta^2} - (4 - \Delta + \Delta^2)}{3\Delta} \begin{cases} 1, & \Delta \equiv 1 - v_\sigma, & A = L, \\ -1, & \Delta \equiv 1 + v_\sigma, & A = R. \end{cases} \quad (\text{B.11})$$

Taking the limit $\Delta \rightarrow 0$, one trivially gets the following result

$$v_{LL,A} \Big|_{\Delta^2 \ll 1} = \left(\frac{3}{8} \Delta + o(\Delta^2) \right) \begin{cases} -1, & \Delta \equiv 1 - v_\sigma \\ 1, & \Delta \equiv 1 + v_\sigma \end{cases} = \frac{3}{8} \begin{cases} v_\sigma - 1 + o(\Delta^2), & A = L, \\ v_\sigma + 1 + o(\Delta^2), & A = R. \end{cases} \quad (\text{B.12})$$

Thus, direct comparison with the expression (B.6) indicates that the modulus of the Eckart velocity exceeds the Landau-Lifshitz one if the time-like **FHS** is close to the corresponding light cone, i.e., if $0 < \Delta^2 \ll 1$

$$|v_{LL,A}(\Delta)| < |v_{E,A}(\Delta)|. \quad (\text{B.13})$$

It can be shown that inequality (B.13) holds always for the physical values of the velocity $v_\sigma^2 < 1$ for the time-like **FHS** or for any physical values of Δ . Indeed, considering only the case of right hemisphere, one can find all roots of the equation

$$\begin{aligned} v_{LL,R}(\Delta) = v_{E,R}(\Delta) &\Rightarrow 4 - \Delta + \Delta^2 - (2 - \Delta) \sqrt{4 + 2\Delta + \Delta^2} = \frac{3}{2} \Delta^2 \quad (\text{B.14}) \\ &\Rightarrow \left(1 - \frac{\Delta}{2}\right) \sqrt{1 + \frac{\Delta}{2} + \frac{\Delta^2}{4}} = \left(1 - \frac{\Delta}{2}\right) \left(1 + \frac{\Delta}{4}\right), \end{aligned}$$

which are then $\Delta = \{0; 2\}$, and only the zero root is physical. Therefore the Eckart and Landau-Lifshitz velocities coincide only for the case $\Delta = 0$, hence inequality (B.13) cannot be broken.

B.3. Anisotropy of the Energy-Momentum Tensor of the Massless Gas

Results of the previous subsection enable us to study the spatial structure of the energy-momentum tensor of the massless particles. The spatial anisotropy of the Cooper-Frye spectra was originally found for the space-like **FHS** [12]. Here we would like to discuss the spatial anisotropy of the energy-momentum tensor on the time-like **FHS**. The nontrivial structure of the gas energy-momentum tensor on the time-like **FHS** already indicates that such anisotropy might exist. Now we can prove it rigorously for the gas of massless particles. For this purpose we diagonalize the energy-momentum tensor by the Lorentz transformation of Eq. (B.8), first, calculate the $T_{g,A}^{XX}$ component, next, and compare it with the $T_{g,A}^{YY}$ one.

After the diagonalization of the energy-momentum tensor the $T_{g,A}^{XX}$ and $T_{g,A}^{00}$ components read as

$$T_{g,A}^{XX'}(v_\sigma, T, \mu_c) = \gamma^2(v_{LL,A}) \left(T_{g,A}^{XX} - 2v_{LL,A} T_{g,A}^{0X} + v_{LL,A}^2 T_{g,A}^{00} \right), \quad (\text{B.15})$$

$$T_{g,A}^{00'}(v_\sigma, T, \mu_c) = \gamma^2(v_{LL,A}) \left(T_{g,A}^{00} - 2v_{LL,A} T_{g,A}^{0X} + v_{LL,A}^2 T_{g,A}^{XX} \right), \quad (\text{B.16})$$

with the Landau-Lifshitz velocity $v_{LL,A}$. It is sufficient to consider just the case of the right hemisphere, i.e., $A = R$. Then in terms of the difference Δ , introduced in Eq. (B.11), the energy-momentum tensor in the **RFG** becomes

$$T_{g,R}^{\mu\nu}(v_\sigma(\Delta)) = \begin{pmatrix} \varepsilon_g(T, \mu_c) \left(1 - \frac{\Delta}{2}\right) & T_{g,R}^{00} \frac{\Delta}{2} & 0 & 0 \\ T_{g,R}^{00} \frac{\Delta}{2} & T_{g,R}^{00} \frac{1-\Delta+\Delta^2}{3} & 0 & 0 \\ 0 & 0 & T_{g,R}^{00} \left(1 - \frac{\Delta}{2}\right) \frac{(1+\Delta)}{3} & 0 \\ 0 & 0 & 0 & T_{g,R}^{00} \left(1 - \frac{\Delta}{2}\right) \frac{(1+\Delta)}{3} \end{pmatrix} \quad (\text{B.17})$$

Employing this convenient form of the energy-momentum tensor and the expression (B.11) for the Landau-Lifshitz velocity, one can find the XX component in the Landau-Lifshitz rest frame where the energy-momentum tensor is diagonal. After some algebra one gets the following result for Eqs. (B.15) and (B.16)

$$T_{g,A}^{XX'}(v_\sigma, T, \mu_c) = \varepsilon_g(T, \mu_c) \left(1 - \frac{\Delta}{2}\right)^2 \frac{\left(\sqrt{1 + \frac{\Delta}{2} + \frac{\Delta^2}{4}} + 1 - \frac{\Delta}{2}\right)^2}{6 \left(\sqrt{1 + \frac{\Delta}{2} + \frac{\Delta^2}{4}} + 1 + \frac{\Delta}{4}\right)}, \quad (\text{B.18})$$

$$T_{g,A}^{00'}(v_\sigma, T, \mu_c) = \varepsilon_g(T, \mu_c) \left(1 - \frac{\Delta}{2}\right)^2 \frac{\left(2 \sqrt{1 + \frac{\Delta}{2} + \frac{\Delta^2}{4}} + 1 + \Delta\right)}{3}. \quad (\text{B.19})$$

It is only important to mention that in deriving the equations above it is convenient to use the polynomial $S(\Delta) = 1 + \frac{\Delta}{2} + \frac{\Delta^2}{4}$, in terms of which all expressions are greatly simplified, for example,

$$1 \pm v_{LL,R} = \frac{2}{S^{\frac{1}{2}}(\Delta) + \left(1 - \frac{\Delta}{2}\right)} \begin{cases} S^{\frac{1}{2}}(\Delta), \\ 1 - \frac{\Delta}{2}. \end{cases} \quad (\text{B.20})$$

Then a direct comparison with the YY component of the energy-momentum tensor from Eq. (B.17) indicates that for the physical values of Δ , i.e., $0 < \Delta < 2$, in the Landau-Lifshitz rest frame the pressure in X direction is always smaller than in Y or Z one

$$T_g^{XX'}(v_\sigma, T, \mu_c) < T_g^{YY}(v_\sigma, T, \mu_c). \quad (\text{B.21})$$

Evidently this result is valid for the left hemisphere as well.

References

- [1] F. Cooper and G. Frye, *Phys. Rev.* **D 10** (1974) 186.
- [2] K. A. Bugaev, *Nucl. Phys.* **A 606** (1996) 559.
- [3] J.J. Neumann, B. Lavrenchuk and G. Fai, *Heavy Ion Physics* **5** (1997) 27.
- [4] L. P. Csernai, Z. Lázár and D. Molnár, *Heavy Ion Physics* **5** (1997) 467.
- [5] Cs. Anderlik *et al.*, *Phys. Rev.* **C 59** (1999) 3309.
- [6] Cs. Anderlik, Zs. Lázár, V.K. Magas, L.P. Csernai, H. Stöcker and W. Greiner, *Phys. Rev.* **C 59** (1999) 1.
- [7] V. Magas, *Freeze out in hydrodynamical models*, Master of Science Thesis, University of Bergen, January 1999.
- [8] H. Stöcker and W. Greiner, *Phys. Rep.* **137** (1986) 277.
- [9] R.B. Clare and D.D. Strotman, *Phys. Rep.* **141** (1986) 177.
- [10] For recent discussions see, for instance, U. Heinz. Strange Messages: Chemical and Thermal Freeze-out in Nuclear Collisions. *Preprint nucl-th/9810056* (1998) 15p.
- [11] L. D. Landau, *Izv. Acad. Nauk SSSR* **17** (1953) 51.
- [12] M. I. Gorenstein and Yu. M. Sinyukov, *Phys. Lett.* **B 142** (1984) 425;
Sov. Nucl. Phys. **41** (1985) 797.
- [13] Yu. M. Sinyukov, *Sov. Nucl. Phys.* **50** (1989) 228;
Yu. M. Sinyukov, *Z. Phys.* **C 43** (1989) 401.
- [14] H. Heiselberg, *Heavy Ion Physics* **5** (1997) 435.
- [15] S. Muroya, H. Nakamura and M. Namiki, *Progr. Theor. Phys (Suppl)* **120** (1995) 209.
- [16] S. R. de Groot, W. A. van Leeuwen and Ch. G. van Weert, *Relativistic Kinetic Theory*, North-Holland Publishing Company, Amsterdam (1980).
- [17] E. Schnedermann, J. Sollfrank and U. Heinz, *Particle Production in Highly Excited Matter*, edited by H.H. Gutbrod and J. Rafelski, Plenum Press, N.Y. (1993) 175.
- [18] S. Bernard *et al.*, *Nucl. Phys.* **A 605** (1996) 566.
- [19] L. P. Csernai, *Zh. Eksp. Teor. Fiz. (Russ.)* **92** (1987) 379; *Sov. Phys. JETP* **65** (1987) 216.
- [20] M.I. Gorenstein, *Preprint UFTP 251/1990* of the University of Frankfurt (1990).
- [21] T. Csörgő and L.P. Csernai, *Phys. Lett.* **B 333** (1994) 494.

- [22] M.I. Gorenstein, H.G. Miller, R.Q. Quick and R.A. Ritchie, *Phys. Lett.* **B 340** (1994) 109.
- [23] L.D. Landau and E. M. Lifshitz, *Fluid Mechanics*, Pergamon, New York (1979).
- [24] A. H. Taub, *Phys. Rev.* **74** (1948) 328.
- [25] see, for instance, J.- P. Blaizot and J.- Y. Ollitraut, *Phys. Rev.* **D 35** (1987) 916; M. I. Gorenstein and V. I. Zhdanov, *Z. Phys.* **C 34** (1987) 79; K. A. Bugaev and M. I. Gorenstein, *J. of Phys.* **G 13** (1987) 1231.
- [26] K.A. Bugaev, M.I. Gorenstein, B. Kämpfer and V.I. Zhdanov, *Phys. Rev.* **D40** (1989) 2903.
- [27] B.L. Rozhdestvensky and N.N. Yanenko, *Systems of Quasi-Linear Equations*, Nauka, Moscow (1978).
- [28] K.A.. Bugaev, M.I. Gorenstein, B. Kämpfer and V.I. Zhdanov, *Sov. J. Nucl. Phys.* **50** (1989) 1172;
K.A. Bugaev, M.I. Gorenstein and V.I. Zhdanov, *Teor. Mat. Fizika* **80** (1989) 138.

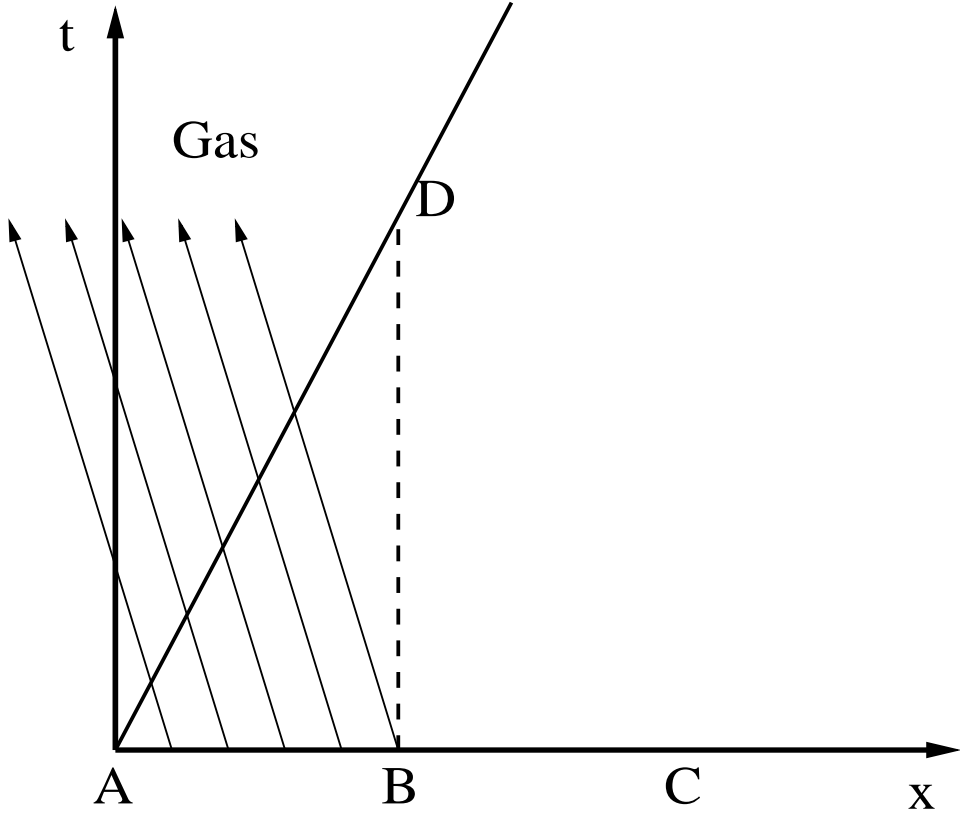
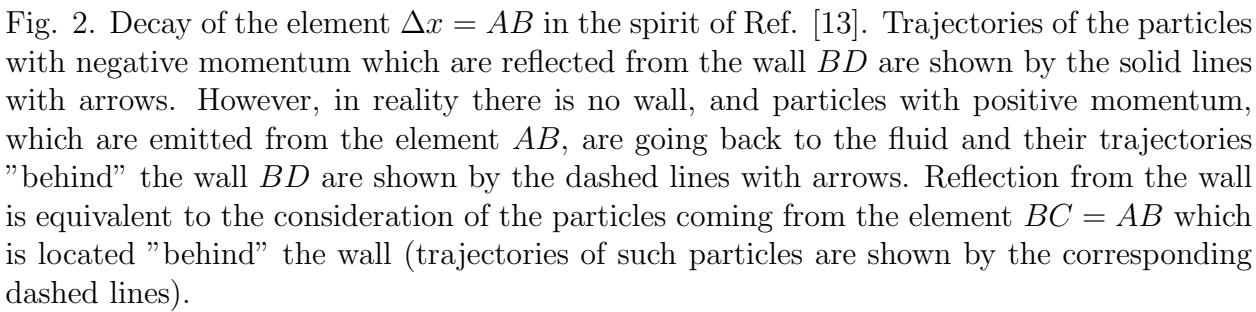


Fig. 1. Decay of the element $\Delta x = AB$ during the time $\Delta t = BD$ in the reference frame of the gas. Particles cross the time-like hypersurface AD . Trajectories of the particles that have negative momenta and are not reflected from the wall BD in the meaning of Ref. [13] are shown by arrows.



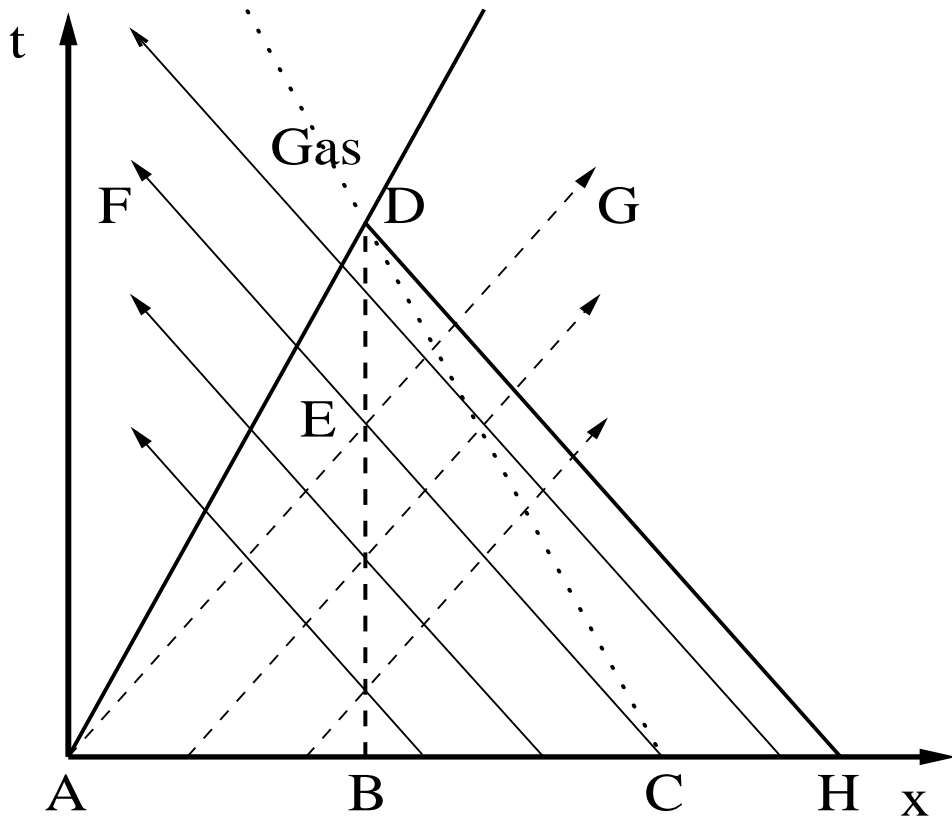


Fig. 3. Decay of the element $\Delta x = AB$ during the time $\Delta t = BD$. Trajectories of the particles that have negative momenta and are reflected from the wall BD in the meaning of Ref. [13] are shown by the dashed lines with arrows. In the real situation those particles are going back to the fluid. The correct trajectories of the free streaming particles are shown by the solid lines with arrows. Thus one can see that in addition to the contribution from the element $BC = AB$ that is taken by the reflection, the contribution from the element CH should be taken into account for the momenta $-1 < \frac{p^x}{p^0} < -\frac{AB}{BD}$. It is only necessary for the time-like freeze-out hypersurfaces.

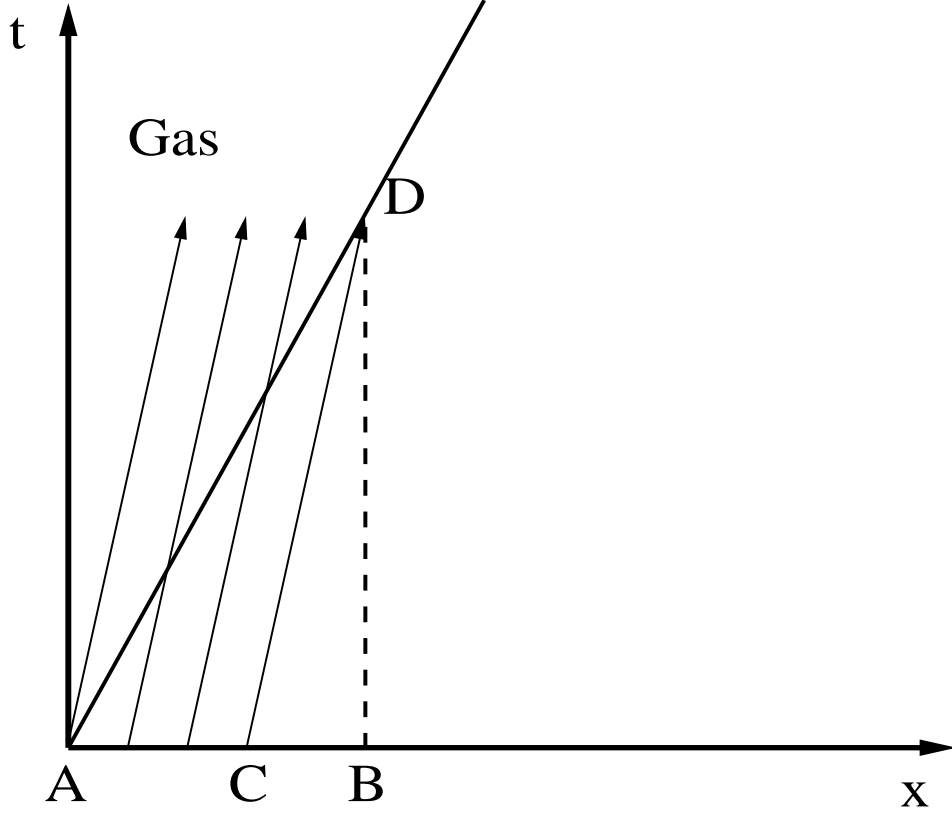


Fig. 4. Decay of the element $\Delta x = AB$ during the time $\Delta t = BD$. Trajectories of the particles with positive momenta are shown by the lines with arrows. Such particles will cross the decay hypersurface AD only if they are emitted from the element $AC = \Delta x - \frac{p^x}{p^0}\Delta t$ or, equivalently, if the following inequality for the velocities $\frac{\Delta x}{\Delta t} \geq \frac{p^x}{p^0}$ holds.

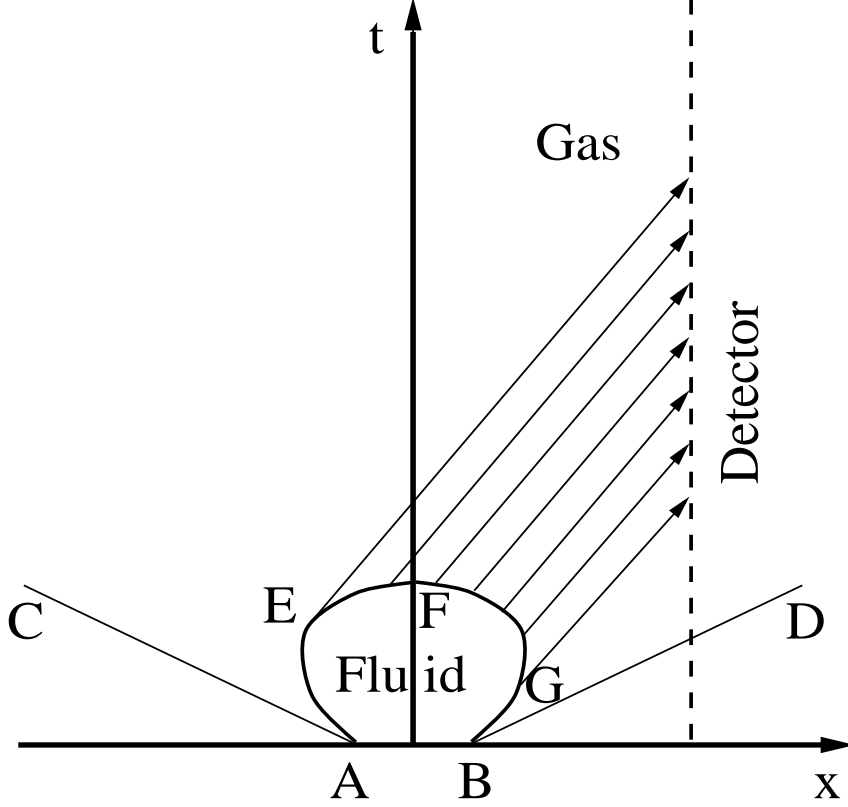


Fig. 5. Decay of the fluid into the gas of free particles on the convex freeze-out hypersurface $AEFGB$. Trajectories of the particles are indicated by the lines with arrows. Dashed line represents the detector's world line. Lines AC and BD denote the light cones. For the given particle velocity $v = \frac{v^x}{p^0}$ the integration limits in coordinate space, points E and G , are found from the condition $p_\rho d\sigma^\rho = 0$. The geometrical meaning of points E and G is evident from the construction: they are tangent points of the particle velocity to the freeze-out hypersurface in $t - x$ plane. In contrast to the cut-off formula for invariant spectra which ensures such limits automatically, the Cooper-Frye one takes into account the particles emitted from all points of the freeze-out hypersurface $AEFGB$.

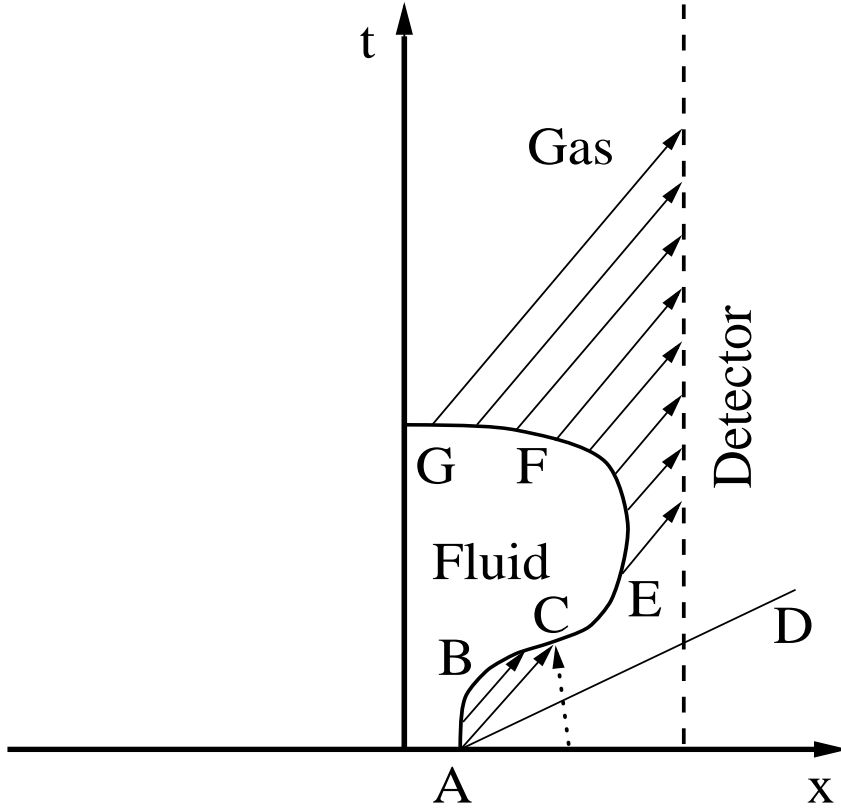


Fig. 6. Decay of the fluid into the gas of free particles on the concave freeze-out hypersurface $ABCEFG$. Notations correspond to the previous figure. In this case, however, one has to take into account the particles feeding back to fluid on the part ABC of the freeze-out hypersurface. These particles were emitted earlier and do not appear from rescattering. The latter is forbidden by the assumption that particle spectra are "frozen" once they belong to the gas of free particles. Hence, particle trajectories, like the one shown by the dotted line, are not allowed in the freeze-out picture because those particles appear from nothing.

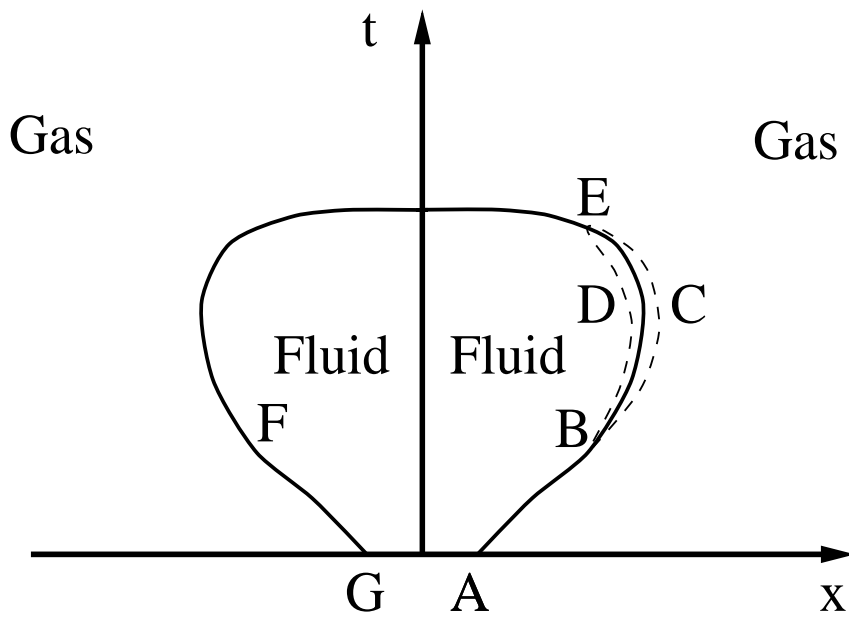


Fig. 7. Integration contour $BCED$ showing the derivation of the boundary conditions between the fluid and the gas of free particles on the **FHS** $ABEFG$.

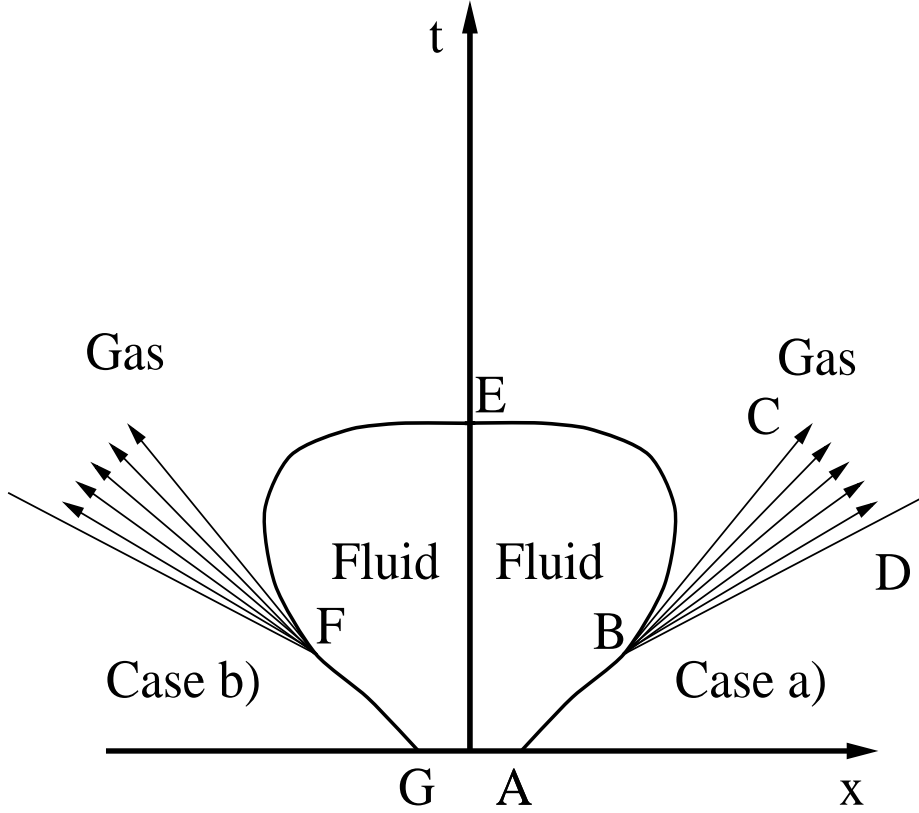


Fig. 8. Decay of the fluid into the gas of free particles on the freeze-out hypersurfaces ABE and EFG is shown for the right hemisphere (Case a)) and for the left one (Case b)). Emission trajectories with possible momenta from point B are indicated by the line with arrows. They are restricted by the tanged line BC to the hypersurface and light cone BD . For the point F the construction is symmetric with respect to reflection.

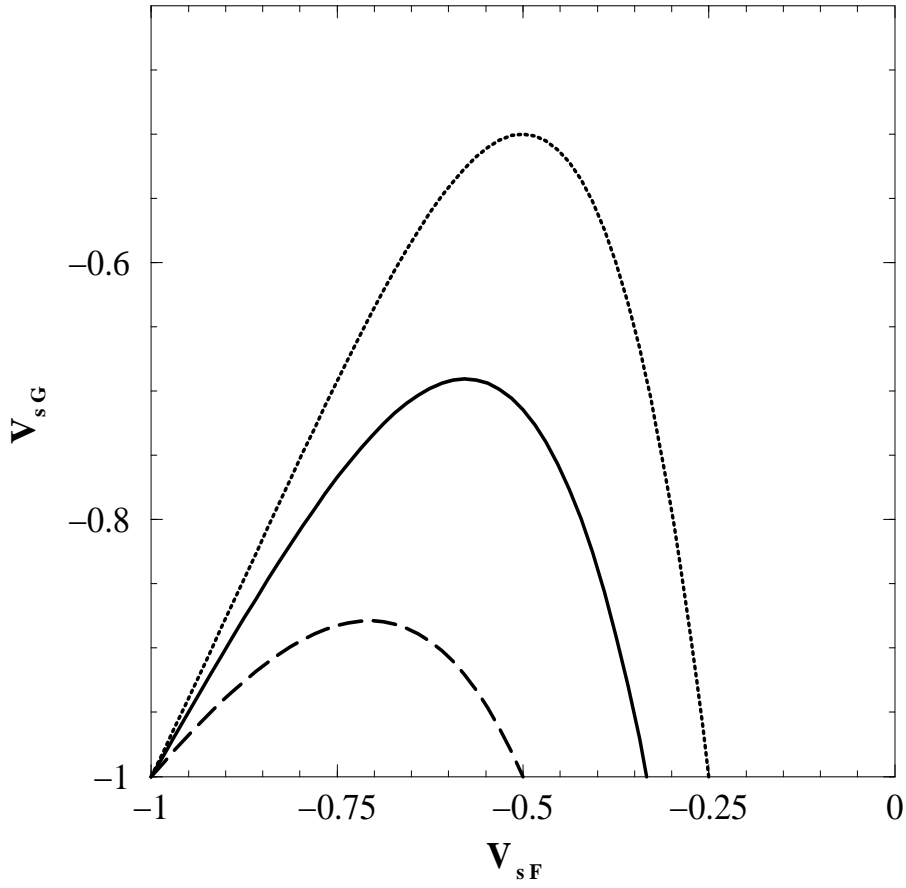


Fig. 9. Dependence of the shock velocity $v_{s\mathbf{G}}$ in the **RFG** upon the the shock velocity $v_{s\mathbf{F}}$ in the **RFF** for three different fluid EoS . The values of the fluid velocity of sound are as follows: $c_s = \frac{1}{\sqrt{3}}$ (solid line), $c_s = \frac{1}{\sqrt{2}}$ (dashed line) and $c_s = \frac{1}{\sqrt{4}}$ (dotted line).

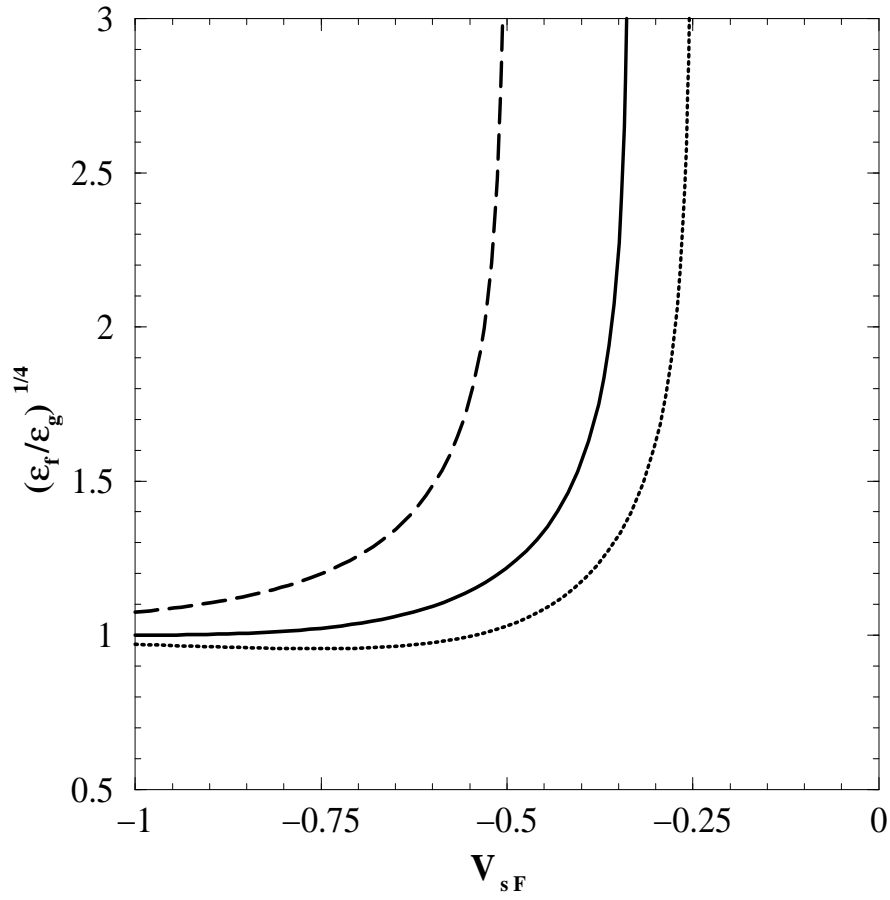


Fig. 10. Ratio of the energy densities on the both sides of the freeze-out shock as a function of the shock velocity $v_{s\mathbf{F}}$ in the **RFF** for three different fluid EoS . The legend corresponds to Fig. 9.

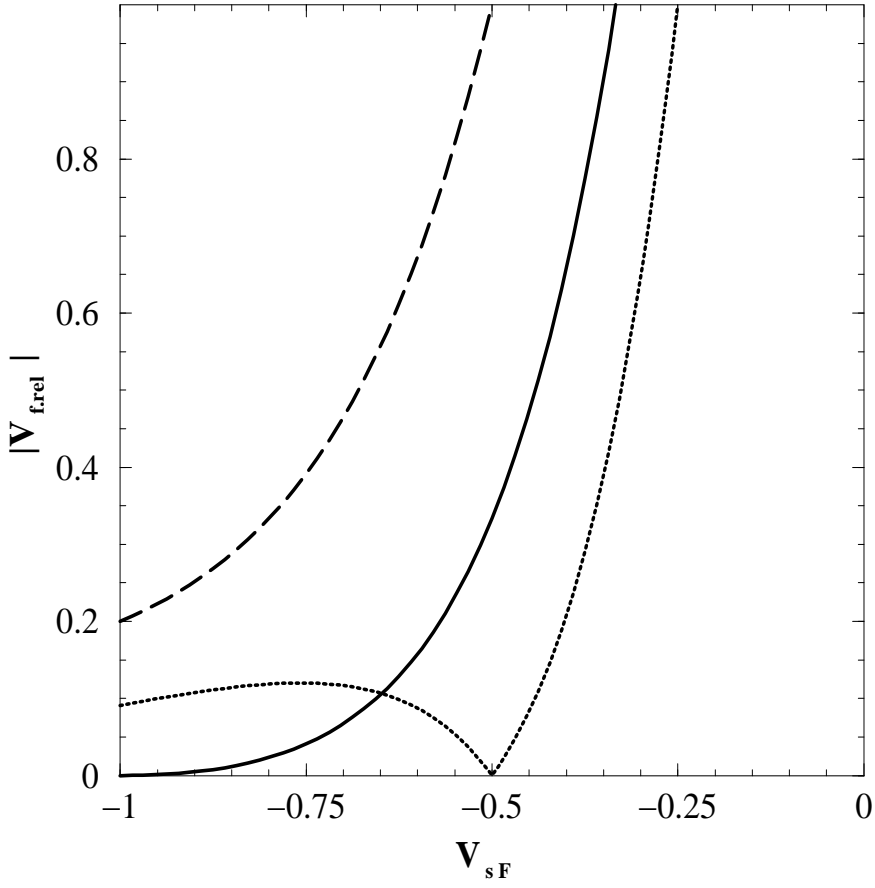


Fig. 11. Relative velocity of the fluid in the **RFG** as a function of the shock velocity v_{sF} in the **RFF** for three different fluid EoS . The legend corresponds to Fig. 9.

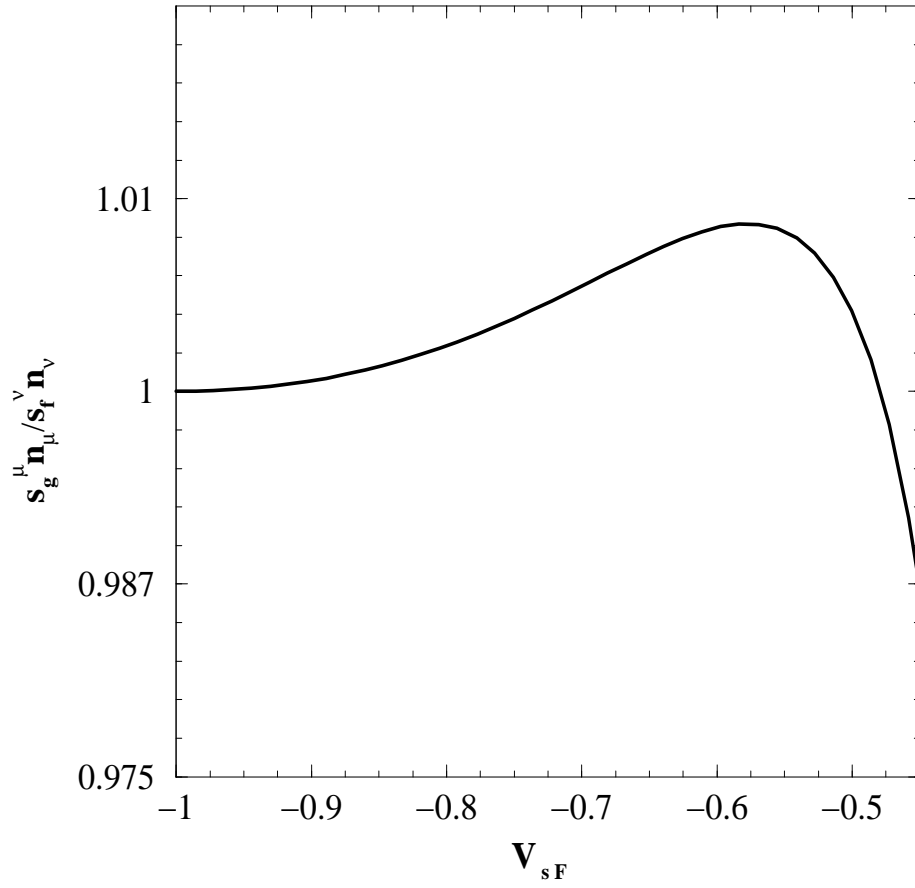


Fig. 12. Ratio of the entropies on the both sides of the freeze-out shock as a function of the shock velocity v_{sF} in the **RFF** for the fluid velocity of sound $c_s = \frac{1}{\sqrt{3}}$.

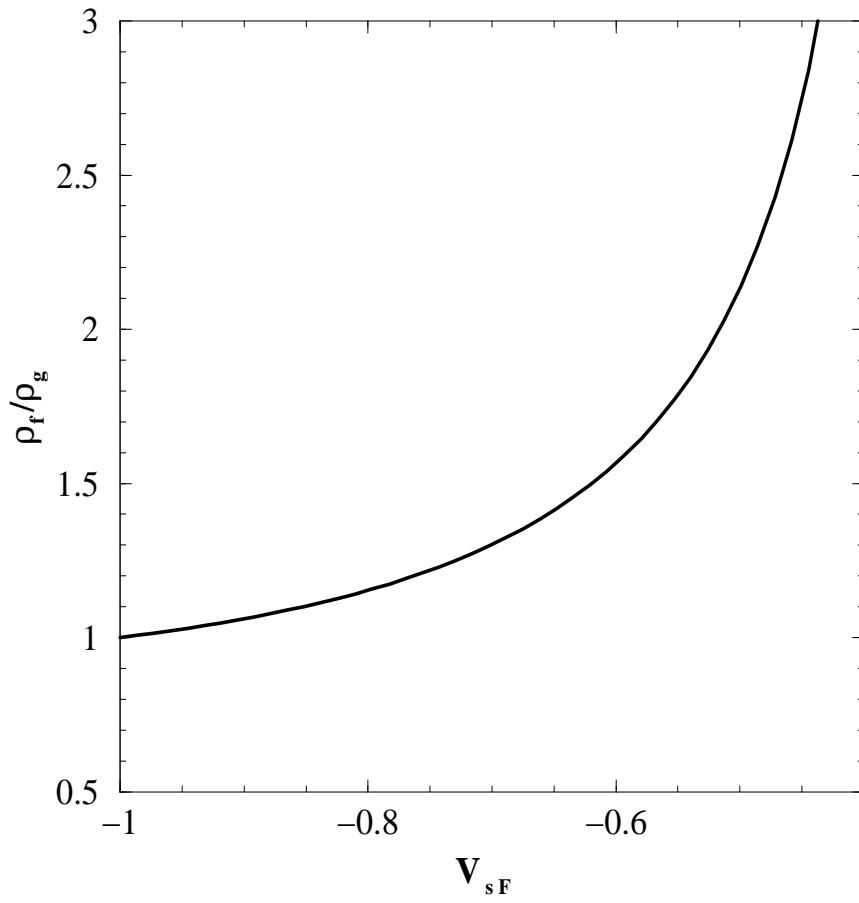


Fig. 13. Ratio of the particle densities on the both sides of the freeze-out shock as a function of the shock velocity v_{sF} in the **RFF** for the fluid velocity of sound $c_s = \frac{1}{\sqrt{3}}$.

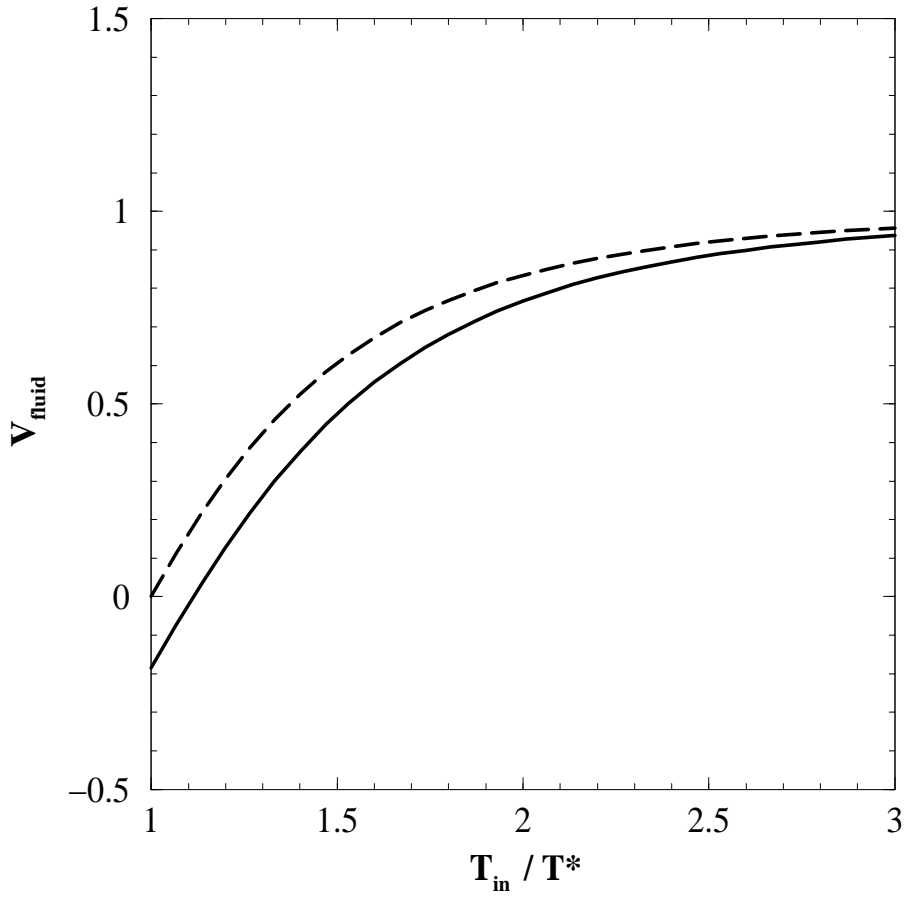


Fig. 14. Fluid velocity of the freeze-out of the simple wave as a function of the initial temperature of the fluid T_{in} . The dashed line corresponds to the Cooper-Frye freeze-out scheme, and the solid one corresponds to the cut-off freeze-out scheme.

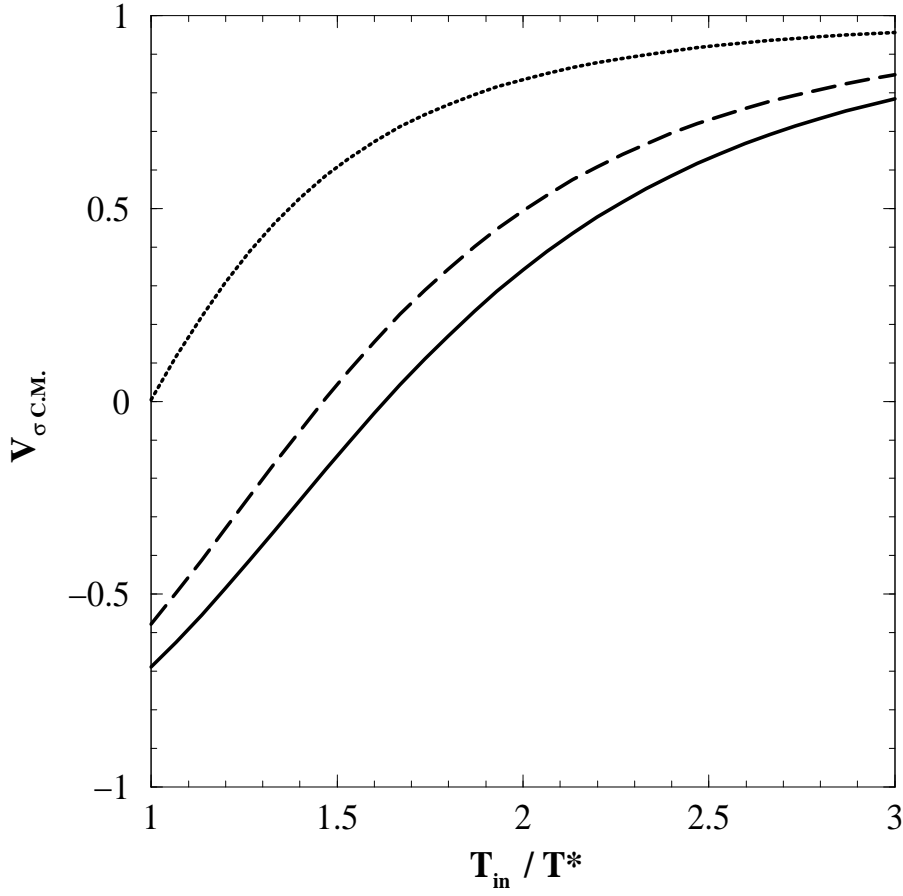


Fig. 15. Velocity of the freeze-out boundary v_{σ} in the **C.M.** frame as a function of the initial temperature of the fluid T_{in} . The dashed line corresponds to the Cooper-Frye freeze-out scheme, and the solid one corresponds to the cut-off freeze-out scheme. The dotted line represents the velocity of the **RFG** in the **C.M.** frame.

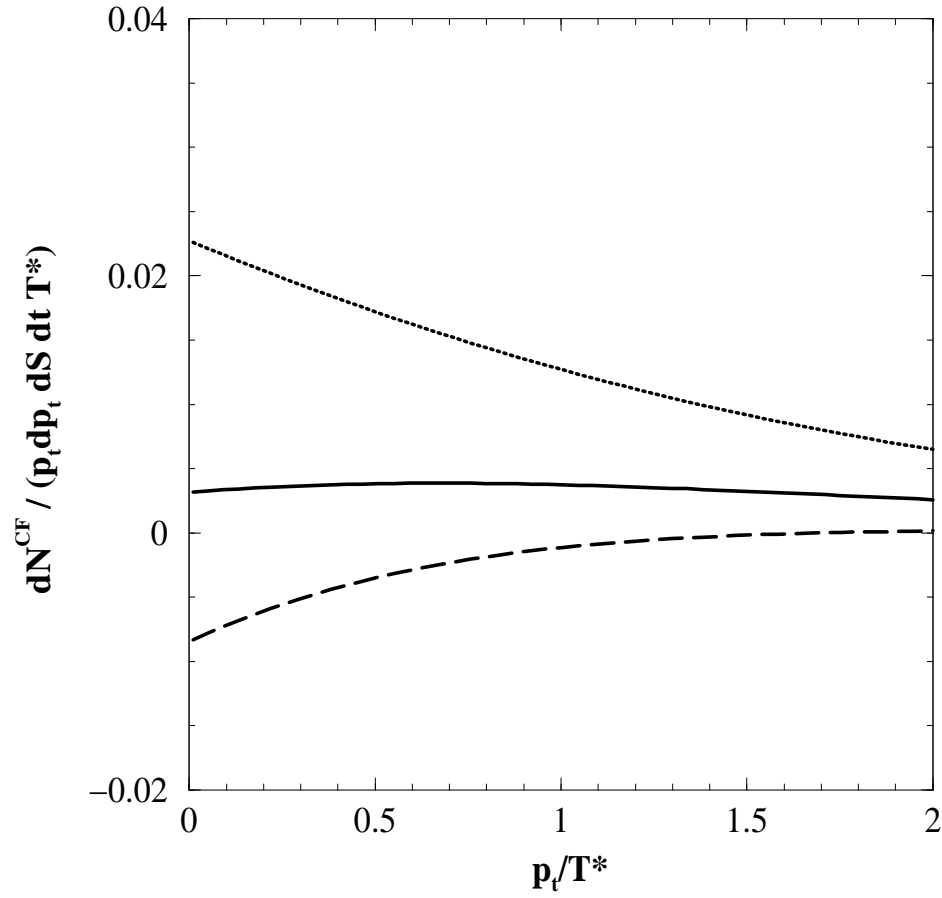


Fig. 16. Momentum distribution of the Cooper-Frye freeze-out scheme integrated over the C.M. rapidity $y_{\text{C.M.}} \in [-1; 1]$. The spectra are found for the three values of the initial temperature of the fluid: $T_{in} = 1.1T^*$ (dotted line), $T_{in} = 1.5T^*$ (solid line), and $T_{in} = 1.9T^*$ (dashed line).

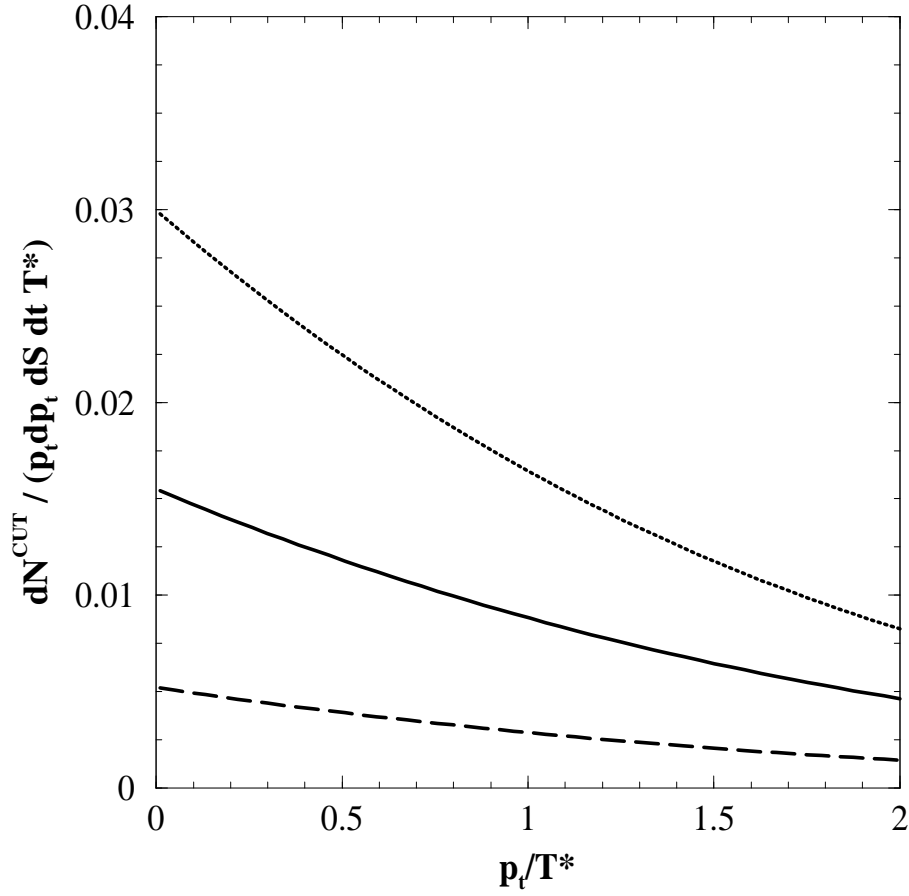


Fig. 17. Momentum distribution of the cut-off freeze-out scheme integrated over the **C.M.** rapidity $y_{\text{C.M.}} \in [-1; 1]$. The spectra are found for the three values of the initial temperature of the fluid: $T_{in} = 1.1T^*$ (dotted line), $T_{in} = 1.5T^*$ (solid line), and $T_{in} = 1.9T^*$ (dashed line).

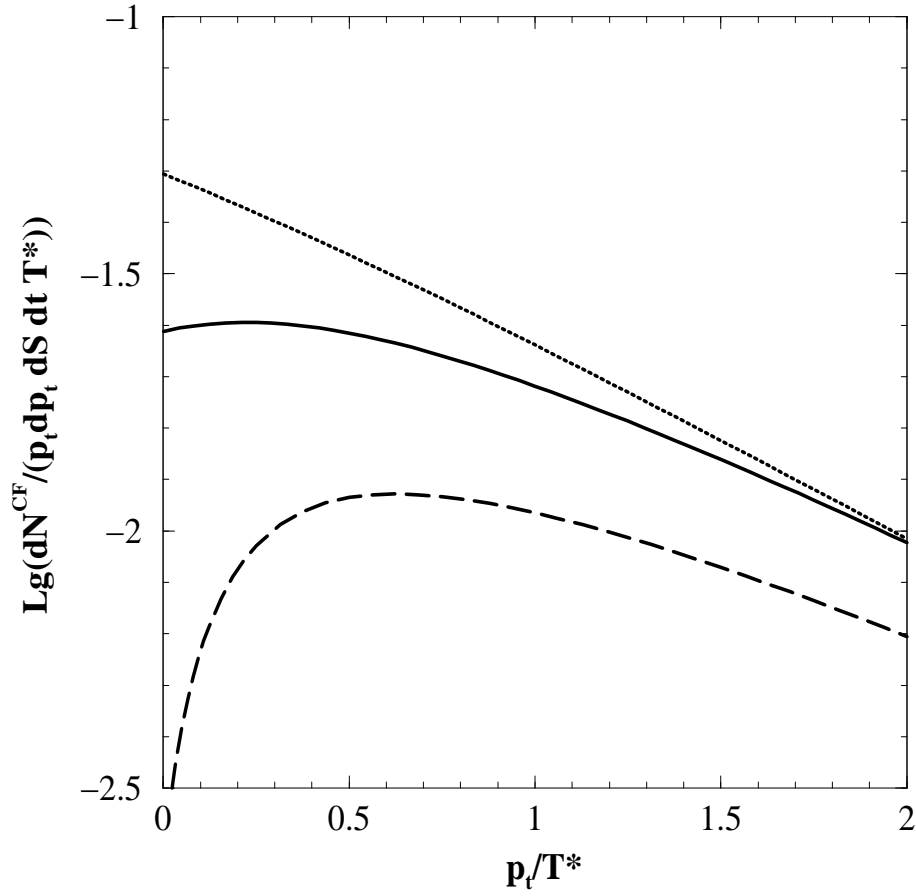


Fig. 18. Momentum distribution of the Cooper-Frye freeze-out scheme integrated over the C.M. rapidity $y_{\text{C.M.}} \in [-2; 2]$. The spectra are found for the three values of the initial temperature of the fluid: $T_{in} = 1.1T^*$ (dotted line), $T_{in} = 1.5T^*$ (solid line), and $T_{in} = 1.9T^*$ (dashed line).

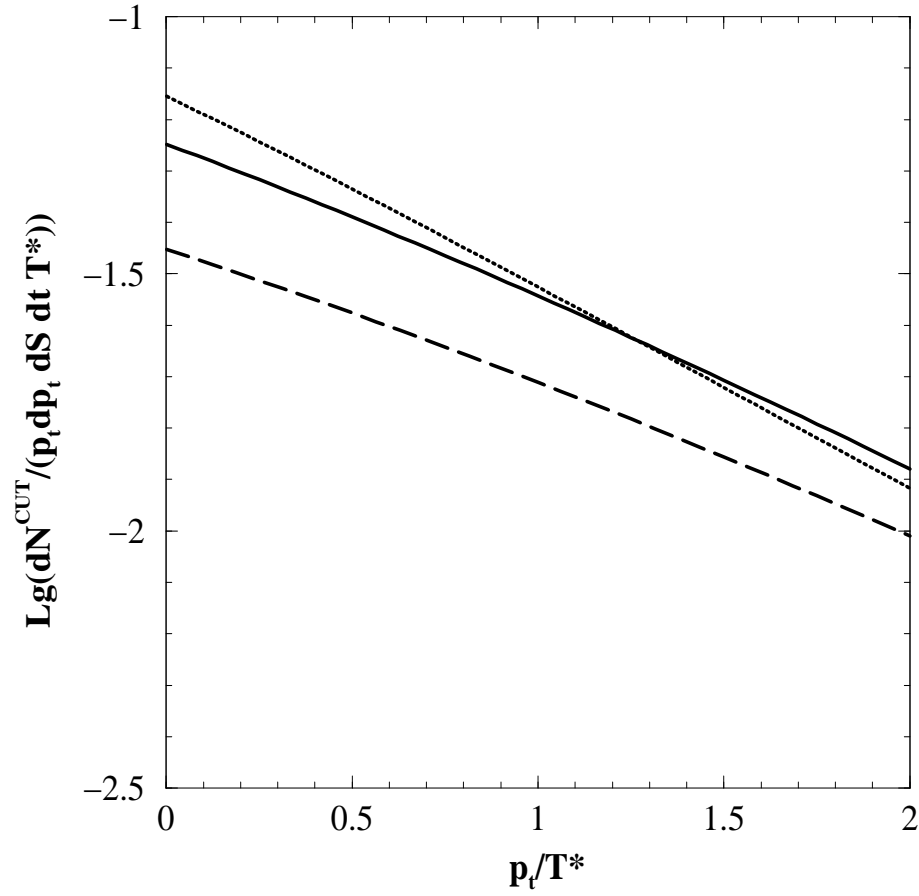


Fig. 19. Momentum distribution of the cut-off freeze-out scheme integrated over the **C.M.** rapidity $y_{\text{C.M.}} \in [-2; 2]$. The spectra are found for the three values of the initial temperature of the fluid: $T_{in} = 1.1T^*$ (dotted line), $T_{in} = 1.5T^*$ (solid line), and $T_{in} = 1.9T^*$ (dashed line).

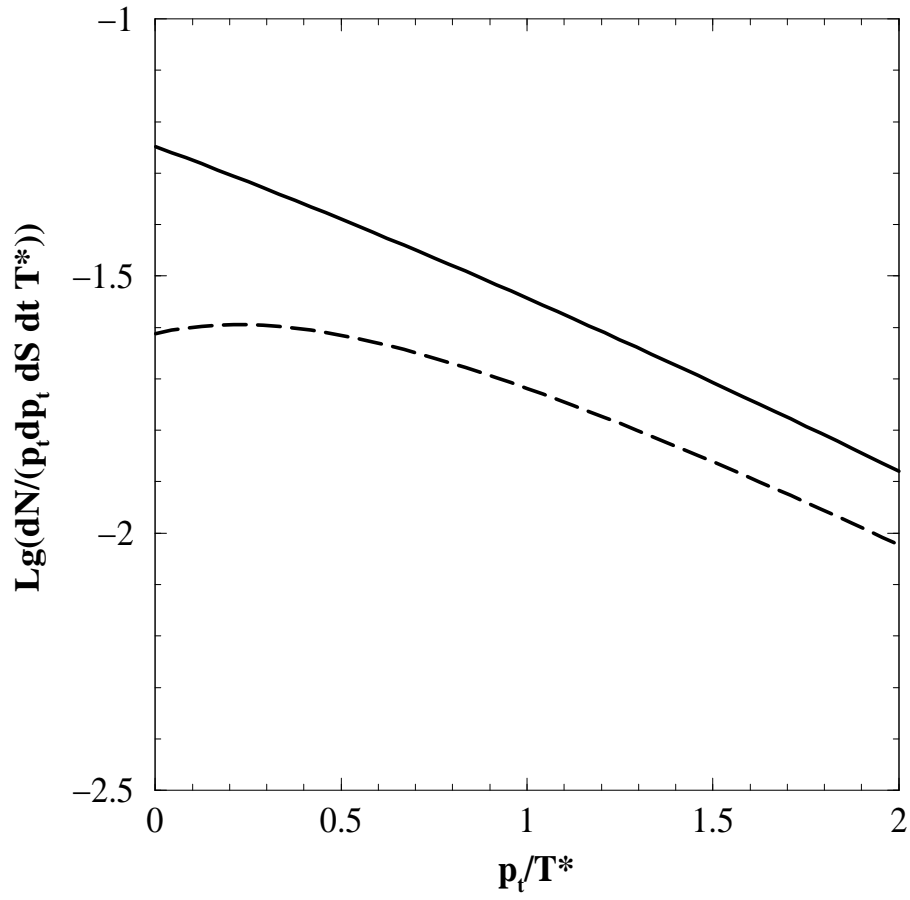


Fig. 20. Comparison of the momentum distribution of the Cooper-Frye (dashed line) and the cut-off (solid line) freeze-out schemes integrated over the **C.M.** rapidity $y_{\text{C.M.}} \in [-2; 2]$. Initial temperature of the fluid is $T_{in} = 1.5T^*$.

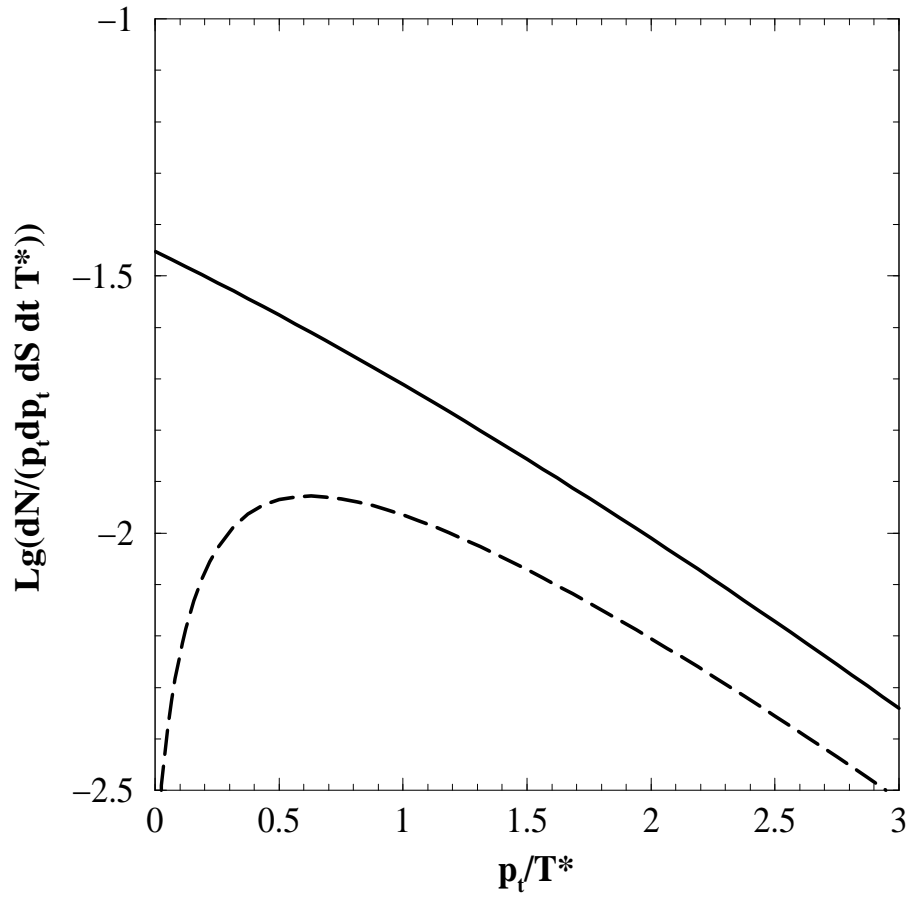


Fig. 21. Comparison of the momentum distribution of the Cooper-Frye (dashed line) and the cut-off (solid line) freeze-out schemes integrated over the **C.M.** rapidity $y_{\text{C.M.}} \in [-2; 2]$. Initial temperature of the fluid is $T_{in} = 1.9T^*$.

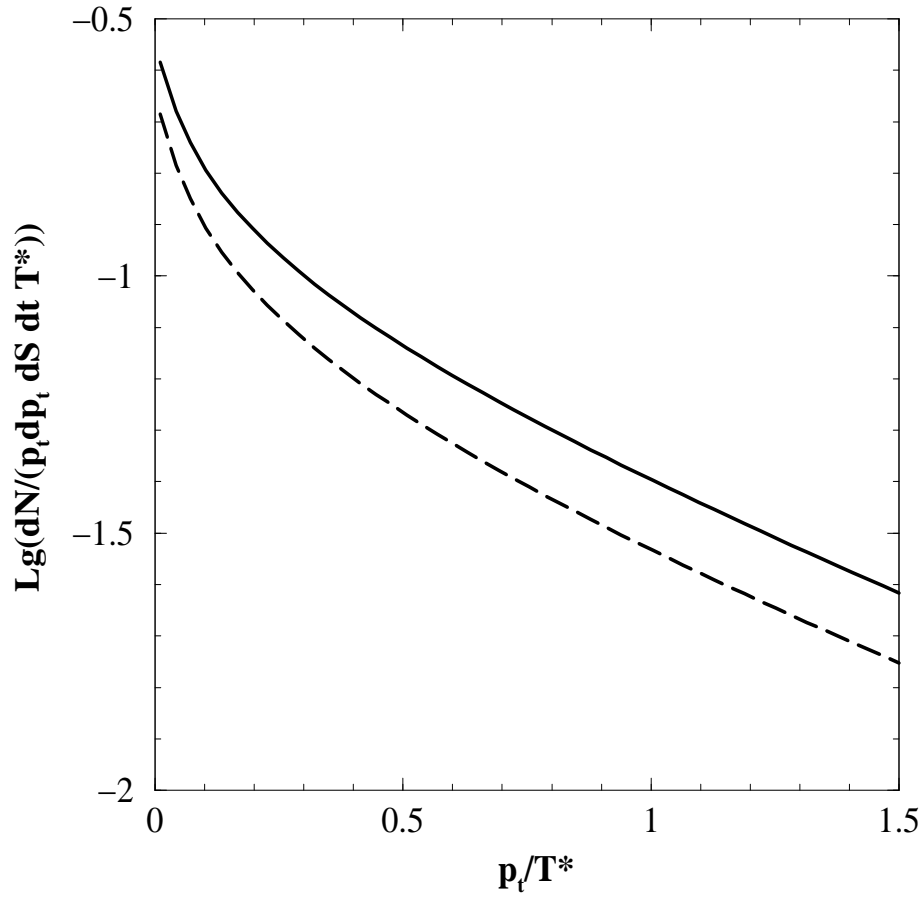


Fig. 22. Comparison of the momentum distribution of the Cooper-Frye (dashed line) and the cut-off (solid line) freeze-out schemes integrated over the **C.M.** rapidity $y_{\text{C.M.}} \in [-1; 6]$. Initial temperature of the fluid is $T_{in} = 1.5T^*$.

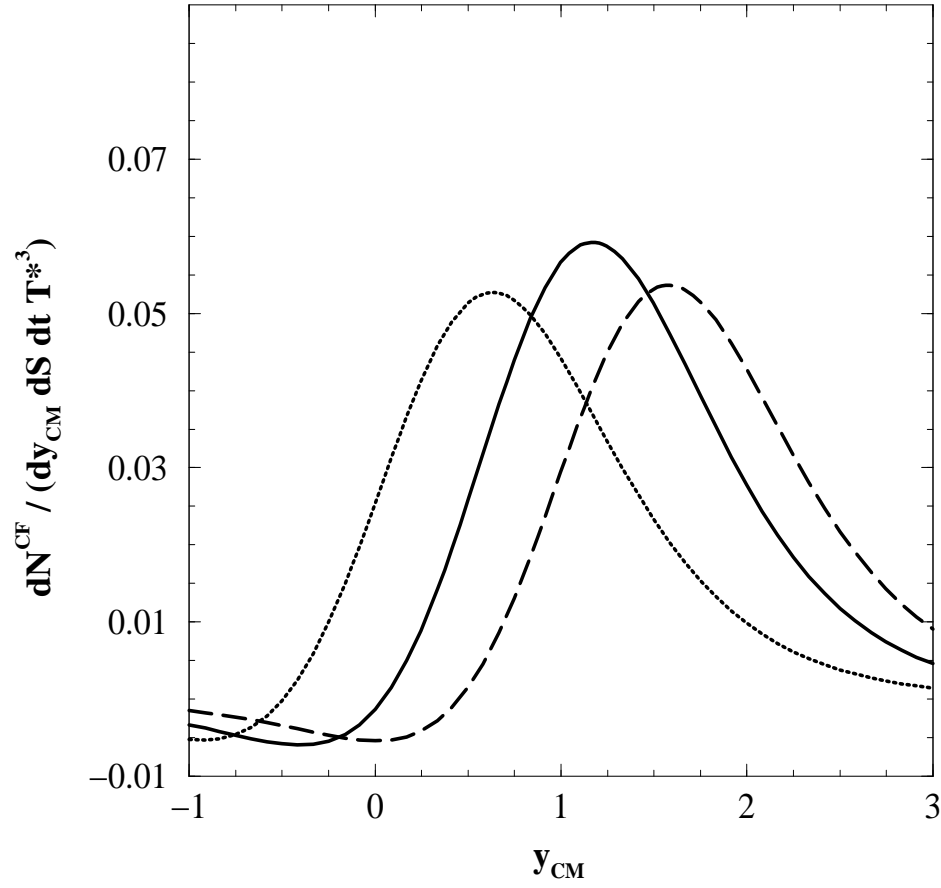


Fig. 23. Momentum distribution of the Cooper-Frye freeze-out scheme integrated over the **C.M.** transverse momentum $p_t \in [0.01; 6]T^*$. Initial temperatures of the fluid are: $T_{in} = 1.1T^*$ (dotted line), $T_{in} = 1.5T^*$ (solid line), and $T_{in} = 1.9T^*$ (dashed line).

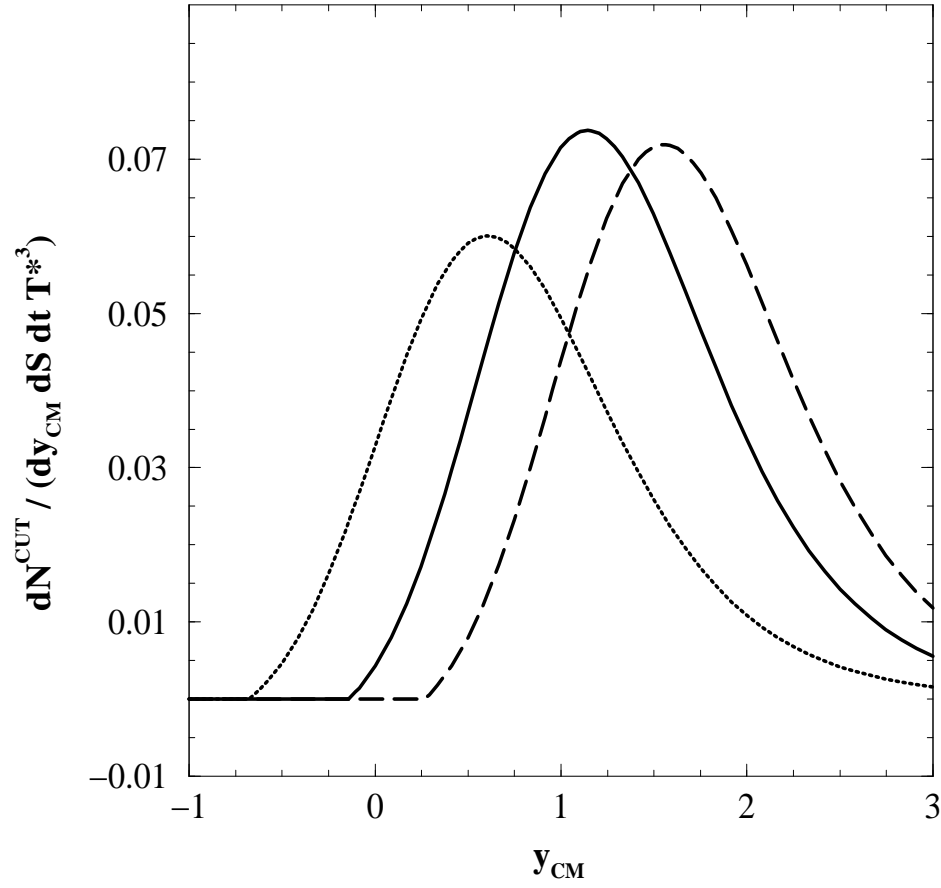


Fig. 24. Momentum distribution of the cut-off freeze-out scheme integrated over the **C.M.** transverse momentum $p_t \in [0.01; 6]T^*$. Initial temperatures of the fluid are: $T_{in} = 1.1T^*$ (dotted line), $T_{in} = 1.5T^*$ (solid line), and $T_{in} = 1.9T^*$ (dashed line).

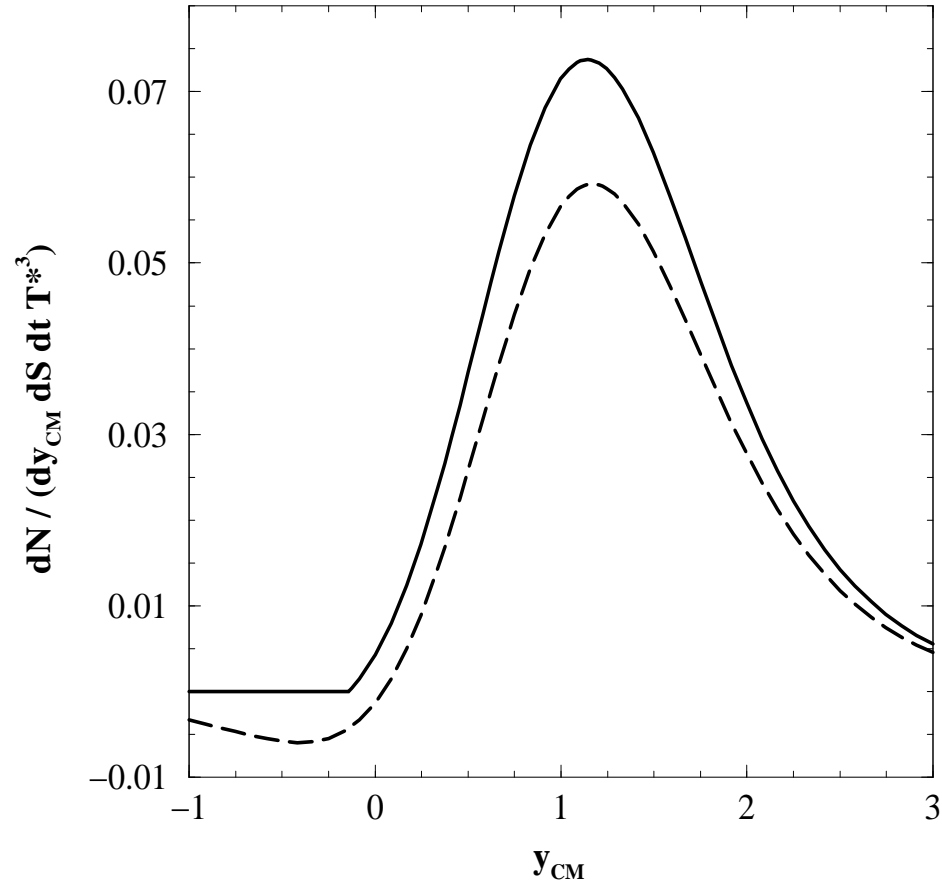


Fig. 25. Comparison of the Cooper-Frye momentum distribution (dashed line) and the cut-off one (solid line) integrated over the **C.M.** transverse momentum $p_t \in [0.01; 6] T^*$. Initial temperature of the fluid is $T_{in} = 1.5 T^*$.

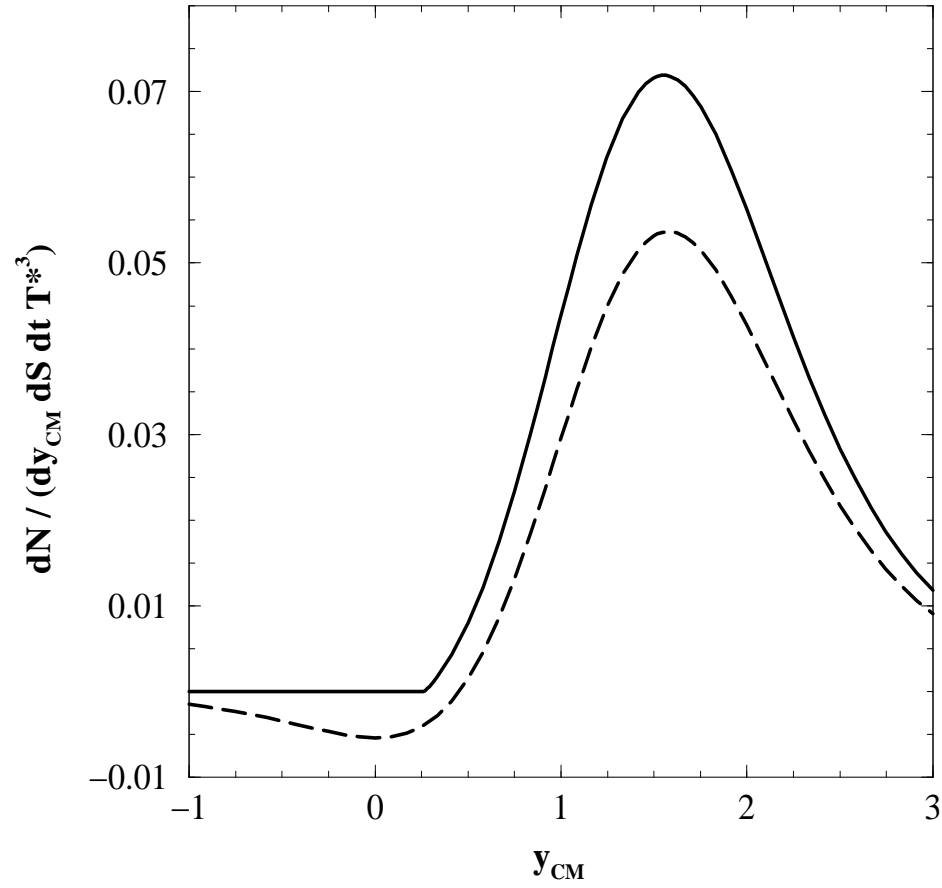


Fig. 26. Comparison of the Cooper-Frye momentum distribution (dashed line) and the cut-off one (solid line) integrated over the **C.M.** transverse momentum $p_t \in [0.01; 6] T^*$. Initial temperature of the fluid is $T_{in} = 1.9 T^*$.